THE INNATE AND ADAPTIVE IMMUNE RESPONSE TO PNEUMONIA VIRUS OF MICE IN A RESISTANT AND A SUSCEPTIBLE MOUSE STRAIN

A Thesis Submitted to the College of

Graduate Studies and Research

in Partial Fullfillment of the Requirements

for the Degree of Master of Science

in the Department of Veterinary Microbiology

University of Saskatchewan

Saskatoon

By

ELLEN RUTH TYNDALE WATKISS

PERMISSION TO USE

In presenting this thesis in partial fulfilment of the requirements for a Postgraduate degree from the University of Saskatchewan, I agree that the Libraries of this University may make it freely available for inspection. I further agree that permission for copying of this thesis in any manner, in whole or in part, for scholarly purposes may be granted by the professor or professors who supervised my thesis work or, in their absence, by the Head of the Department or the Dean of the College in which my thesis work was done. It is understood that any copying or publication or use of this thesis or parts thereof for financial gain shall not be allowed without my written permission. It is also understood that due recognition shall be given to me and to the University of Saskatchewan in any scholarly use which may be made of any material in my thesis.

Requests for permission to copy or to make other use of material in this thesis in whole or part should be addressed to:

Head of the Department of Veterinary Microbiology

University of Saskatchewan

Saskatoon, Saskatchewan S7N 5B4

Canada

ABSTRACT

Respiratory syncytial virus (RSV) is the leading cause of infant bronchiolitis, but the mechanisms underlying host susceptibility to severe infection are still largely unknown. The closely related pneumonia virus of mice (PVM) causes a similar immune-mediated disease in rodents, which makes possible the analysis of host factors that lead to severe illness in mice. This project was designed to compare the immune responses to lethal and sublethal doses of PVM strain 15 in the Balb/c mouse strain with those of the more resistant C57Bl/6 strain. The two strains often show opposite T-helper responses, with C57Bl/6 mice having a greater bias towards Th1 responses and Balb/c mice towards Th2 responses. Based on studies of PVM and RSV in mice, we expected the greater susceptibility of Balb/c mice to PVM 15 infection to be associated with enhanced proinflammatory chemokines, Th2-biased cytokines, and eosinophilic disease.

We found that the two strains have Th1-biased responses to PVM infection in both the innate and adaptive arms of the immune response. Eosinophilia did not develop in either strain upon infection with PVM 15. Balb/c mice responded to PVM infection with an earlier and stronger innate response that failed to control viral replication. Neutrophils were more predominant in infected Balb/c lungs than in C57Bl/6 mice. In contrast, C57Bl/6 mice were capable of suppressing both viral replication and innate inflammatory responses, and clearance appeared to be mediated by lymphocytes rather than neutrophils. PVM-specific IFN-γ production by splenocytes in C57Bl/6 mice was stronger earlier and weaker at late time points after a sublethal infection than that of Balb/c mice. Additionally, the antibodies produced in the blood and in the lungs of sublethally infected C57Bl/6 mice reached an earlier peak and were more capable of neutralizing PVM *in vitro* than that of Balb/c mice, despite similar IgG titres and

lower mucosal IgA titres in C57Bl/6 mice. Overall, the difference in susceptibility of these two strains appeared to be related not to an inherent T helper bias, but to the capacity of the C57Bl/6 mice to control both viral replication and the immune response elicited by PVM.

ACKNOWLEDGEMENTS

There are more people to thank for the help and support I received at VIDO than words allotted for acknowledgements. I would like to thank my supervisor, Dr. Sylvia van den Hurk, for her support and guidance throughout this project. Thanks to my advisory committee, Dr. George Mutwiri, and graduate chairs, Dr. Vikram Misra and Dr. Janet Hill. I would like to thank the VIDO Animal Care staff for their technical assistance and the countless hours they put in, especially on weekends and holidays. A special thanks to Laura Latimer for her support, both technical and emotional, throughout this project. The support and friendship of my lab mates and coworkers at VIDO, both past and present, have been a constant source of strength for me, and there are too many names to list. Thanks to Dr. Pratima Shrivastava for help with qPCR, to Marlene Snider for analysing BAL cells, and to Natasa Arsic for establishing the PVM model in our lab and assisting me with FACS. Additional thanks go out to Dr. Susantha Gomis for histopathological analysis, Dr. Samuel Attah-Poku of Chemistry Services, and the staff in Glassware and Media Preparation. Funding for this project stems from grants provided by NSERC and CIHR and scholarships from the Department of Veterinary Microbiology. Thanks to my roommates, especially Taryn, for the warmth of shared food and dreams. Finally, I would like to thank my family for reminding me that no task is too difficult and no dream too big to follow.

DEDICATION

This work is dedicated to the 1040 mice that were killed over the course of this project. Their lives contributed to the more than 14,000 data points that were generated and used for the purpose of statistical analyses, the development of assays, and establishing new protocols. I want to remind the reader that as a species, mice will not benefit from this research, and it is through their suffering and death that we have gained the knowledge presented here. Their contribution to science is often, if not always, overlooked, which is why I felt it necessary to dedicate this work to their sacrifice. May this serve as a reminder to those who have become desensitized to this aspect of research.

In addition to the animals that gave their lives for this project, I want to dedicate this work to my family and to my surrogate family that has developed in our household here in Saskatoon. They have taught me that laughter and community are the greatest sources of strength that we have.

Table of Contents

LIST OF TABLES

LIST OF FIGURES

LIST OF ABBREVIATIONS

AP	alkaline phosphatase
APC	antigen presenting cell
BAL	bronchoalveolar lavage
BCR	B cell receptor
BHK	baby hamster kidney
BRSV	bovine respiratory syncytial virus
BSA	bovine serum albumin
CCL	C-C chemokine receptor ligand
CCR	C-C chemokine receptor
CD	cluster of differentiation
cDC	conventional dendritic cells
ConA	Concanavalin A
CTL	cytolytic T lymphocytes
DC	dendritic cell
dd	double-distilled
ds	double-stranded
ECP	eosinophil cationic protein
EDTA	ethylenediaminetetraacetic acid
ELISA	enzyme-linked immunosorbent assay
ELISPOT	enzyme-linked immunospot assay
FBS	fetal bovine serum
FLT3L	fms-related tyrosine kinase 3 ligand
GAPDH	glyceraldehyde 3-phosphate dehydrogenase
G-CSF	granulocyte colony-stimulating factor
GM-CSF	granulocyte macrophage colony-stimulating factor
Gro	growth-regulated protein
H&E	hematoxylin and eosin
hr	hour
ICAM	intercellular adhesion molecule
IFN	interferon
Ig	immunoglobulin
IL	interleukin
IP	interferon gamma-inducible protein
IRF	interferon regulatory factor
LFC	lung fragment culture
LRT	lower respiratory tract
LRTI	lower respiratory tract infection
MCP	monocyte chemotactic protein
mDC	myeloid dendritic cell
MEM	minimum essential medium
MHC	major histocompatability complex
MIP	macrophage inflammatory protein
MOI	multiplicity of infection

MyD88	myeloid differentiation primary response gene 88
NF-κB	nuclear factor kappa B
NK	natural killer
NKT	natural killer T
NS	non-structural
ORF	open reading frame
p.i.	post infection
PAMP	pattern-associated molecular pattern
PBS	phosphate-buffered saline
PBST	PBS with 0.05% Tween20
pDC	plasmacytoid dendritic cell
pfu	plaque forming units
PMSF	phenylmethylsulfonyl fluoride
PRR	pattern recognition receptor
PVM	pneumonia virus of mice
qPCR	quantitative real time polymerase chain reaction
RANTES	regulated upon activation, normal T-cell expressed and secreted
RBC	red blood cell
RIG-1	retinoic acid-inducible gene-1
RNA	ribonucleaic acid
rpm	revolutions per minute
RSV	respiratory syncytial virus
RSV_{CM}	RSV conditioned media
RT	room temperature
RT-PCR	real-time polymerase chain reaction
sec	second
SH	small hydrophobic
SP	surfactant protein
STAT	signal transducer and activator protein
$TCID_{50}$	50% tissue culture infective dose
TCR	T cell receptor
TLR	toll-like receptor
TNF	tumor necrosis factor
URTI	upper respiratory tract infection
UV	ultraviolet

1.0 Introduction and Literature Review

1.1 Burden and Epidemiology of Respiratory Syncytial Virus

Respiratory syncytial virus (RSV) is a common human pathogen that circulates through communities on a yearly basis, causing mild cold-like symptoms in most healthy adults and children. In infants and young children predisposed to severe RSV, however, RSV infection is more likely to move into the lower respiratory tract (LRT), leading to pneumonia and inflammation of the small airways, or bronchiolitis. RSV can be isolated from the majority of children hospitalized for bronchiolitis during the RSV season and is the most common respiratory virus associated with infection of infants [1-3]. The winter and spring months of November through April are the peak season of RSV infections in temperate climates of the Northern hemisphere, while in tropical climates RSV outbreaks occur most frequently during the rainy season [4-7].

RSV is highly transmissible, spreading through communities rapidly and infecting most of the population within their first year of life [8]. The virus spreads by direct contact with infected individuals or their respiratory secretions [9, 10]. Although relatively harmless on a population-wide basis, it is a ubiquitous pathogen throughout all age groups, reinfecting individuals multiple times over the course of a lifetime [8, 11]. Based on evidence from children followed from birth to their fourth year of life, almost half of the infants experienced reinfection with RSV in their second year of life, which dropped to one third in the fourth year of life [8]. In agreement with this, in a trial examining the rate of reinfection in adults experimentally infected with RSV six times over the course of 26 months it was observed that even subjects with the highest neutralizing antibody titres had a 25% chance of becoming reinfected, with at least one

reinfection occuring in 73% of individuals over the 26 month period [12]. Furthermore, the majority of healthcare workers working with infected infants become infected during an RSV season, and some have been reported to experience reinfection multiple times during a single RSV season [9]. Since RSV infections can be much more serious in immune compromised individuals and those with underlying heart and respiratory disorders, it is of critical importance to limit the nosocomial spread of RSV in hospitals.

Hall et al. found that hospitalized infants shed RSV at levels of around 10^4 50% tissue culture infectious dose ($TCID_{50}$) per millilitre of nasopharyngeal aspirate for an average of a week following admission, with younger infants shedding higher amounts and children with more severe infections shedding for longer periods of time [13]. This parallels another more recent study in which RT-PCR was used to detect RSV transcripts in hospitalized infants, finding over 10^6 copies per microlitre of nasopharyngeal aspirate, again with higher levels in infants under one month of age [14]. In order to examine the means of transmission, Hall et al. found that RSV can survive in respiratory secretions for 12 hours or more when they land on hard surfaces such as plastic, and survives on skin as long as 25 minutes after contact with contaminated surfaces [10, 11]. Further work showed that individuals who touched infants directly had the highest risk of infection, with the next highest risk in those who touched surfaces that had been handled by infected children, while those who sat near the infected infants without any contact showed no signs of infection [15]. These results also explain why such a high proportion of staff in hospitals acquire nosocomial RSV infections during the height of the RSV season, despite practices such as wearing gloves and gowns, although these precautions do lower the spread of RSV from staff to other hospitalized infants admitted during an RSV outbreak [11, 16].

In developed nations, the rate of hospitalization for RSV-associated illness in infants is around 1-3%, although premature infants can have rates as high as 10% and those with chronic lung conditions over 50% [2, 3, 17-22]. Infants who are hospitalized for RSV usually require lengthy stays, an average of 5-7 days in otherwise healthy infants and 9-12 days in infants with other complicating factors [23]. Interestingly, the rates of hospitalization for infant bronchiolitis have been rising steadily both in Canada and the United States. Two independent studies showed a trend toward increased bronchiolitis and pneumonia case admissions to hospitals in North America, though neither examined the rate of RSV specifically. An examination of hospital admissions between 1980 and 1996 in children under 5 years in the United States showed that rates of hospitalization due to bronchiolitis increased 2.4-fold in infants less than one year of age [19]. Similarly, a study of Canadian children admitted to hospitals between 1980 and 2000 showed a 2.6-fold increase in hospitalizations due to bronchiolitis in children under four [24]. These numbers cannot be directly associated with an increased number of RSV infections, although a large proportion of the children with bronchiolitis have an RSV infection. However, this increase points to a greater burden on the health care system. The economic burden associated with RSV is a combination of the expense due to lengthy hospital stays, sick days taken due to nosocomial infection of hospital staff, and sick days taken by parents to care for outpatients with RSV, which makes the rising rates of infant bronchiolitis concerning [2, 25].

Beyond the economic burden that RSV poses, the loss of life associated with RSV is quite high on a population-wide basis. Mortality rates are relatively low in North America and other developed nations worldwide, with around 2% of hospitalized infants succumbing to infection, the majority of whom fall into high risk categories like preterm or extremely young infants, especially those with underlying conditions [21]. RSV has also been shown to be an

important cause of mortality in elderly patients, although influenza continues to be the more important respiratory pathogen associated with death over 65 years of age [26]. RSV-associated mortality is a far greater problem in areas where access to healthcare is limited, such as in developing nations and remote areas of North America. Several studies have shown higher than normal rates of severe bronchiolitis in North American aboriginal populations in Alaska, which is likely due to the culmination of a variety of factors [18, 27, 28]. A recent meta-analysis suggested that 99% of the deaths associated with RSV world-wide occur in developing nations [29]. The researchers pooled the results of multiple studies from across the world and estimated that in the year 2005, between 66 000 and 199 000 children under 5 years of age died of RSV infection world-wide, though this has been suggested to be an overestimate [29, 30]. As the death toll of infants, immune compromised, and elderly individuals continues to rise, the need for a better understanding of the mechanisms behind RSV pathogenesis grows along with it.

1.2 Animal Models of RSV

Studying the pathogenesis of severe LRTIs in humans is difficult for a number of reasons. Many RSV infections in healthy individuals are mild enough to remain untreated and unreported, so often only the most severe infections requiring medical intervention are available for study [31, 32]. Also, the site of infection in the LRT is not readily accessible, making studies limited to non-invasive procedures such as the analysis of peripheral blood cells, nasal washes, lung aspirates from intubated infants, and post-mortem lung tissue. In addition, the availability of appropriate control samples and the ethical implications of sampling the LRT in severely ill infants further limit the effectiveness of these studies. Animal models of RSV infection overcome these limitations by providing access to the site of inflammation without the ethical constraints of working with human infants.

Natural host-pathogen interactions have evolved over the course of millennia, and the host-specificity of RSV and other pneumoviruses makes the study of RSV infection in small animal models, such as mice and cotton rats, difficult to interpret in the context of human infections [33]. While RSV replicates in these animals, they do not show clinical illness. Consequently, rather than providing a model of pathogenesis, these small animals are more useful for studies of clearance mechanisms and protection through vaccination [34]. Bovine RSV (BRSV) is the closest relative of human RSV, and as a natural pathogen in cattle, it causes enhanced pathology in calves under 6 months of age, making it a good model of a natural pathogen in an outbred species. In addition, a large animal model of RSV is more relevant to the pathogenesis of RSV in humans, since the morphology of the lungs is more similar than that of rodents and the genetic variability is more realistic than using inbred mouse strains. Chimpanzees can be infected with human RSV, providing an even more relevant large animal model of RSV infection, but both of these models are hindered by the expense of handling these animals and the availability of reagents. Thus, an alternate model of the immune mechanisms involved in susceptibility to natural pneumovirus infection is to infect mice with the closely-related pneumonia virus of mice (PVM) [35, 36].

PVM was isolated from laboratory mice in the late 1930's and as a natural pathogen in rodents, a low dose inoculum replicates to high levels and causes immune-mediated respiratory illness that is quite similar to that described for RSV in children [35-37]. Its potential as a natural model of severe pneumovirus pathogenesis was not established until the 1990's by Cook et al. [38]. Since immunological tools for evaluating the murine response *in vivo* and *in vitro* are widely available, this gives the PVM model a great advantage over large animal models like bovine RSV in cattle. Different mouse strains show different degrees of susceptibility to

infection with PVM, which allows for examination of host genetic background in pneumovirus pathogenesis [39, 40]. Furthermore, there is a wide variety of transgenic and gene deleted mouse strains already developed, making the evaluation of individual genes in the pathogenesis of severe illness possible. Thus, the PVM model of RSV pathogenesis is a promising model for evaluating the immunological mechanisms contributing to the development of severe pneumovirus infection in a natural host.

1.3 Pneumovirus Biology

There are several review articles and book chapters available on the pneumovirus family. The following is a synopsis of pneumovirus molecular genetics reviewed by Easton et al. [41]. The pneumoviruses, a subfamily of the paramyxovirus family, are a group of enveloped viruses with a single-stranded, negative sense RNA genome. They cause respiratory illness in a variety of hosts, with each virus having a fairly narrow range of host-specificity, usually limited to a few closely related species. There are two genera in the subfamily: the metapneumovirus genus contains the human and avian metapneumoviruses, and the pneumovirus genus contains the respiratory syncytial viruses (human, bovine, ovine, and caprine RSV) and pneumonia virus of mice (PVM). The genome of the pneumovirus genus is organized into 10 open reading frames (ORF), coding for 11 proteins, while the metapneumoviruses have a slightly different genome organization and lack the two genes for the nonstructural proteins, NS1 and NS2.

In pneumoviruses, the nonstructural proteins are transcribed from small ORFs at the 3' end of the genome. Because they are so small and they are the first genes transcribed, the NS gene products accumulate rapidly after infection. They are known to play a role in antiviral responses, blocking the type I interferon (IFN) response at multiple levels, which may explain

why the pneumovirus genus is more resistant to IFN-α treatment compared to the metapneumoviruses and other paramyxoviruses. Three glycoproteins are anchored into the viral membrane: the G protein is heavily glycosylated and involved in attachment, the F protein is necessary for fusion of the virus with the cell and syncytium formation and can mediate attachment, and the non-essential small hydrophobic (SH) protein's function remains elusive. The F and G proteins, as the primary envelope proteins, are the main targets of neutralizing antibodies. The G protein, through glycosylation, is highly variable, and it is also produced in a secreted form by infected cells, which can protect virus particles from detection and neutralization by G-specific antibodies. At least three proteins are associated with the RNA genome in the nucleocapsid complex: the nucleoprotein (N), which binds the genome, the phosphoprotein (P), which is required for RNA processing, and the large polymerase protein (L). The phosphoprotein gene encodes a number of related products that are translated into different proteins from the same mRNA transcript because of internal AUG start codons, but their role in replication and infection have not yet been established. The matrix protein (M) is essential for particle formation and packaging. It is critical for the association of the lipid envelope with the nucleocapsid and suppressing transcription to allow packaging of the genome. Two additional proteins, M2-1 and M2-2, are transcribed from overlapping ORFs. In the RSV genome, the M2 region also overlaps with the beginning of the L gene, but this overlap is not present in the PVM genome. M2-1 is thought to allow for proper transcription of the mRNA from the genome, acting as an elongation factor, though M2-deleted viruses can still assemble viable virions. The M2-2 product has a more elusive function, and it may act as a transcription repressor, allowing the virus to move from the early phase of infection to the later phase which requires a switch from transcription and production of viral products to assembly of the virions.

1.4 Cells Involved in Pneumovirus Pathogenesis

1.4.1 Innate Immune Cells

As the first cells to encounter virus upon RSV infection, alveolar macrophages and respiratory epithelial cells set the stage for the innate response and can direct the adaptive response. In culture, both cell types respond to RSV infection by upregulating and secreting a number of chemokines and cytokines that are critical for recruiting and activating immune cells *in vivo* [42, 43]. These cells include neutrophils, natural killer (NK) cells, dendritic cells (DCs), monocytes, and different subsets of T cells. Some of these cell populations can support RSV replication, though the cycle is usually abortive in cells other than the respiratory epithelium. However, even without productive infection, *in vitro* evidence suggests that RSV replication can affect the function of neutrophils, eosinophils, and monocytes [42, 44-51]. Furthermore, there is evidence that soluble mediators from infected cells have as great or greater an impact on the effector function of these cells than interactions with the virus alone [44, 52-54].

The activation of the antiviral response occurs through the interaction of viral pathogen-associated molecular patterns (PAMPs) with cellular pattern recognition receptors (PRRs). In host cells, the Toll-like receptor (TLR) family of PRRs plays a critical role in the detection of pneumoviruses. They detect foreign material by binding to signature molecular patterns that are unique to pathogens, such as molecules of double-stranded RNA produced during viral replication. PAMPs can be proteins, glycoproteins, lipids, or nucleic acids, and different TLRs are capable of binding different types of PAMPs. For the majority of TLRs, detection of viral PAMPs causes a signal cascade involving the adaptor protein MyD88, which, depending upon the signal detected and the receptor type, results in the activation of transcription factors that

upregulate antiviral pathways in the cell. These pathways not only allow the cell to protect itself from the invading pathogen, but also to warn neighbouring cells of an infection, and to signal immune cells to become activated and migrate to the area.

The unique combination of PRRs in different cell types and areas of the body allows for each cell type to play a specialized role in responding to an infection and contributing to the immune response *in vivo*. The role of important immune cells in pneumovirus pathogenesis will be discussed below, with special consideration of the interaction between cell types and their "communication" through the production of inflammatory mediators.

1.4.1.1 Epithelial Cells

Respiratory epithelial cells are the major target of RSV replication, although epithelial cells of the eye are also a primary site of replication and self-inoculation [11, 55, 56]. Within hours of infection with RSV, epithelial cells show an upregulation of pathways involved in the cellular antiviral response, both *in vivo* and *in vitro* [47, 57, 58]. They are one of the key cells that produce proinflammatory chemokines and cytokines, activating and recruiting immune cells to the lung. Their interactions with macrophages, neutrophils, DCs, and T cells have all been examined in the context of RSV infection, which will be the highlight of this section.

Type I interferons are known as the first defense against viral infection, and epithelial cells are a critical source of this important cytokine during RSV infection. The activation of the interferon response gene networks is critical for the production of proinflammatory cytokines and chemokines. The most commonly reported chemokines upregulated upon RSV infection of epithelial cells include CC chemokines MCP-1(CCL2), MIP-1-α(CCL3), and RANTES (CCL5), and CXC chemokines IL-8 (CXCL8), Gro-α (CXCL2), and IP-10 (CXCL10) [42, 49, 59, 60].

Of the chemokines, MIP-1α, MCP-1, RANTES, and IL-8 are well known to be upregulated in the lung washes of infants intubated for severe RSV as well as in mice inoculated with RSV, although IL-8 is a human-specific chemokine whose functional homologue in mice, MIP-2, is likewise upregulated upon RSV infection [61-67]. Cytokines produced by RSV-infected epithelial cells include TNF-α, IFN-β, IL-6, IL-1α and IL-1β [60, 68-72]. The role of individual cytokines and chemokines in signalling to immune cells will be discussed in later sections.

In cultured respiratory epithelial cells, initiation of the type I interferon response depends on the detection of double-stranded RNA (dsRNA) by the retinoid-inducible gene -1 (RIG-1) protein, an RNA helicase that functions as a cytosolic PRR [47]. This signalling event results in the activation of the transcription factors NF-κB and IRF-3 between 6 and 9 hours after infection, which leads to upregulation of IFN-β and other IFN response genes, including the chemokines RANTES and IP-10 [47]. IFN-β signalling in turn activates the expression of TLR3 in epithelial cells, and this receptor is critical for activation of NF-κB and production of chemokines by RSV-infected epithelial cells between 18 and 24 h p.i. [47]. Similarly, another group found that TLR3 signalling was required for the production of chemokines RANTES and IP-10 in response to RSV infection, while IL-8 was dependent on MyD88-mediated signalling, suggesting the involvement of at least one other TLR in IL-8 production [60]. Indeed, silencing of MyD88 had no effect on RANTES production by airway epithelial cells, but drastically reduced the production of IL-8 upon infection of RSV [60]. RSV-infection has also been shown to upregulate the expression of other TLRs on airway epithelial cells, including TLR2, TLR4, and TLR6, all of which have been implicated during RSV pathogenesis [73-77]. As such, these alternative pathways may explain the MyD88-dependent release of IL-8 by infected epithelial cells reported above.

Concurrent with TLR upregulation, there is evidence that RSV induces apoptosis in cultured airway epithelial cells. The authors of the study found that by 24 hr p.i. 11% of RSV-infected airway epithelial cells expressed surface TLR4, compared to 1% of uninfected cells, and almost all of the RSV-infected TLR4-expressing cells were positive for the apoptosis marker Annexin-V [77]. Apoptosis can therefore play a further role in the pathogenesis of RSV, as phagocytic macrophages, DCs, and neutrophils clear the apoptotic bodies of the epithelial cells and are further stimulated by internal PRR receptors.

The importance of epithelial cells in contributing to the immune response will become clear upon examination of other cell types involved in RSV pathogenesis. Through the secretion of soluble inflammatory mediators, RSV-infected epithelial cells can have drastic effects on the activity of macrophages, neutrophils, eosinophils, monocytes, and other important cells of the immune system. They can change the level of response of these cells to RSV, and can inhibit or enhance signalling pathways involved in further chemokine secretion, apoptosis, and initiation of the adaptive immune response.

1.4.1.2 Alveolar Macrophages

While epithelial cells of the respiratory tract are likely the first cells to become infected with RSV, *in vivo* and *in vitro* evidence suggests that macrophages are capable of responding to RSV hours earlier than epithelial cells. They are able to respond more quickly because they can detect RSV before it begins to replicate, unlike epithelial cells that require replication of the virus before it can be detected. Like epithelial cells, macrophages are critical for signalling to the immune system and initiating the response elicited upon encountering RSV. As phagocytic cells of the innate immune system, they are responsible for clearing foreign material and dead or

dying cells from the lungs, including infected epithelial cells and the remains of infiltrating immune cells. They play a critical role in local antigen presentation, in the activation of NK cell responses, and in enhancing the secretion of mediators from epithelial cells and other infiltrating immune cells.

The rapidity of the response to RSV by macrophages is impressive. *In vitro*, human alveolar macrophages infected with RSV show upregulation of the cytokines IL-6, IL-8 and TNF-α within an hour of infection, while the mouse macrophage cell line RAW264.7 responded slightly slower, with NF-κB activation occurring between 1 and 4 hours p.i. [46, 78]. *In vivo* evidence in the Balb/c model of RSV corroborates the earlier activation of the antiviral response by macrophages, as macrophage depletion prior to RSV infection lowered the activity of NF-κB by 1.5 hours post infection, but had no effect on NF-κB activity by 24 hours p.i. [79]. In macrophages, early NF-κB activation relies on the interaction of RSV F protein with CD14 and TLR4, a process that occurs whether viral particles are viable or not [74]. The initial activation of the immune response through NF-κB, as with epithelial cells, triggers the production of inflammatory mediators including RANTES, IL-8/MIP-2, TNF-α, IL-1, and IL-6 [46, 78].

The importance of the macrophage response to RSV *in vivo* has been highlighted by studies in mice where alveolar macrophages have been selectively depleted by treatment with liposomes containing clodronate. Upon infection with RSV, these mice developed impaired cytokine and chemokine responses to the virus, with lower levels of TNF-α, IL-6, IFN-α, MIP-1α, and RANTES detected in the lungs at the initial peak of cytokine production, which occurs at 24 h p.i. in normal mice [80]. In addition to the decrease in early cytokine levels, the mice had higher levels of virus on day 4 p.i., suggesting that macrophages are important for controlling viral replication, either directly or indirectly [80]. The increased viral load in macrophage-

depleted mice may be due to reduced NK cell killing of virus-infected epithelial cells, as macrophage depletion abolished the influx of NK cells to the lung, which peaked on day 4 in normal mice [80]. In addition, the authors found that the NK cell activation marker CD69 was lower in macrophage-depleted mice upon infection with RSV [80]. Surprisingly, despite decreased numbers and activation of NK cells in the lungs, there was no significant decrease in IFN-γ levels during this time [80].

Similar results were found in experiments with a mouse strain that lacks functional TLR4, which is critical for macrophage signalling. $TLR4^{-/-}$ mice had lower levels of NK cells and CD14+ cells in the lung between days 5 and 7 p.i., which was the peak of NK cell recruitment in the closely related $TLR4^{+/+}$ strain used as a comparison [81]. The authors found that IL-12 secretion was impaired in $TLR4^{-/-}$ mice, and NK cell-mediated cytotoxicity could be restored *in vitro* by supplementing IL-12 [81]. As in macrophage-depleted mice, RSV replicated to higher titres and its clearance from the lungs was delayed in $TLR4^{-/-}$ mice, suggesting a role for TLR4 in promoting viral clearance [81]. Interestingly, in both studies, there was no difference in the long-term response to RSV infection between control and macrophage-impaired mice. Despite evidence that NK cell activation and IFN-γ secretion can enhance CTL responses in a DC- and IL-12-dependent manner, there was no difference in the development of RSV-specific CD8 T cell responses in TLR4 deficient mice nor in macrophage depleted mice [80-82]. This suggests that while macrophages and TLR4 are critical for early antiviral responses, other mechanisms can compensate for this loss during the development of the adaptive response.

In addition to their central role in the development of the NK response *in vivo*, macrophages can enhance the interaction of neutrophils and epithelial cells through the secretion of TNF-α and IL-1. These cytokines are important for upregulating intercellular adhesion

molecule-1 (ICAM-1) on epithelial cells, which facilitates the adhesion of neutrophils to the epithelium, a critical step in neutrophil-mediated killing of infected cells [68, 83, 84]. The secretion of IL-8/MIP-2 by macrophages further contributes to neutrophil recruitment and activation [45, 46]. Since TNF-α and IL-8/MIP-2 are produced by RSV-infected epithelial cells, and treatment of cells with TNF-α induces further production of these cytokines *in vitro*, epithelial cells and macrophages clearly have overlapping and mutually enhancing roles in the development of the immune response *in vivo* [46, 70, 85].

1.4.1.3 Neutrophils

Neutrophils are the major infiltrating cell type during RSV infection of mice and in infants with bronchiolitis [56, 86, 87]. They may contribute to RSV-induced lung pathology, as the severity of RSV in infants has been associated with higher levels of neutrophil elastase production, along with the neutrophil chemoattractant, IL-8 [61]. *In vitro*, the activation of neutrophils by RSV appears to be induced primarily by the cytokines and chemokines secreted by infected epithelial cells, as purified RSV shows a lowered capacity to activate neutrophils compared to crude RSV preparations or the clarified supernatants of RSV-infected cells [44]. Similarly, another study showed treatment of neutrophils with UV- or heat-inactivated RSV lead to similar activation levels and IL-8 expression as treatment with live RSV, further suggesting that replication is not required for neutrophil activation [45]. Neutrophils secrete IL-8 and IL-6 in response to incubation with RSV *in vitro*, and the secretion of these cytokines was enhanced by incubating RSV with an antibody to the F protein, giving credence to the concept of neutrophil activation being at least partially mediated by the phagocytosis of viral particles [44, 88].

Neutrophils isolated from the blood appear to have higher levels of activation, measured by CD11b expression, in infants with severe RSV compared to control infants [89]. Likewise, the activation of neutrophils isolated from the BAL of infected infants was higher than those isolated from the blood of these infants, and, in turn, greater than those isolated from control infants [89]. Another study examining the activation of neutrophils in the lungs and peripheral blood of RSV-positive infants admitted to hospital for bronchiolitis showed similar, but not identical, results. RSV infection was associated with enhanced activation of neutrophils in both lungs and peripheral blood, as measured by CD18 expression, while CD11b was upregulated only on lung neutrophils [90]. Another interesting finding was that both circulating and lung-resident neutrophils isolated from infants with RSV bronchiolitis expressed apoptosis markers Annexin V and propidium iodide, while Fas was upregulated only on lung neutrophils [90]. These studies suggest that the activation of neutrophils begins in the periphery and is enhanced by local factors in the lung. Their activation in the lung is associated with enhanced cytokine and chemokine production, and non-specific damage to the tissue through respiratory burst and the secretion of enzymes like myeloperoxidase and neutrophil elastase [44, 61, 88]. Also, since RSV has been shown to enhance apoptosis in both epithelial cells and neutrophils, this likely puts greater pressure on alveolar macrophages in clearing the cell debris from the lungs. Thus, as the primary granulocyte infiltrating the lungs, neutrophils play a key role in RSV pathogenesis *in vivo*.

1.4.1.4 Eosinophils

The role of eosinophils in pneumovirus infection is still unclear. In RSV-infected children, eosinophils have been detected in the BAL of children with bronchiolitis, along with eosinophil degranulation products, eotaxin, and Th2 cytokines [91-94]. However, these features

are not universally present during severe bronchiolitis, which has led some groups to separate their research cohorts on the basis of the presence or absence of eosinophils and/or Th2 cytokines. In these studies, children exhibiting eosinophilic disease were more likely to have enhanced Th2-biased responses either locally or peripherally [92, 95]. Also, the comparison of RSV-mediated URTI with RSV bronchiolitis has suggested that eosinophils are more important in bronchiolitis than URTI. Some groups also found that wheezing during primary infection and the development of recurrent wheeze during childhood was associated with enhanced eosinophilia during primary infection, but others have not been able to document the same association [96].

Eosinophils, like neutrophils, are granulocytes that are recruited to the site of inflammation and activated by local inflammatory mediators. They are capable of killing cells through a process of degranulation, whereby enzymes are released across an immunological synapse, triggering lysis of the target cell. This process is not specific to virus-infected cells; rather, it occurs through activation via local signals like GM-CSF and IL-5, and can be sustained by the degranulation products released by surrounding eosinophils, providing an autocrine positive feedback loop [97].

Eosinophils isolated from the blood can be infected with RSV, which leads to the production of IL-6 [51]. In addition, the authors report that eosinophils cultured in the presence of heat-inactivated RSV produced IL-1, IL-13, IL-15, and growth factors G-CFS and GM-CSF [51]. In another study that examined the interaction between epithelial cells and eosinophils upon infection with RSV, the authors found that eosinophil degranulation required the presence of epithelial cells in culture. Incubation of eosinophils with purified RSV or UV-inactivated culture medium from infected epithelial cells (RSV_{CM}) did not increase levels of eosinophil cationic

protein (ECP), a marker of eosinophil degranulation, while incubation of eosinophils with either infected epithelial cells or a combination of uninfected epithelial cells with RSV_{CM} caused significant increases in ECP in the medium [98]. As previously reported, RSV_{CM} induced the upregulation of ICAM-1 on epithelial cells and, additionally, the activation marker CD11b on eosinophils [98]. They found that eosinophil degranulation could be inhibited by blocking the adhesion molecule, CD18, using a number of different monoclonal antibodies [98]. Blockade of ICAM-1 had no effect on eosinophil degranulation, however, suggesting that the β-integrin CD18/CD11b interacts with other adhesion molecules on the surface of epithelial cells [98]. It must be noted, however, that eosinophils isolated from blood have to be supplemented with IL-5 *in vitro* to maintain their viability beyond a 24 hour period, and at the same time, IL-5 acts as an eosinophil activation factor. Only low levels of IL-5 are detected in the lungs of RSV infected infants, so how relevant the *in vitro* studies are to RSV pathogenesis is still uncertain [95].

1.4.1.5 Natural Killer Cells and Natural Killer T cells

Natural killer (NK) cells and NKT cells are involved in the early innate response to infection and also play an important role in the adaptive response through the secretion of cytokines that can sway the development of T-helper bias. Activated NK cells are the primary source of early IFN-γ production in many viral infections, while NKT cells can produce either IFN-γ or IL-4 in high concentrations upon activation. Much information is still lacking on the role of these cells in RSV pathogenesis, and, indeed, on their role in many infectious models.

NK cells are critical for responding to and killing virus-infected cells before the adaptive response has been activated. They monitor for signs of infected cells through a number of different receptors that either inhibit or activate their capacity to kill the target cell upon

recognition of ligands displayed on the cell surface. Type I IFN and IL-12 are two of the most prominent activation signals, both of which are primarily provided by activated DCs during viral infection [99]. The interaction between NK and DC populations has been widely reviewed in a number of publications [99-102].

In RSV infection, the role of NK cells is not entirely clear. Indirect evidence for their importance in primary pathogenesis comes from histopathological analysis of the lungs of infants who died as a result of severe RSV infection. The authors found a striking absence of NK cells and CD8 T cells in the lung tissue, and virtually no evidence of granzyme in the lung, which is a marker of cell-mediated cytotoxicity [103]. However, since the authors were only able to examine tissue from healthy and lethally infected infants, the role of these cells in non-lethal infections is unclear. The role of NK cells has been much more thoroughly examined during RSV pathogenesis in mice.

As discussed above, studies of RSV pathogenesis in mice suggest that the recruitment of NK cells to the lungs is dependent on macrophages and TLR4 [80, 81]. Further elucidation of this mechanism was carried out in both the C57Bl/10 strain and Balb/c strain by comparing the effect of mutations in TLR4 and IL-12 following infection with RSV. Here, the authors found that NK cell recruitment and activity was reduced by blocking IL-12 signalling in both Balb/c and C57Bl/10 backgrounds, but not by blocking TLR4 signalling in either strain [104]. The results of this study appear to conflict with those of the report discussed above, where NK cell trafficking was impaired in the $TLR4^{-/-}$ strain, C57Bl/10ScNCr, compared to that in the closely related $TLR4^{+/+}$ strain, C57Bl/10Sn [81]. However, both studies indicate a role for IL-12 in NK cell trafficking, as the C57Bl/10ScNCr produced decreased IL-12 in response to RSV infection. The authors also suggest that their results may contrast with those of Haynes et al. due to

interference with NK cell detection by the expression of NK markers on activated CD8 T cells in the C57Bl/10 strain at late time points in the infection [104]. In light of these findings, the role of NK cells has yet to be precisely defined in murine RSV pathogenesis, in part because of the lack of a single distinct marker of NK cells. Despite this, NK cells are known to be recruited to lungs upon infection with RSV and there is evidence that they contribute to the clearance of RSV *in vivo*.

The role of chemokines and cytokines in NK activation is thoroughly reviewed in a number of publications [102, 105, 106]. More than one subset of NK cells in circulation are differentiable on the basis of the expression of various surface markers, and they are capable of responding to different chemokines on the basis of the expression of the appropriate chemokine receptor [107]. Several chemokines produced upon infection with RSV are reported to act as chemoattractants to NK cells. MIP-1α, MCP-1, IL-8, RANTES, and IP-10 have all been suggested to recruit NK cells either *in vitro* or *in vivo* [102, 105, 107]. The cytokines IFN-α/β, IL-12, IL-1, IL-15, and TNF-α are also capable of enhancing NK activation and cytotoxicity [105]. As mentioned above, these mediators are produced in response to RSV by the combined efforts of epithelial cells, macrophages, DCs, and neutrophils, among other infiltrating immune cells. Thus, although the role of NK cells in human RSV infection is not entirely clear at this point in time, they are likely to play a role in the antiviral response to this virus, given that they are capable of responding to several key inflammatory mediators involved in RSV pathogenesis.

The role of NKT cells in RSV pathogenesis, like that of NK cells, has not yet been fully elucidated. Indeed, as a relatively recent discovery in the field of immunology, their role in helping to bridge the innate and adaptive arms of the immune system is only beginning to be explored. NKT cells, as their name suggests, are a group of cells that display markers and

properties of both NK cells and T cells. They are described as innate-like α/β T cells, because they express T cell receptors (TCRs) that combine an invariant α chain with either a variant or invariant β chain, depending on the animal and strain. In addition to TCR they also express NK markers, which likewise depend upon the species and strain of animal in question. NKT cells are capable of recognizing pathogens and infected cells using their TCR, which triggers the production of large quantities of cytokines and killing of the target cell.

In RSV pathogenesis in humans, little is known about NKT cell activation *in vivo*. Interestingly, in a study examining the histopathology induced by RSV infection in untreated infants CD3 T cells were shown to outnumber the combined CD4 and CD8 T cells in the lungs, and the authors suggested that a CD3 double negative population was present in the lungs of the index case [56]. Although the group examined three archived cases of fatal untreated RSV infections that occurred between 1930 and 1950, the index case was an infant that had been diagnosed with RSV in 1999 and then died as a result of an accident the following day. As such, the index case was not a fatal infection, so the finding that there was a substantial contribution from a population of CD3 double negative T cells may indicate the presence of NKT cells in the lungs of infected infants. Additionally, the index case had high numbers of CD8 T cells in the lungs, along with neutrophils and macrophages. Since NKT cells are thought to be able to promote CD8 T cell responses *in vivo*, the results of this study are quite intriguing. However, another potential population of CD3 double negative cells that could be indicated by this case is the gamma/delta T cells, which can also be CD4 and/or CD8 negative.

The role of NKT cells in RSV infection has only been studied directly in mice. The authors examined CD1d-deficient mice bred onto both the Balb/c and C57Bl/6 genetic backgrounds. The results of this study showed that CD1d-deficiency had slightly different effects

in Balb/c mice compared to C57Bl/6 mice. NKT cell numbers were low in both wild-type strains during the course of infection. Despite this, in both strains NKT cell-deficiency led to a decrease in the number of CD8 T cells in the lungs on day 7, which in the Balb/c strain continued to day 10 p.i. [108]. In addition, the authors found that the C57Bl/6 mice with CD1d-deficiency had enhanced NK cell responses on day 4 p.i. [108]. In agreement with this, gene-deleted C57Bl/6 mice showed no difference in IFN-γ production between days 4 and 10, while NKT-deficient Balb/c mice had significantly reduced levels of IFN-γ on days 7 and 10 p.i.. Since Balb/c mice are more susceptible to RSV infection, the deletion mutants in Balb/c mice were still more susceptible, in terms of viral replication, IFN-γ production, and weight loss than either wild-type or mutant C57Bl/6 mice [108]. Intriguingly, however, Balb/c mice with NKT cell deficiency cleared the virus as efficiently as wild-type mice, while gene-deleted C57Bl/6 mice showed impaired viral clearance [108]. In agreement with this finding, gene-deleted Balb/c mice displayed reduced weight loss compared to wild-type mice, while C57Bl/6 mice with the same deletion experienced weight loss that was not seen in wild-type mice [108].

Since CD8 T cell responses are known to be critical for viral clearance, and are also associated with pathology and weight loss, this study points to some interesting differences between the response of Balb/c and C57Bl/6 mice to RSV. As Balb/c mice are inherently more susceptible to RSV infection, the decrease in the CD8 response in Balb/c mice appeared to be enough to protect mice from the pathological effects of the CTL response, while still maintaining control over replication. In contrast, because C57Bl/6 mice are capable of controlling viral replication without intervention, the weakened CD8 T cell response led to reduced control of the virus, despite similar production of IFN-γ in the lungs and early compensation by NK cells. The

results of this study show that regardless of mouse strain NKT cells enhance the CD8 T cell response to RSV *in vivo*.

Since Johnson et al. found that double-negative T cells were present in the lungs of an RSV-infected infant, along with high numbers of CD8 T cells, these studies may indicate a role for NKT cells in human RSV infection and a similar enhancement of the CD8 response to that seen in mice [56]. However, the study in mice above showed no evidence of NKT cell infiltration upon infection with RSV, so whether they play a role, either locally or peripherally, during infection in humans remains to be seen.

1.4.1.6 Dendritic Cells

Dendritic cells (DCs) play a critical role in linking the innate and adaptive arms of the immune system. While myeloid DCs, often called "conventional" DCs (cDCs), are the major antigen-presenting cell (APC) in the body, the plasmacytoid DCs (pDCs) are important producers of IFN-α, especially during viral infection. The latter cell type was originally designated as a professional IFN-α producing cell, until they were later recognized as a DC subtype rather than as a class of cells unto themselves. Conventional DCs are critical for the development of the adaptive response by activating naive T cells and directing them toward a Th1 or Th2 phenotype based on the secretion of cytokines. Plasmacytoid DCs, on the other hand, are less capable of antigen presentation, but respond to viral infection with the production of large quantities of IFN-α, which promotes the antiviral response as well as the activation of macrophages, NK cells, mDCs, and other immune cells. The capacity of RSV to reinfect individuals throughout life, in addition to the immune-mediated nature of RSV infection, has led to much research in examining the role of DCs in the innate and adaptive responses to RSV.

In humans, much of the work on DC function has been focused on monocyte-derived DCs, since their precursors in the peripheral blood are easily accessible and the generation of immature DCs that display phenotypic properties of either myeloid or plasmacytoid DCs has been thoroughly characterized. A recent report on primary mDC and pDC populations isolated from the peripheral blood showed that they responded to RSV infection in a similar manner to monocyte-derived DCs, although the maturation markers CD40 and CD80 were not as strongly upregulated in primary DC cultures [109]. Coculture of infectious RSV with immature mDC and pDC showed that a small proportion of the cells become infected, with mDC populations being more susceptible (<10% of mDC compared to <2% of pDC) [109]. Both infected and uninfected DCs of either subtype underwent maturation in response to RSV, showing upregulation of the maturation markers CD86 and MCH class II [109, 110]. These molecules are critical for antigen presentation to T cells and provide costimulatory support to allow for the activation and proliferation of T cells into effector and memory phenotypes during the adaptive response. In primary DC populations isolated from the peripheral blood, there were slight differences in the expression of maturation markers in the small population of DCs that experienced productive infection with RSV compared to the DCs incubated with RSV that showed no signs of infection [109]. Specifically, infected pDCs displayed enhanced expression of maturation markers, while the relatively rare mDC population designated mDC2 showed a reduction in CD86 expression in infected cells compared to uninfected cells [109]. Since mDC2 cells are suggested to be present in the lungs in higher numbers compared to pDC or mDC1, this decrease in maturation marker in infected mDC2 cells could affect their capacity to activate local T cell responses in the lung.

The authors of this paper also found, surprisingly, that IL-12 was not secreted by any of the three primary DC subsets isolated from the blood upon exposure to RSV, despite reports that

DCs generated from peripheral or cord blood secrete IL-12 in response to RSV [109]. Upon stimulation with RSV, the DCs produced RANTES, IL-8, MIP-1α, MIP-1β, and IFN-α, but not IL-12, IFN-γ, TNF-α, or IL-10, in contrast to studies on monocyte-derived DC populations [109]. The study of primary cells rather than cells generated *ex vivo* is important to understand differences that stem from the differentiation process that occurs in the natural environment compared to that in a laboratory. In addition, the examination of DC maturation and their interaction with different cell populations *in vivo* is critical to understand the role they play in the process of RSV infection in humans. Thus, mouse models are invaluable for understanding the role of DCs in the immune response to RSV *in vivo*.

Upon infection with RSV, Balb/c mice show enhanced numbers of pDC in the lung as early as 24 h p.i., reaching a peak on day 3 p.i.. In the lymph nodes, pDC were elevated by day 2, and reached a peak on day 6 p.i. [111]. Another group examining pDC infiltration in the lungs of infected C57Bl/6 mice found that these cells first appeared on 48h p.i. and remained above mock-infected levels through to day 6 p.i., with a modest peak at 48 h [112]. Since pDCs are involved in the local response to RSV by producing cytokines, their presence in the lung early during the course of infection points to their role in supporting the development of NK and macrophage responses in lung. Their later migration to the lymph node, which was not examined in the C57Bl/6 model, would thereby allow them to further interact with cDCs and T cells in the lymph node, directing the nature of the adaptive response through cytokine secretion.

Interestingly, however, *ex vivo* infection of Balb/c pDC populations with RSV yielded no upregulation of IFN-α or, indeed any cytokine examined other than MIP-1α and MIP-1β [111]. Conversely, Smit et al. found that pDC populations from Balb/c mice displayed a strong production of IFN-α in response to RSV, although the two groups used different molecular

markers to sort their pDC populations, which could alter the phenotype of the resulting cell population [113]. In support of this, the latter group found a significant increase in IL-6, TNF-α, MCP-1, and IP-10 production by pDC in response to *ex vivo* RSV infection, which was not detected in the study by Guerrero-Plata et al. [111, 113]. Thus, the experimental design of studies on the role of these cells in infection has a drastic impact on the results, and comparison between different systems is difficult. However, the fact that pDC are seen to infiltrate the lungs of mice infected with RSV and subsequently move into the draining lymph nodes at the same time as the onset of the adaptive response strongly points to a role for them in directing both the innate and adaptive responses to RSV infection *in vivo*.

Indeed, by experimentally enhancing or deleting the function of pDC *in vivo*, the critical role of these cells in both innate and adaptive responses has been widely documented. Smit et al. used a combination of FLT3L, which stimulates both cDC and pDC expansion *in vivo*, with 120G8, which partially depletes pDC, to evaluate the role of these two DC populations during RSV infection. From this study, they found that concurrent enhancement of pDC and cDC populations with FLT3L treatment prior to RSV infection resulted in decreased Th2 cytokines and increased Th1 cytokines, both in the lungs following RSV infection and upon stimulation of T cells isolated from these animals with an anti-CD3 antibody [113]. When pDCs were selectively depleted by including 120G8 in the FLT3L treatment, the T-helper response was drastically skewed toward a Th2 bias, with similar levels of IFN-γ as the untreated RSV-infected mice and heightened IL-4, IL-5, and IL-13 production in the lungs and by stimulated T cells [113]. Thus, an increase in DC levels *in vivo* led to heightened IFN-γ production and decreased Th2 cytokine production in the lungs and by T cells, and these changes were dependent on pDCs. Furthermore, the total number of CD8 T cells, in addition to the number of RSV-specific CD8 T

cells and IFN-γ+ CD8 T cells, were enhanced in a pDC-dependent manner in the lungs of infected mice [113]. In summary, pDC promote the development of a Th1-biased response, in particular by enhancing the CD8 T cell response. In contrast to the enhanced IFN-γ induced by NK or NKT cell responses, the RSV-specific activation of CD8 T cells was enhanced, suggesting that pDC could contribute directly or indirectly through cDCs to promote Th1 responses in RSV infection.

The results of the above study also highlight the role of cDC in modulating the T helper response, as evidenced by the enhanced Th2-biased responses to RSV in mice with elevated numbers of cDCs and normal numbers of pDCs [113]. Their role in directing the T helper bias and innate responses in mice has been further examined by a number of groups. Upon infection with RSV, cDCs were rapidly recruited to the lymph nodes by day 2 p.i. and their numbers increased through to day 7, while in the lungs, they remained at background levels until day 5 p.i., and reached a peak on day 8 [111]. As the primary antigen presenting cell that directs the adaptive response to RSV, the early accumulation of cDCs in the lymph nodes is necessary for the activation of naive T cells in the peripheral lymphoid tissue. Their later presence in the lungs of infected mice suggests that they can enhance the local T cell mediated response which begins around one week p.i..

Infection of cDCs *in vitro* induced maturation marker expression and the secretion of IL-10, IL-12, IL-6, and IP-10 [113]. These cytokines are important for directing the adaptive response to RSV. For example, during priming of naive T helper cells, IL-12 secretion by APCs promotes the differentiation of these cells into Th1 cells that preferentially secrete IFN-γ, as reviewed in [114]. IL-10, on the other hand suppresses IFN-γ production and thus promotes Th2 biased responses [115]. The combination of the two cytokines produced by the RSV-infected

cDCs agrees with the notion that T helper responses to RSV infection are mixed Th1 and Th2, with a greater tendency toward Th1 responses.

1.4.2 Cells of the Adaptive Immune System

The combined effects of cytokines produced by epithelial cells, macrophages, NK cells, NKT cells, and DCs lead to the development of the long-term adaptive response, which during RSV infection is both critical for the clearance of the virus and contributes to pathology. The cell-mediated response, in particular, may lead to enhanced pathology in the murine model, and there is some evidence for this in humans as well. The cell-mediated response plays a further role in directing the humoral response to RSV, which is critical in developing protective neutralizing antibody titres. Together, the adaptive responses are meant to protect animals from reinfection, but in RSV pathogenesis the memory responses to the virus appear to be only partially protective, offering a reduction in the severity of illness without protecting from reinfection.

1.4.2.1 T Cells and the Cell-mediated Response to RSV

There are several schools of thought on what drives the pathogenesis of pneumoviruses. The immune-mediated nature of RSV pathology was highlighted by the failed vaccine that led to severe, non-protective, Th2-biased immunopathology upon RSV infection [116]. This, in combination with the striking association between severe bouts of RSV in infancy and the development of Th2-mediated conditions like asthma and allergies in childhood, led many researchers to focus on the T-helper bias of the immune response to RSV in severe and mild infections [117-122]. However, the debate over whether severe RSV is associated with predominantly Th1 or Th2 biased responses still continues. Others have moved beyond T-helper bias and are more concerned with the innate responses produced in the lungs in the form of pro-

inflammatory chemokines, which are responsible for the influx of immune cells involved in pathogenesis [62, 121]. Regulatory T cells and gamma/delta T cells, though not considered here, are also possible contributors to RSV pathogenesis *in vivo*. Several papers and review articles are available on the subject, although the data is much more limited than that on typical CD4 and CD8 T cells [123-127].

Examining the T-helper bias of the immune response to RSV in humans has yielded a great deal of conflicting data, the interpretation of which depends on the method used to examine the response, as well as the cell types sampled and their location. Although some studies have shown the Th-2 biased cytokine IL-4 to be upregulated in nasopharygeal secretions of RSV-infected children [64, 95], there is also a great deal of evidence that the levels of IFN-γ are upregulated over uninfected children to a higher degree than IL-4, indicating the local response is primarily Th1-biased [128, 129]. However, another study on the IFN-γ/IL-4 ratio in bronchoalveolar lavage (BAL) samples from infants with severe bronchiolitis showed that half the group had a Th-2 biased response, secreting only IL-4, a quarter had only IFN-γ, and a quarter of them had low levels of both cytokines [130]. Studies on the activation level and T-helper bias of serum or T cells isolated from the blood of children with and without RSV are equally discordant [120-122, 131].

When examining the difference in T-helper balance between severe and mild infections, the controversy continues. Some groups have split their patients into cohorts based on the involvement of the upper or lower respiratory tract, and others make a further distinction between severe and mild forms of LRTI. These studies are often limited by patient numbers and therefore lack proper age- and health-matched controls. Despite this there is evidence that severe and fatal LRTI in infants, especially those under 3 months of age, may be attributed to

exceptionally low levels of Th1 cytokines and activated cytotoxic T lymphocytes (CTL) [62, 103, 121, 124]. Milder forms of RSV infection, on the other hand, tend to be characterized by a Th1-biased response with low levels of IL-4 and moderate IFN-γ production both in the lungs and in activated peripheral blood lymphocytes [120, 122, 129].

Since cytokines alone are not indicative of T-helper bias, other researchers use alternative methods such as measuring the activation of the cell-mediated cytotoxic response through the detection of effector molecules and activation markers. For example, granzyme A and B are enzymes released from the granules of cytotoxic lymphocytes like NK cells and CTLs. These molecules were detected in higher quantities in the BAL of children hospitalized for severe RSV, suggesting that strong cell-mediated responses were associated with severe illness [132]. The authors found that primarily CD8 T cells expressed high levels of granzyme and, to a lesser degree NK cells [132]. In agreement with this, another group found high numbers of activated CD8 T cells in the lungs and blood stream of infants with severe RSV that proliferated upon incubation with RSV antigen [133]. Thus, there is a strong indication that cytotoxic T cells are active in severe RSV, which is indicative of a Th1 response.

Overall, mixed T helper responses to RSV are a prominent feature of RSV infection in infants. The same is seen in mice infected with RSV. Smit et al. found that T cells from RSV-infected Balb/c mice produced IL-4, IL-5, IL-13, and IFN-γ in response to TCR stimulation with an anti CD3 antibody [113]. Likewise these cytokines were all upregulated in the lungs of RSV-infected Balb/c mice [113]. IFN-γ is readily produced in the lungs beginning as early as day 3 p.i. and the infiltration of RSV-specific CD4 and CD8 T cells begins around day 6 p.i.. As described in the preceding sections, the early immune response is critical for the development of appropriate CD4 and CD8 T cell responses in order to clear the virus.

During the infection, virus specific effector T cells proliferate to high numbers, and once the virus is cleared, the majority of these effector CD4 and CD8 T cells die off as a result of the lack of TCR stimulation. A small proportion of them remain as memory T cells that can respond quickly to a secondary infection with the virus. Circulating T cells regularly pass through the spleen and lymph nodes, guided by the homing receptor CCR7. In these lymphoid tissues, T cells filter through dense networks of myeloid DCs that present antigen to T cells. The homing of these two cell types to the lymphoid tissue increases the likelihood of the relatively rare populations of antigen-specific cells coming into contact with APCs that bear their cognate antigen. Exposure to the antigen once T cell memory has been established results in rapid proliferation following antigen presentation by activated DCs. Several reviews are available on these processes. In addition to circulating central memory cells, there is also a population of effector memory cells that reside in the tissue and can act quickly upon infection with the pathogen.

Since memory T cell responses to RSV infection can only be measured in the peripheral blood in humans, there is little data on the proliferative capacity of RSV-specific pulmonary T cells. A study of the mRNA expression of cytokines in PBMC cultured with RSV antigen showed that these cells produced predominantly Th1 biased cytokines both in infants and in adults [134] . Both IL-10- and IFN-γ-secreting CD4 T cells have been detected in the PBMC of adults and elderly subjects in response to RSV antigen stimulation. [135]. Although there was a trend towards lower RSV-specific IL-10 production in older subjects, the difference was not significant. However, when the ratio of IL-10- and IFN-γ-secreting cells was calculated for each patient, the elderly cohort had a significantly lower RSV-specific IL-10/IFN-γ ratio [135].

Interestingly, in a rare study with lung tissue isolated from patients who underwent a lobectomy for carcinoma screening, the authors found that the lung contained high numbers of RSV-specific CD8 T cells with a memory phenotype based on cell surface markers that responded to HLA-restricted peptides already identified [136]. Compared to the phenotype of T cells isolated from the blood, the lung RSV-specific CD8 T cells had reduced expression of lymph node-homing receptor CCR7 and showed a more differentiated phenotype, based on the expression of activation markers [136]. In another study, the same group found that normal elderly individuals had reduced numbers of RSV-specific memory CD8 T cells in the blood compared to healthy young adults [137].

The non-protective nature of the cell-mediated immune response, measured by the IFN-γ production and proliferation of RSV-stimulated whole blood cultures, is highlighted by a study on the cell-mediated response to RSV during the peak of disease severity, four weeks after infection, and one year after infection. The authors found that the highest level of RSV-specific cell-mediated response occurred 4 weeks after infection, when 80% of infants demonstrated cell-mediated immunity, while by one year after infection only 38% of infants had any cell-mediated response [138]. There was also no difference between infants who had experienced reinfection during that time and those who had not, suggesting that secondary RSV infection did not enhance the RSV-specific cell-mediated immune response [138].

In mice, the pulmonary and peripheral memory T cell response following RSV infection has been well documented. A CD8 T cell epitope on the M2 protein has been shown to be important in the memory response in Balb/c mice. When the number of M2-specific CD8 T cells is compared to the number of IFN-γ secreting M2-specific cells, there is a considerable discrepancy between these numbers, indicative of poor effector function of this population of

CD8 T cells [139, 140]. IFN-γ production could be induced in a much higher number of M2-specific cells by including IL-2 in the culture medium during peptide stimulation [139, 140].

CD8 T cell responses are also directed toward the F protein in Balb/c mice. The CTL response directed toward the F protein epitope is not as strong as that directed toward the M2 epitope, as evidenced by the ~10-fold lower number of F-specific CD8 T cells infiltrating the lungs during primary infection compared to those specific for the M2 epitope [141]. The two populations of CD8 T cells infiltrated the lungs along the same time course during primary infection, peaking in numbers on days 8-10 p.i. [141]. A similar defect in the activation and cytokine secretion from tetramer-stained F-specific CD8 T cells was seen to that reported for M2-specific T cell, suggesting that RSV infection can inhibit the activation of RSV-specific T cells [141].

On the other hand, Ostler et al. found that Balb/c mice have effector CD8 T cells in the lung up to day 20 that were capable of lysing infected target cells without prior antigen stimulation [142]. The mice were also protected from infection with a recombinant virus that expressed RSV proteins but did not incorporate them into the viral membrane [142]. Thus, the protection could not have been mediated by antibodies, but had to be due to cell-mediated responses to the RSV antigens displayed by MHC molecules [142]. Further analysis by this group showed that RSV-specific CD8 T cells displaying a memory phenotype remained in the lung up to day 50, but they were no longer capable of lysing target cells, suggesting that these cells were in a resting state [143].

The majority of the studies on CD4 memory T cells involve immunization with the G protein of RSV, which primes Balb/c mice toward a Th2 biased eosinophilic lung disease. While

the G protein is capable of priming mice toward both Th1 and Th2 responses, the lack of CD8 T cells induced due to the absence of the M2 epitope causes the Th2 biased response to overtake the Th1 response during reinfection, leading to eosinophilia [144, 145]. The Th2-biased response in G-primed Balb/c mice was dependent on their genetic background rather than the MHC class haplotype, since Balb/b mice expressing the H2-D^b haplotype developed the same mixed Th1/Th2 CD4 response and similar levels of eosinophilia. In C57Bl/6 mice, which also express H2-D^b, eosinophilia did not develop, but could be induced by depletion of CD8 T cells during reinfection [144, 146]. The suppression of the Th1 response upon priming with G protein was due to enhanced IL-10 production in the Balb background [146]. The T cell response to RSV is critical for viral clearance, but also plays a role in immunopathology. The memory response is important for protection against further challenges, and the susceptibility of humans to repeated RSV infections suggests an impairment of the cell-mediated immune response. In addition, T helper cells play a role in the development of humoral immunity, providing cognate help to B cells in the spleen and in tissues along with directing isotype switching of the antibody repertoire produced by B cells during infection and memory development.

1.4.2.2 B Cells and the Humoral Response to RSV

The interplay of the T helper bias and the humoral response has been well characterized *in vivo*. B cells that encounter a pathogen that is specific for its BCR, which is a bound form of the IgM antibody, endocytose the pathogen and are thereby stimulated to mature, usually due to the recognition of PAMPs following endocytosis. They upregulate surface MHC-II molecules and home to the lymphoid tissue where they interact with DCs and T cells. In the spleen and lymph nodes, antigen-primed B cells differentiate into activated B cells and subsequently into antibody-secreting plasma cells or memory cells with the support of DCs and T helper cells. DCs

can present soluble antigens to B cells that are otherwise not available to them and antigen-pulsed DCs can stimulate isotype switching and strong B cell responses *in vitro*. T helper cells are required to provide costimulatory signals and cytokines while the two cells are joined through the interaction of the T cell receptor and its matching MHC-II restricted epitope expressed on the surface of the B cell. DC and T helper-derived cytokines drive isotype switching during the differentiation of B cells through their association in the peripheral lymphoid tissues. The Th1 cytokine IFN-γ helps induce IgG_{2a} production, IL-4 promotes IgG_1 and IgE, and IL-5 is important in the induction of IgA [97, 147].

The role of the humoral response to RSV has been examined in humans with regards to the poor capacity of RSV-specific antibodies to protect individuals from reinfection. Neutralizing antibody can be protective, as shown by the successful use of prophylactic immunoglobin against RSV in high risk infants [148, 149]. In infants, neutralizing antibodies against RSV recognize the two major surface proteins that are displayed to the immune system, the F and G proteins [150, 151]. A number of studies have suggested a threshold neutralizing antibody level protects against severe disease, either through maternal antibodies or following infection [150, 152-154]. On the other hand, in these studies a relatively low proportion of individuals displayed neutralizing levels sufficient to prevent reinfection, and even when neutralizing antibody was detected at high levels in healthy adults, these individuals were still relatively susceptible to RSV reinfection [12, 152]. Therefore neutralizing antibody is more effective in preventing severe illness than preventing reinfection.

Age appears to play a role in the development of the antibody response, as significantly fewer infants under 8 months of age mounted G- or F-specific IgA and IgG responses in serum and nasal washes compared to infants over 9 months of age [151]. In addition, the younger

cohort also had lower levels of neutralizing antibody in the serum and nasal washes, further supporting the impairment of the humoral response elicited in neonates [151]. The kinetics of antibody production for the different classes of immunoglobin in response to RSV was examined in hospitalized infants by Welliver et al. in 1980. They found that RSV-specific IgA and IgG in the serum were produced starting on day 10, peaked 3-4 weeks after infection, and became very low to undetectable by one year p.i. for IgG and IgA, respectively [155]. In this study, too, the authors noted that infants under 6 months of age displayed impaired antibody responses, supporting the findings reported above [155].

RSV-specific IgE responses have been reported in infants with wheeze, and this response is in some cases associated with Th2-mediated pathology including eosinophils [156, 157]. IgE and IgA were reported to be predominantly mucosal, while IgG was predominantly found in the serum of RSV-infected infants [158].

1.5 Innate and Adaptive Immunity in the PVM Model of RSV Pathogenesis

The use of PVM as a model of RSV pathogenesis is relatively recent compared to studies of RSV infection in mice. In addition, far fewer research laboratories are currently concerned with this pathogen. In the majority of studies, the mouse-adapted strain PVM J3666 is used, although PVM 15 is also virulent in mice. The infection is far more severe than RSV in mice, although the cell types recruited in response to PVM are similar, and may play a similar role in the development of the immune response. There is still much research to be done to determine how PVM causes disease in mice, and whether this model is appropriate for examining host susceptibility to RSV infection in humans.

In terms of inflammatory mediators involved in PVM pathogenesis, similar to RSV infection, the chemokines MIP-1α, MCP-1, and MIP-2 are a prominent response during PVM infection of mice [35]. In addition, IFN-γ is also associated with disease severity, and in combination with MIP-1α controls the infiltration of neutrophils, lymphocytes, and eosinophils [87, 159-161]. IFN-α was produced in the lungs of PVM infected mice on day 6 p.i., and the deletion of its receptor caused an overall reduction in leukocyte infiltration and a shift toward greater Th2 bias in the inflammatory mediators and cell types involved in the infection [162].

Although neutrophils remain the dominant granulocyte infiltrating upon infection with PVM, eosinophilia is also typical of PVM J3666 infection in C57Bl/6 and Balb/c strains [159]. Interestingly, IL-5 is not required for this response [159, 163]. The eosinophil-related chemokine eotaxin (CCL11), along with MIP-1α, was still produced in IL-5 deletion mutant C57Bl/6 mice, and eosinophils migrated to the lungs unhindered in these mice [163]. The role of eosinophils in PVM pathogenesis has been further elucidated by infecting them with PVM *in vitro*. Similar to RSV, upon infection with PVM, bone-marrow derived eosinophils produced the cytokine IL-6, and, additionally, the chemokines MIP-1α, MCP-1, and IP-10 [51]. Deletion of the TLR signalling intermediate MyD88 caused enhanced replication of PVM in eosinophils and diminished production of inflammatory mediators, which could be returned to normal levels by the addition of exogenous IL-6 [51]. Infection of a macrophage cell line also resulted in the production of MIP-1α, MIP-2, and TNF-α, suggesting that these cells are important for the production of these inflammatory mediators *in vivo* [164].

In the Balb/c strain, infection with a low dose of PVM J3666 induced the infiltration of IFN-γ secreting NK cells, CD8 T cells, and CD4 T cells by day 6 p.i. [161]. T cells were the most numerous of the IFN-γ secreting cells in the lungs of these mice [161]. Similarly, a

sublethal dose of PVM 15 in C57Bl/6 mice induced strong CD8 T cell responses that were associated with weight loss [165]. Both CD4 and CD8 T cells contributed to viral clearance and weight loss during PVM pathogenesis, similar to the findings for RSV in mice [165, 166].

An analysis of the reactivity of the CD8 T cells that infiltrated the lung showed that they were specific for epitopes on the F, M, and P proteins of PVM [167]. Similar to reports of CD8 T cells specific for the M2 protein on RSV, PVM-infected Balb/c mice showed a deficiency in IFN-γ production by CD8 T cells specific for the P protein [167]. This inactivation was even more dramatic than that seen in RSV infection, with only 10% of the cells specific for the P-derived peptide showing an activated phenotype, compared to 60% activated for M2-specific T cells from mice infected with RSV [167]. Also, CD4 T cell responses were generated against epitopes on the PVM G protein, with mixed Th1/Th2 cytokines produced upon stimulation of splenocytes with G-protein peptides [168]. Partial protection against lethal challenge could be achieved by immunizing with PVM peptides to stimulate the CD8 and CD4 T cell responses, and combination of the two peptides was required to achieve greater than 50% protection [168].

The humoral response to PVM infection and its role in protection have not yet been established. In addition, one of the problems with the current knowledge of PVM pathogenesis is the use of both Balb/c and C57Bl/6 mice interchangeably, without any direct comparison between them. Since these two strains have very different responses to pathogens and antigenic stimulation, as discussed below, it will be important to compare these strains in the context of PVM infection.

1.6 Comparison of the Immune Response in Balb/c and C57Bl/6 Mouse Strains

Two of the most commonly used mouse strains in laboratory research are the Balb/c and C57Bl/6 strains. They are often compared because of their differential responses to numerous pathogens, in particular because they are thought to have predominantly Th2 and Th1 biased responses, respectively. The best example of this difference has been established in *Leishmania* infection, where a lack of early IL-12 and strong IL-4 production in Balb/c mice renders them more susceptible to Leishmaniasis due to overwhelming Th2-biased responses, while C57Bl/6 mice clear the pathogen through IL-12 and IFN-γ dependent mechanisms [169-171]. Dendritic cells and macrophages are the predominant source of IL-12 in these mice. The basis of this difference has been examined in both cell types, with similar results.

Peritoneal macrophages isolated from Balb/c mice have been found to produce less IFN-β in response to IL-12 stimulation, due to lower upregulation of the IL-12 receptor following IFN-β treatment [172]. In addition, levels of intracellular STAT4, a critical molecule involved in the type I IFN response, were reduced in Balb/c macrophages [172]. Similarly, DCs isolated from Balb/c mice have lower levels of STAT4 and a lower capacity to produce IL-12 in response to stimulation, which plays a role in the susceptibility of Balb/c mice to infection with the intracellular bacteria, Listeria [173].

The basis for the enhanced susceptibility of Balb/c mice to RSV infection has not been determined. In G-protein sensitized mice, the two strains clearly have a difference in their genetic background that enhances the capacity of Balb/c mice to respond in a Th2 biased manner. As discussed above, although Th1 and Th2 biased T helper responses to the G protein are observed *in vivo*, CD8 T cell responses are completely absent and eosinophilia predominates

the response to RSV infection in G-primed Balb/c mice [144, 145]. This priming to eosinophilic disease occurs in the closely related Balb/b strain that has the same genetic background as Balb/c, but expresses the same MHC haplotypes as C57Bl/6 mice [144]. Therefore the resistance to eosinophilia in C57Bl/6 mice is not merely related to the difference in MHC haplotype, but to unrelated differences in their genetic background. Depletion of CD8 responses in C57Bl/6 mice caused this strain to become susceptible to a degree of eosinophilia similar to that seen in Balb/c mice, further suggesting that this strain is inherently capable of promoting Th1 biased responses [146].

On the other hand, the Balb/c mice are still capable of producing excessive IFN-γ responses compared to C57Bl/6. Indeed, this is a prominent feature of their response to RSV infection and is associated with T cell-mediated weight loss. An indirect comparison of PVM J3666 in Balb/c and C57Bl/6 mice showed that the Balb/c strain also appears to be more susceptible to PVM infection, with enhanced IFN-γ production in the susceptible strain. In Balb/c mice infected with the intracellular bacteria *Burkholderia pseudomallei*, detrimental immunopathology based on the proinflammatory mediators IFN-γ and TNF-α, which are also associated with the Th1 response, is associated with their enhanced susceptibility compared to C57Bl/6 mice [174]. Similar to the case for RSV infection, the two strains have mixed T helper responses to the bacteria, but the Balb/c strain produces higher levels of the cytokines IFN-γ TNF-α, IL-1, and IL-6 that contribute to their susceptibility to severe illness [174]. Thus, rather than the enhanced susceptibility of Balb/c mice to numerous infections being due to an inherent Th2 biased response, they may have depressed regulatory capacity. Evidence for this stems from the loss of control that is typically seen in infectious disease models with Balb/c mice, whereby

the magnitude of the cytokine response, be it CD8- or CD4-T cell-mediated, and Th1 or Th2 biased, tends to be stronger than the response of C57Bl/6 mice.

Since these two strains of mice are commonly used for immunological research, a better understanding of the host genetic determinants for severe illness in the pneumovirus model will provide a great deal of pertinent information regarding the use of these strains as models of RSV and the genetic factors that differentiate their responses to pathogens.

2.0 Hypothesis and Objectives

The purpose of this study is to examine the immune response to PVM infection in Balb/c and C57Bl/6 mice, and to understand the difference in the relative susceptibility of these strains to pneumovirus infection, and their suitability as a model of RSV pathogenesis in infants.

The first objective was to examine the innate response to acute infection with PVM in Balb/c and C57Bl/6 mice. We examined the role of proinflammatory mediators and T-helper bias in the lung during primary infection with PVM, and the resulting infiltration of immune cells into the lung. We hypothesized that the more susceptible Balb/c strain would produce higher levels of proinflammatory mediators and Th2-biased cytokines, and would therefore experience enhanced cellular infiltration and eosinophilic lung disease.

Our second objective was to measure the innate and adaptive responses to a sublethal dose of PVM in Balb/c and C57Bl/6 mice. We expected that Balb/c mice would experience stronger Th2-biased cell-mediated responses to PVM and that the humoral response would reflect this bias in the antibody isotypes secreted *in vivo*.

3.0 Materials and Methods

3.1 Cell Culture and Virus Propagation

Original stocks of PVM strain 15 and Baby Hamster Kidney (BHK)-21 cells were purchased from American Type Culture Collection. BHK cells were propagated in minimum essential medium (MEM) (Sigma-Aldrich) supplemented with 0.1 mM non-essential amino acids (Invitrogen), 1 mM sodium pyruvate (Invitrogen), 50 μg/ ml gentamicin (Invitrogen), and 5% fetal bovine serum (FBS; PAA Laboratories Inc.). BHK-21 cells cultured in T150 flasks (BD Biosciences) at 37°C in 5% CO_2 were split at a ratio of 1:6 two to three times a week.

To propagate PVM 15, BHK cells were grown to ~80% confluency in T150 flasks (BD Biosciences) the medium was removed and the cells were washed with Dulbecco's Modified Eagle Medium (Sigma) supplemented with 0.1 mM non-essential amino acids (Invitrogen), 10 mM HEPES (Invitrogen), 50 μg/ ml gentamicin (Invitrogen) and 2% FBS (PAA Laboratories Inc.) (PVM medium). After washing cells gently, the medium was replaced with 14.5 ml of PVM medium and 1.5 ml of PVM (~10^6 pfu, equivalent to an MOI of 0.01-0.1) per flask, and the cells were incubated at 37°C, 5% CO_2. After 72 hr, the virus was harvested by scraping cells into the supernatant using a 15 mm cell scraper (Corning Inc.), and the cell debris disrupted as much as possible by pipetting up and down. This mixture was used as viral stock to infect additional flasks of BHK cells or aliquotted and stored at -80°C. For assays requiring PVM-infected and mock-infected cell lysates, an equal number of flasks were inoculated with 16 ml of PVM medium alone and treated as described above.

3.2 Challenge of Mice with PVM

Five to six week-old specific pathogen-free mice were purchased from Charles River Laboratories, housed in groups of 4-6 animals, and allowed up to one week to acclimatize. Under light isofluorane anaesthesia, the mice were inoculated intranasally with 50 μl of PVM 15 diluted in serum-free PVM medium or with medium alone. Prior to dilution, the viral stock was thawed on ice and sonicated five times for 30 sec to release cell-associated particles using a cup sonicator, with ice in the sonication chamber at all times. Mice were individually weighed and monitored daily for signs of clinical illness according to a modified version of the scoring system used by Morton and Griffiths [175]. Animals that scored a 2 or higher based on clinical signs of illness, those that scored a 3 for weight loss (weighing <80% of its starting weight), and those scheduled for sample collection were euthanized by an overdose of isofluorane, bled out by cardiac puncture, and sampled as described below. All experiments were performed within the guidelines of the Canadian Council for Animal Care.

3.3 Lung Samples

3.3.1 Lung Homogenates

The single-lobed lung was homogenized in medium for isolation of virus and to measure cytokine and chemokine levels in the lungs. After opening the chest cavity, the single-lobed lung was clamped from the multi-lobed lung at the bifurcation and removed sterilely. The lung was placed into a 2 ml screwcap tube (VWR International), filled up to the 1 ml mark with 2.4 mm zirconia beads (Biospec Products, Inc.) and 1 ml of serum-free PVM medium supplemented with 1x antibiotic/antimycotic (Invitrogen). After the lung was placed in the tube, an additional volume of 500 μl medium was added to displace air bubbles, and the lung homogenized for 10

sec at 4800 rpm using a Mini-beadbeater (Biospec Products, Inc.). Immediately following homogenization, the tube was centrifuged at 4°C for 1 min at 10,000xg, and the supernatant was aliquotted into two 500 µl portions. One aliquot without protease inhibitors was used to measure PVM titres, and one aliquot containing a protease inhibitor (PI) cocktail was used for cytokine and chemokine analysis. The PI contained10 µg/ ml aprotinin (Sigma-Aldrich), 10 µg/ ml leupeptin (Sigma-Aldrich), 50 µM EDTA, and 1 mM PMSF (Sigma-Aldrich). No protease inhibitors were added to the lung homogenates in the long-term trials because they appeared unnecessary for cytokine and chemokine detection. The two aliquots, along with the original bead-filled tube, were flash frozen in liquid nitrogen immediately, within 5 min of collecting the sample.

3.3.2 Histology

On day 6 p.i. of the short-term trials, the multi-lobed right lung was sent for histological examination. After removal of the single-lobed lung, as described above, the multi-lobed lung was perfused with 1 ml of 10% buffered formalin (VWR) through the trachea and placed in a cassette, which was then immersed in formalin. The perfused lungs were sent to Prairie Diagnostic Services, where they were embedded in paraffin wax and cut into two sections that were stained with hematoxylin and eosin. The H&E sections were sent to a pathologist and scored in a blinded manner. Scores were given based on the presence and severity of, as well as the dissemination of lesions characterized by cellular infiltrates and edema in the tissue surrounding the bronchioles and blood vessels visible in lung sections. A score of 0 denotes a normal lung, 1 indicates signs of perivascular edema and mild perivasculitis, limited to small foci that were not widespread, while a score of 2 denotes moderate levels of perivasculitis, vasculitis, and multifocal perivascular edema. Finally, a score of 3 represents animals with extensive,

severe, multifocal perivasculitis, vasculitis, and vascular edema, and/or necrotic and fibrinous areas. Examples of animals with representative scores are shown in Figure 4.3**.**

3.3.3 Bronchoalveolar Lavage (BAL)

The multi-lobed lung was washed with 500 µl of BAL solution, composed of phosphate buffered saline pH 7.2 (Invitrogen) supplemented with 2% FBS (PAA Laboratories Inc.) and 50 µM EDTA. The lung washes from each group of four mice were pooled and stored on ice until they could be processed further. To analyse the cellular infiltrates in the lung, the cells were counted with a Coulter counter (BeckmanCoulter) and the sample was centrifuged at 311 *xg* for 10 min. After centrifugation, the supernatant was collected and stored at -80°C, while the remaining cell pellet was resuspended at $2.5x10^5$ cells/ ml in fresh BAL solution. Two slides were prepared using a Cytospin 4 (Thermo Shandon), by spinning 200 µl and 400 µl onto a slide (the equivalent of $5x10^4$ and $1x10^5$ cells) at 500 rpm for 5 min. The slides were stained with a Giemsa-Wright stain (Bayer HealthCare) using an automated slide stainer, and differential analysis of the cell populations was performed by counting at least 200 cells.

3.3.4 Trizol® Homogenates

In the short-term trials, on days 1-5 p.i., the multilobed lung was collected for analysis of mRNA expression and homogenized in Trizol® reagent (Invitrogen). A 2 ml screw-cap tube filled with 2.4 mm zirconia beads and 1 ml of Trizol® reagent (Invitrogen) was used to collect the washed lung, followed by homogenization as described for the medium homogenates. After centrifugation, the tube was immediately flash-frozen in liquid nitrogen, and transferred to -80°C until processed for RNA isolation.

3.3.5 Lung Fragment Culture

In the long-term trials, the multilobed lung was collected for lung fragment culture (LFC) following the lavage in order to assess antibody levels in the lungs. The lung was placed into a tube containing 5 ml of LFC medium, which is composed of RPMI 1640 medium (Invitrogen) supplemented with 0.1 mM non-essential amino acids (Invitrogen), 10 mM HEPES buffer (Invitrogen), 1 mM sodium pyruvate (Invitrogen), 2 mM L-glutamine (Invitrogen), 1x antibiotic/antimycotic (Invitrogen), 50 μg/ml gentamicin (Invitrogen), and 10% FBS (PAA Laboratories Inc.). After collection, the lung was kept on ice until it could be further processed. It was cut into four roughly equal-sized pieces and placed into four wells of a 48-well plate (Corning Inc.) and then minced into pieces ~1 mm in diameter using scissors. Each well contained 500 μl of LFC medium plated ahead of time and allowed to warm to 37°C in an incubator. The lung fragments were cultured for 5 days at 37°C, at which point the culture medium was collected into a 15 ml polypropylene tube (BD Biosciences) and centrifuged at 4°C and 311 *xg*, for 10 min. The supernatant was transferred to two sterile 2 ml screw-cap tubes (VWR) and stored at -80°C for analysis of lung antibody levels.

3.4 Splenocyte Isolation

In the long-term trials, splenocytes were isolated on days 14, 28, and 42 p.i. according to a previously described protocol [176]. Mice were euthanized and spleens were collected sterilely into tubes containing wash medium, which consists of MEM (Sigma) supplemented with 50 μg/ml gentamicin (Invitrogen) and 10 mM HEPES buffer (Invitrogen), and held on ice for further processing. The spleens were trimmed of fat and cut into small pieces over a 100 μm cell strainer (BD Biosciences). The cells were gently pressed through the strainer using a glass plunger (Poppers & Sons, Inc.) and rinsed with wash medium into a sterile petri dish (VWR).

The cells were passed through the strainer 3-4 times to remove clumps and then centrifuged at 4°C and 1200 rpm, for 10 min. The cell pellet was resuspended in 1 ml of room temperature (RT) ammonium chloride lysis buffer to remove red blood cells (RBC). The lysis buffer consists of 0.14 M ammonium chloride in 17 mM Tris, pH 7.2, which is inactivated after 30 sec by the addition of 10 ml wash medium. Following RBC lysis, the splenocytes were washed twice with 10 ml wash medium, and resuspended in ELISPOT medium, which is composed of RPMI 1640 (Invitrogen) supplemented with 0.1 mM non-essential amino acids (Invitrogen), 10mM HEPES buffer (Invitrogen), 1 mM sodium pyruvate (Invitrogen), 2 mM L-glutamine (Invitrogen), 50 μg/ml gentamicin (Invitrogen), 50 μM 2-mercaptoethanol (Sigma-Aldrich) and 10% FBS (PAA Laboratories, Inc.). The cells were counted with a Coulter counter (Beckman-Coulter) and resuspended in ELISPOT medium at $1x10^7$ cells/ml.

3.4 PVM Quantification

PVM was quantified using a standard immunofluorescent plaque assay. Ten-fold serial dilutions of mouse lung homogenates or stock virus in PVM medium were made in sterile 96-well dilution plates (Nalgen Nunc International) and 100 μl was transferred in duplicate onto 80% confluent BHK-21 cell monolayers. After 72 hr incubation at 37°C and 5% CO_2, the supernatants were removed from the cells, and the plates blotted dry. The cell sheets were fixed with an ice-cold solution of 4 parts acetone to 1 part methanol, and dried at RT. After drying, the fixed plates were stored up to 4 days at 4°C.

The staining procedure was carried out at RT, and the plates were washed three times between each incubation and before blocking by immersion in PBS. Plates were blocked for 30 min in PBS containing 5% goat serum (Invitrogen), followed by a 2-3 hr incubation with a 1:500

dilution of a PVM N protein-specific polyclonal rabbit antibody in PBS containing 1% goat serum, and a 1 hr incubation in the dark with an Alexafluor488-congujated goat-anti-rabbit antibody (Invitrogen). After a final two washes, the plates were tapped dry on paper towel and plaques visualized using a fluorescent microscope (Zeiss). Plates were stored, wrapped in foil, at 4°C for up to one week.

Plaques were counted and the titre of the sample was calculated by multiplying the dilution factor at which there were fewer than 12 plaques per well by the number of plaques visible in that well. This results in the number of plaques per 100 µl of sample, which is multiplied by 10 to give the titre in pfu/ ml.

3.5 RT-PCR Analysis of Chemokine and Cytokine Expression

Trizol® homogenates of lung tissue collected on days 1, 3, and 5 p.i. of the short-term trials were processed according to the manufacturer's instructions for RNA isolation, and subsequent genomic DNA removal and cDNA synthesis were carried out using Qiagen's QuantiTect Reverse Transcription Kit according to manufacturer's instructions. Real-time semi-quantitative PCR (qPCR) was carried out using Platinum SYBR Green qPCR Supermix-UDG (Invitrogen) as per manufacturer's instructions. Reactions were set up in 96-well Hardshell Full G/C PCR plates (Bio-Rad Laboratories) sealed with Microseal 'B' Adhesive Seals (Bio-Rad Laboratories) and run on a CFX96 Real Time System (Bio-Rad Laboratories). Primers were purchased from Invitrogen using published sequences for amplifying housekeeping genes β-actin and GAPDH, as well as cytokine and chemokine genes IFN-γ, MIP-1α, MCP-1, IFN-α, IFN-β, and TNF-α (Table 3.1). Primers for IL-4, MIP-2, eotaxin, RANTES, and IP-10 were designed using the online resource NCBI PrimerBlast (http://www.ncbi.nlm.nih.gov/tools/primer-blast/)

and the primer design software, CloneManager Version 9.0. Optimal primer annealing temperatures and qPCR reaction efficiencies were determined using a temperature gradient from 50-70°C and cDNA dilution series. The qPCR reaction was carried out according to the following parameters: 40 cycles of denaturation at 95°C for 30 sec, followed by 30 sec annealing and extension (see Table 3.1 for optimal temperature). Expression levels of cytokine and chemokine transcripts were calculated using the Bio-Rad analysis software (Bio-Rad CFX Manager Version 2.0), normalized against both β-actin and GAPDH, and expressed as the normalized fold-change over mock-infected control animals euthanized on the same day.

Table 3.1: Cytokine and Chemokine Primers and their Optimal Annealing Temperatures

Target gene	Direction	Sequence	Source	Annealing Temp (°C)
β-actin	Forward Reverse	ACTGGGACGACATGGAG GTAGATGGGCACAGTGTGGG	[177]	57.5
GAPDH	Forward Reverse	AACTTTGGCATTGTGGAAGG ACACATTGGGGGTAGGAACA	[178]	57.5
MIP-1α	Forward Reverse	CTTCTCTGTACCATGACACTC AGGTCTCTTTGGAGTCAGCG	[177]	57.5
MIP-2	Forward Reverse	TGCGCCCAGACAGAAGTCATAGC GCTCTAGAGTCAGTTAGCCTTGCCTTTG	designed in house	63.9
MCP-1	Forward Reverse	CTTCTGGGCCTGCTGTTCA CCAGCCTACTCATTGGGATCA	[179]	57.5
IFN-γ	Forward Reverse	TCAAGTGGCATAGATGTGGAAGAA TGGCTCTGCAGGATTTTCATG	[179]	57.5
IL-4	Forward Reverse	GGAGATGGATGTGCCAAACG ACCTTGGAAGCCCTACAGAC	designed in house	63.9
IFN-α	Forward Reverse	CCTGTGTGATGCAACAGGTC TCACTCCTCCTTGCTCAATC	[180]	59.3
IFN-β	Forward Reverse	ATCATGAACAACAGGTGGATCCTCC TTCAAGTGGAGAGCAGTTGAG	[180]	63.9
TNF-α	Forward Reverse	GAACTGGCAGAAGAGGCACT AGGGTCTGGGCCATAGAACT	[180]	68.9
IP-10	Forward Reverse	GAGATCATTGCCACGATGAA CACTGGGTAAAGGGGAGTGA	designed in house	63.9
RANTES	Forward Reverse	CTCACTGCAGCCGCCCTCTG CCTTGACGTGGGCACGAGGC	designed in house	57.5
Eotaxin	Forward Reverse	AGAGGCTGAGATCCAAGCAG CAGATCTCTTTGCCCAACCT	designed in house	63.9

3.6 ELISAs for Cytokine and Chemokine Levels in Lung Homogenates

ELISAs for IFN-γ, MCP-1, MIP-1α, and MIP-2 were carried out on lung homogenates using a DuoSet system from R&D Systems according to the manufacturer's instructions. For the MIP-2 and IFN-γ assays, the capture and detection antibodies were optimized to double the recommended concentration, while the MCP-1 and MIP-1α assays were carried out using the manufacturer's recommended concentrations. The dilution of the lung homogenates was optimized for each assay and found to be within the range of assay detection at 1:50 for MCP-1 and MIP-1α and 1:2 for IFN-γ and MIP-2. The level of these proteins was measured in the diluted lung homogenates in pg/ ml and multiplied by the dilution factor to give the total quantity in the lungs in pg/ ml.

3.7 IFN-γ and IL-5 Enzyme-linked Immunospot (ELISPOT) Assays

One day prior to spleen collection, 96-well Multiscreen-HA ELISPOT plates (Millipore) were coated with murine IFN-γ- and IL-5-specific monoclonal antibodies (BD PharMingen) diluted to 2 μg/ ml in sterile coating buffer. Following an overnight incubation at 4°C, the plates were washed 4 times with sterile PBS, pH 7.2 (Invitrogen) and blocked for at least 1 hr with 1% BSA (Sigma-Aldrich) in PBS pH 7.2 (Invitrogen) at 37°C. In each well, 100 μl of splenocytes were restimulated with 100 μl of medium alone, mock- or PVM-infected cell lysates, or the mitogen Concanavalin A (ConA). To prepare the lysates, mock- or PVM-infected cell lysates were heat-inactivated for 30 min at 56°C and diluted in ELISPOT medium such that the final protein concentration in each well was 25 μg/ml. Medium alone and ConA at a final

concentration of 1 μg/ml were used as negative and positive controls, and each treatment was assayed in triplicate for each animal.

After approximately 40 hr of incubation at 37°C in a 5% CO_2 incubator, the medium was removed from the plate and the wells were filled with double-distilled (dd)H_2O and left for 10 min at RT to lyse the cells. All subsequent incubations were also carried out at RT. Plates were washed three times in PBST (PBS with 0.05% Tween 20 (Sigma-Aldrich)) and twice with ddH_2O, and then biotinylated anti-mouse IFN-γ or IL-5 monoclonal antibodies (BD Biosciences) were added to the wells at a concentration of 2 μg/ml in PBS with 1% BSA (Sigma-Aldrich). After 1-2 hr incubation, the plates were washed as previously and alkaline phosphatase (AP)-conjugated streptavadin (Jackson ImmunoResearch Laboratories) was added at a dilution of 1:1000 in PBS with 1% BSA (Sigma-Aldrich) for 1-2 hr. After a final wash step, the spots created by cytokine-secreting cells were visualized by the addition of 5-bromo-4-chloro-3-indolylphosphate and nitroblue substrate (Sigma-Aldrich) diluted in ddH_2O. After 5-10 min development, plates were washed in ddH_2O and dried at RT overnight. Spots were counted under an inverted microscope (Olympus SZ71) and the results expressed as the number of cytokine-secreting cells per million splenocytes stimulated with mock-infected cell lysates subtracted from the number of cytokine-secreting cells stimulated with PVM-infected cell lysates.

3.8 PVM-specific IgG and IgA ELISA

PVM-specific antibodies were assayed in the lung fragment culture supernatants and sera of infected mice. PVM-infected and mock-infected cell lysates were pelleted at 4°C for 30 min, resuspended in ddH_2O, and frozen at -80°C. Upon thawing, the concentrated cell lysates were treated with 0.05% Nonidet-P40 (Sigma-Aldrich) and sonicated 5 times for 30 sec in a cup

sonicator on ice. The resulting suspensions were centrifuged at 10,000 xg for 1 min, and the supernatants used as PVM-positive or -negative antigen following a 1:500 dilution in ddH_2O. 96-well polystyrene ImmulonII plates (Thermo Electron) were coated with 50 µl of the diluted antigens and dried overnight. Coated plates were stored, wrapped in plastic, at -20°C for use in the PVM ELISA described below.

Washes were performed with PBST and ddH_2O as per ELISPOT protocol. Plates were warmed to RT, washed, and blocked in PBS with 5% gelatin (Sigma-Aldrich). Four-fold serial dilutions of serum or LFC supernatant were prepared in 96-well non-sterile dilution plates (Nalgen Nunc International), starting at a 1:40 dilution for serum and 1:10 for LFC supernatants. The diluted sera and LFC supernatants were added to the blocked PVM ELISA plates and incubated overnight at 4°C. The plates were washed and either AP-conjugated IgG (Kirkegaard & Perry Laboratories) diluted to 1:5000 or biotinylated-anti-mouse IgA (Invitrogen) at 1:2000 was added to the plates and allowed to react for 1-2 hr. For the IgA ELISA, an additional 1 hr incubation with a 1:10,000 dilution of AP-conjugated streptavidin (Jackson ImmunoResearch Laboratories) was carried out at RT. The plates were developed with p-nitrophenyl phosphate (Sigma-Aldrich) and the absorbances read at 405 nm with a reference wavelength of 490 nm. Titres were calculated based on the dilution at which the ELISA read-out for the PVM-positive antigen was equal to the highest reading from the same animal's serum tested with the PVM-negative antigen.

3.9 Virus Neutralization Assay

Sera and LFC supernatants were serially diluted in PVM medium in sterile flat-bottom 96-well tissue culture plates (Nalgen Nunc International) starting at 1:10 and 1:2, respectively

and continuing in 2-fold dilutions down the plate. An equal volume of PVM 15 at a concentration of 500 pfu/ well in PVM medium was added to the dilution plate, such that the resulting dilution of the serum or supernatant was 1:20 and 1:4, respectively. After 1 hr incubation at 37°C and 5% CO_2, the virus mixture was transferred in duplicate onto BHK-21 cell monolayers grown to 80% confluency in flat-bottom 96-well tissue culture plates (Nalgen Nunc International). Following a further 72 hr incubation at 37°C and 5% CO_2, the cells were fixed and stained according to the PVM plaque assay protocol described in section 3.4. Because the addition of normal serum enhanced the growth of BHK cells and thus the degree of infection in the virus neutralization assay, the virus neutralizing antibody titres in the serum were expressed as the dilution at which virus was completely neutralized. For the neutralization assays using LFC supernatants, the lowest dilution of LFC supernatant was inhibitory to PVM even in mock-infected animals, and low numbers of irregular and misshapen plaques were visible in all infected animals. Thus, the neutralization antibody titres in the LFC supernatants were expressed as the dilution at which the number of plaques was reduced by 50% compared to those infected with virus alone.

3.10 Statistical Analysis

Statistical software (GraphPad Prism Version 5.00) was used to analyze all data collected. Since the sample size for the analyses was only 4-8 animals, and the variability in biological systems makes normal distribution unlikely, the data were analyzed using non-parametric tests. The Kruskall-Wallis test was used to determine whether there was a difference between all groups. If the test indicated significant differences between the groups, Mann-Whitney U tests were used to compare the median of individual groups. Differences were considered significant if $p<0.05$.

4.0 Immediate Response to Acute Infection with PVM in Balb/c and C57Bl/6 Mice

4.1 Clinical Response to PVM Infection

4.1.1 Body Weight Loss

To investigate the relative susceptibility of Balb/c and C57Bl/6 strains to PVM infection, we infected mice with different doses of PVM and weighed them daily, which is the best indication of clinical severity. Each mouse's weight was expressed as a percentage of its day 0 weight, such that a weight below 100% is indicative of weight loss. At all time points, the control animals maintained a median weight of more than 100%. Between days 1 and 3 p.i., all infected mice continued to gain weight (Fig. 4.1 A&B).

Balb/c mice infected with 3000 pfu showed the first signs of weight loss on day 4 p.i., becoming statistically different from the control group on day 5 p.i., at 96% ($p<0.0001$) (Fig. 4.1 D). By day 6 p.i., two of the eight remaining mice had died and the rest had dropped to a median of 89% of their starting body weight ($p=0.0024$) (Fig. 4.1 E). The more resistant C57Bl/6 mice, on the other hand, experienced the same degree of weight loss beginning one day later than the Balb/c group. By day 4 p.i., they had increased to a significantly higher weight than the control group, but they dropped to a significantly lower median weight of 96% on day 6 and 89% on 7 p.i. ($p=0.0072$ and 0.0286, respectively) (Fig. 4.1 C-F) . The 3000 pfu dose was found to be lethal in C57Bl/6 mice by day 7, as one of the four mice died just prior to sampling.

When these strains were infected with a 10-fold lower dose, they showed delayed weight loss, with the 300 pfu Balb/c group displaying similar clinical severity to the 3000 pfu C57Bl/6 group, while the 300 pfu C57Bl/6 group had no signs of illness by day 7. The 300 pfu Balb/c mice began losing weight on day 5 p.i., becoming significantly different from the control mice

on day 6 with a median of 93% and dropping further to 85% on day 7 p.i. ($p = 0.0039$ and 0.0286, respectively) (Fig. 4.1 D-F). C57Bl/6 mice infected with 300 pfu, on the other hand, showed virtually no weight loss by day 7 p.i., with the four remaining mice having a median weight of 104%. This was similar to the group of Balb/c mice infected with 30 pfu of PVM, which had a median weight of 102% on day 7 p.i. and was not statistically different from the mock-infected group.

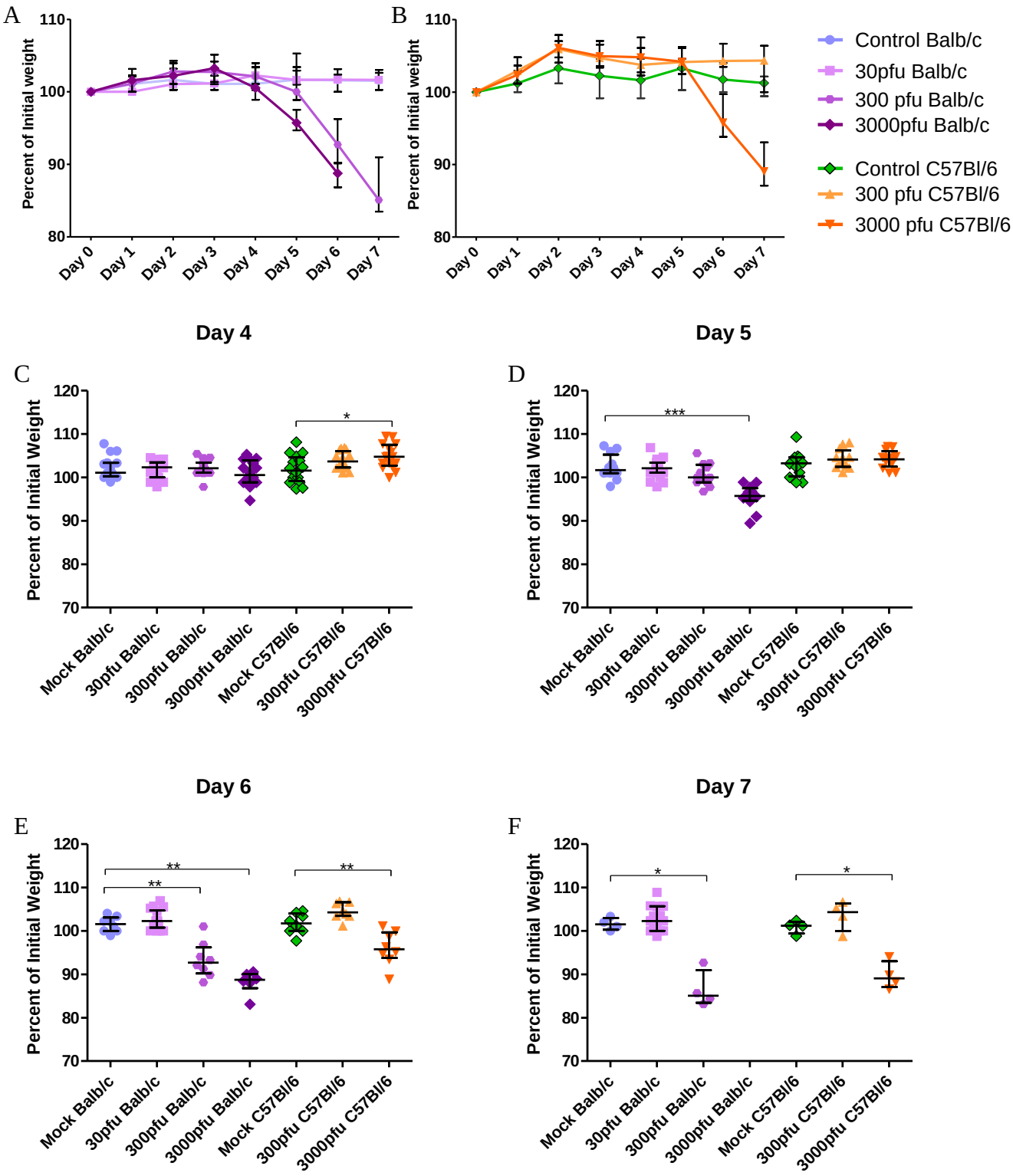
A
B
Percent of Initial weight
110
100
90
80
Day 0
Day 1
Day 2
Day 3
Day 4
Day 5
Day 6
Day 7
Control Balb/c
30pfu Balb/c
300 pfu Balb/c
3000pfu Balb/c
Control C57Bl/6
300 pfu C57Bl/6
3000 pfu C57Bl/6
Day 4
Day 5
C
D
Percent of Initial Weight
120
110
100
90
80
70
*
***
Mock Balb/c
30pfu Balb/c
300pfu Balb/c
3000pfu Balb/c
Mock C57Bl/6
300pfu C57Bl/6
3000pfu C57Bl/6
Day 6
Day 7
E
F
**
*

Figure 4.1

Figure 4.1: Weight change associated with PVM infection. 5-6 week old Balb/c and C57Bl/6 mice were inoculated with medium, 30 pfu, 300 pfu, or 3000 pfu of PVM 15 and weighed daily for 7 days following infection, and 4 mice/group were sacrificed daily. Weights are expressed as a percentage of each mouse's day 0 weight. The top panel, (A) and (B), shows the median weight for each group with error bars indicating the interquartile range. The lower two panels (C-F) show the individual weights of the mice that remained on days 4-7 p.i., with each point representing a single mouse and the line indicating the median. *, $p<0.05$; **, $p<0.01$; ***, $p<0.001$.

4.1.2 Viral Replication in the Lungs

The susceptibility of Balb/c and C57Bl/6 mice was further measured by viral replication in the lungs. Groups of four mice were euthanized daily following intranasal inoculation with medium or 30-3000 pfu of PVM 15, and their lungs were removed and processed for virus isolation. At all three doses, the Balb/c mice had a more rapid accumulation of virus in the lungs than C57Bl/6 mice, and tended to peak earlier and drop off instead of reaching a plateau (Fig 4.2 A and B). In both strains, PVM replication was highly dose-dependent. Balb/c mice had significantly different viral titres in the lung between all dose groups at all time points other than day 4, when the 3000 pfu dose had similar titres as the 300 pfu dose in this strain (Fig. 4.2 C-H). The two C57Bl/6 groups were significantly different on all days other than days 4 and 7 p.i. ($p<0.05$ for all significant comparisons) (Fig. 4.2 C-H).

At a dose of 3000 pfu, the Balb/c mice showed between 25-and 250-fold higher levels of viral replication compared to C57Bl/6 mice. The virus titres in Balb/c mice reached a maximum on day 5 p.i. at $4.5x10^7$ pfu/ml, dropping to $7.8x10^6$ on day 6, while in C57Bl/6 the maximum was reached on day 6 p.i. at $8.5x10^5$ pfu/ml and maintained to day 7 at $5.0x10^5$ pfu/ml. The median viral titre of these two groups was significantly different at all times following infection ($p<0.05$) (Fig. 4.2 C-H).

Given a 10-fold lower dose, Balb/c mice again accumulated virus much more rapidly than C57Bl/6 mice, such that their PVM titres were significantly higher than those in the C57Bl/6 mice from days 2-6 p.i. ($p<0.05$) (Fig. 4.2 C-F). The 300 pfu Balb/c group reached detectible levels of PVM in the lungs on day 2 p.i., one day earlier than C57Bl/6 mice. By day 4 p.i., their viral load had risen to $5.5x10^5$ pfu/ml, which was not significantly different from the

viral load measured on days 5-7, although this group appeared to peak on day 6 at $1.0x10^6$ pfu/ml and drop slightly on day 7 (Fig. 4.2 A). In contrast, C57Bl/6 mice infected with 300 pfu required three days to achieve detectible levels of PVM in the lungs and replicated the virus to a maximum of $2.3x10^5$ pfu/ml on day 6, which was maintained at $2.0x10^5$ pfu/ml on day 7 (Fig. 4.2 B).

Finally, the lowest dose of PVM 15 was examined only in Balb/c mice because of their increased susceptibility to infection. They replicated the virus in a similar pattern to the 10-fold higher dose in C57Bl/6 mice, with viral replication becoming detectible on day 3 p.i., increasing to $2.8x10^5$ pfu/ml by day 6 p.i., and dropping to $3.0x10^4$ pfu/ml on day 7 p.i. (Fig. 4.2 A).

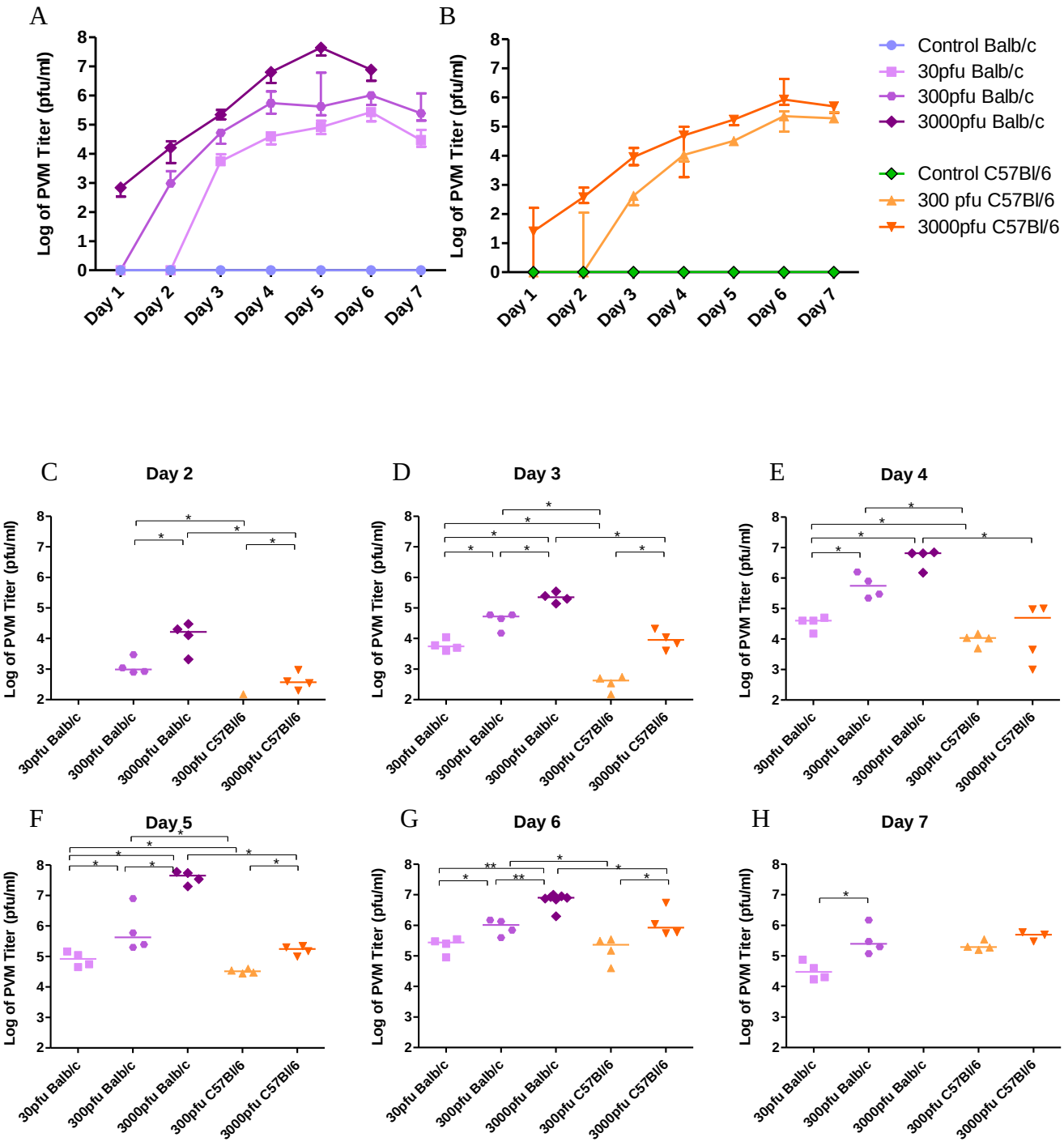
A
B
Log of PVM Titer (pfu/ml)
Day 1
Day 2
Day 3
Day 4
Day 5
Day 6
Day 7
Control Balb/c
30pfu Balb/c
300pfu Balb/c
3000pfu Balb/c
Control C57Bl/6
300 pfu C57Bl/6
3000pfu C57Bl/6
C
Day 2
D
Day 3
E
Day 4
F
Day 5
G
Day 6
H
Day 7
30pfu Balb/c
300pfu Balb/c
3000pfu Balb/c
300pfu C57Bl/6
3000pfu C57Bl/6

Figure 4.2

Figure 4.2: Viral replication in the lungs of PVM infected mice. 5-6 week old Balb/c and C57Bl/6 mice were inoculated with medium, 30 pfu, 300 pfu, or 3000 pfu of PVM 15 and lungs were collected daily from four mice/group. The viral load is expressed as the log10 of the viral titre in pfu/ml. In (A) and (B), the symbols represent the median weight for each group with error bars indicating the interquartile range. In (C-H), each data point represents a single animal and the line represents the group median. *, $p<0.05$; **, $p<0.01$.

4.1.3. Histopathological Analysis

In order to assess the level of lung pathology induced by different doses of PVM in Balb/c and C57Bl/6 mice, groups of four mice were euthanized on day 6 p.i., and the lungs were collected and processed for histopathological analysis of lung sections. Scores were given based on the dissemination and severity of lesions visible in duplicate lung sections (Fig. 4.3 A). All mock-infected animals had normal lungs, whereas all but two infected mice had visible pathology in the lungs. The two infected mice with normal lungs were in the 300 pfu C57Bl/6 group. Scores were quite variable, with at least one mouse in each group scoring the highest possible score of 3, indicating widely disseminated and severe lesions. Although there was no significant difference in lung score between groups, there appeared to be a trend towards a dose-dependent increase in lung score for both strains of mice.

As can be seen in Figure 4.3 B, mice with a score of zero, or normal lungs (upper left panel), had few cells dispersed throughout the alveolar space, and the airway epithelium appeared intact and free of fluid and infiltrating immune cells. A score of one indicates a localized, mild inflammation of the peribronchiolar and perivascular space involving fluid accumulation with few infiltrating immune cells. A representative lung section shows the presence of edema surrounding the blood vessel (V), indicated with an arrow pointing downward (Fig. 4.3 B, upper right panel). The upward arrow is pointing at the inflammatory cells infiltrating the tissue.

A mouse scoring two may exhibit multiple lesions or a single extensive lesion, and the lesions are more severe, with higher numbers of infiltrating cells in the inflamed tissue and the alveolar space. The photo in figure 4.3 B (lower left panel) shows a representative lesion with

moderate numbers of inflammatory cells in the tissue, though the alveolar space is still relatively clear of cellular debris.

A score of three indicates broadly dispersed lesions with cellular infiltrates in the alveolar space and surrounding tissues. A representative photo is shown in figure 4.3 B (lower right panel), and the severity of the lesion is evident by the presence of inflammatory cells in the alveolar space and surrounding the blood vessel and bronchiole (B). There is little air space left in the lung, as so much cell debris has accumulated in the alveoli.

A

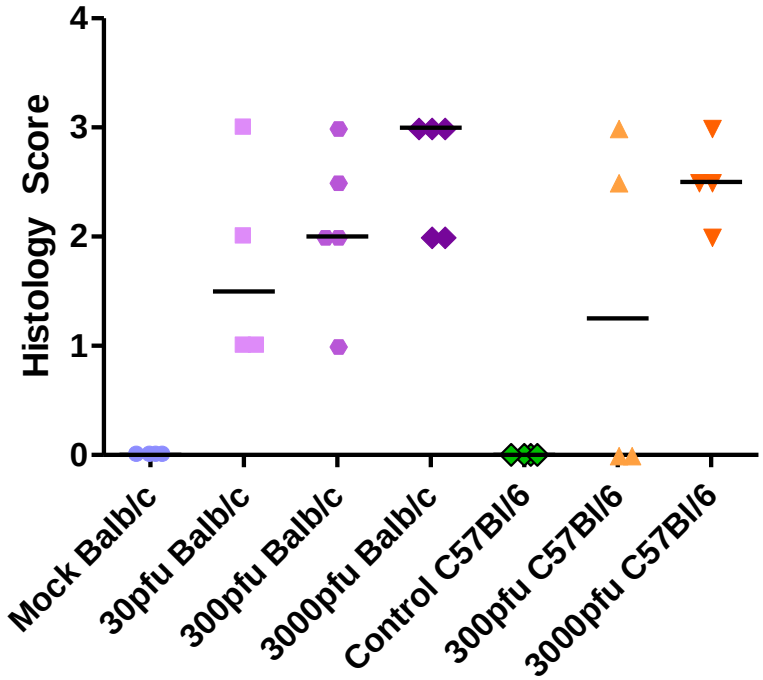
Histology Score
4
3
2
1
0
Mock Balb/c
30pfu Balb/c
300pfu Balb/c
3000pfu Balb/c
Control C57Bl/6
300pfu C57Bl/6
3000pfu C57Bl/6

B

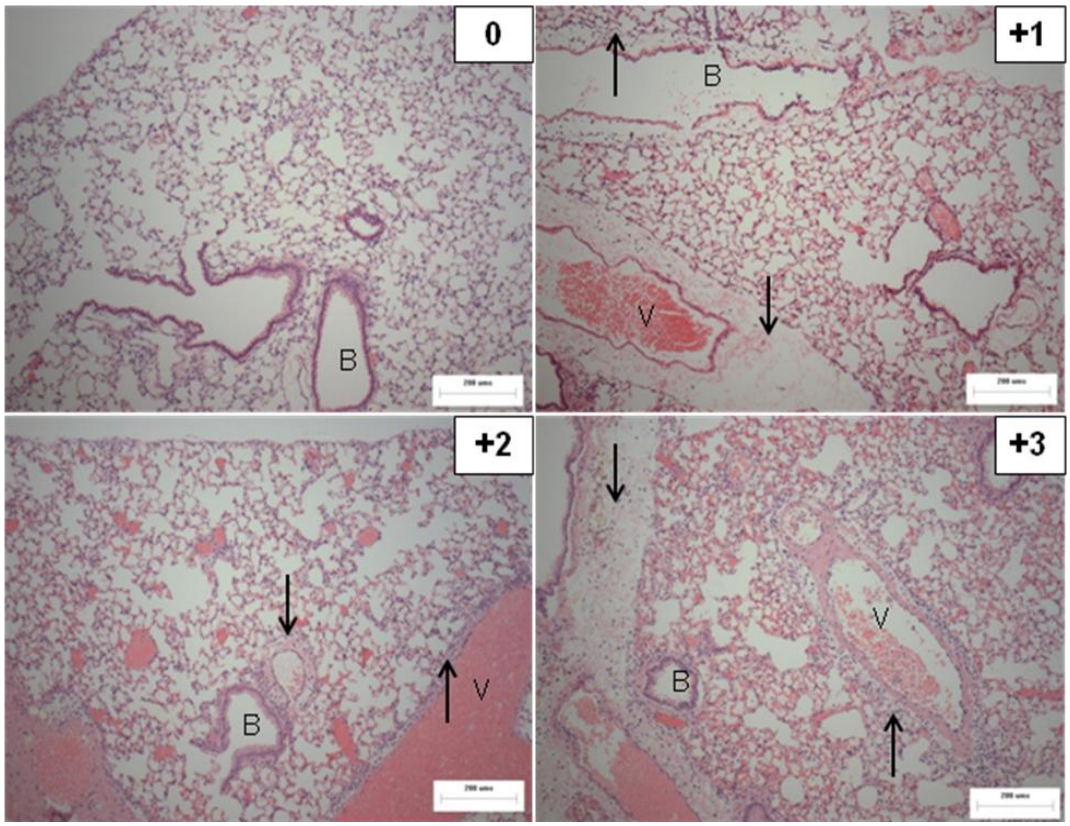
0
B
+1
B
V
+2
B
V
+3
V
B

Figure 4.3

Figure 4.3: Histopathological analysis of PVM-infected mice. 5-6 week old Balb/c and C57Bl/6 mice were inoculated with medium, 30 pfu, 300 pfu, or 3000 pfu of PVM 15 and lungs were collected from four mice on day 6 p.i. for histopathological analysis. Scores were given on the basis of the severity and dissemination of the lesions visible in duplicate lung sections, depicted in (A), where each data point represents a single animal. In (B), representative lung sections for animals scoring 0, 1, 2, and 3 are shown, with the upward arrows (↑) indicating infiltrating inflammatory cells and the downward arrows (↓) indicating edema in the tissue. The bronchiole is labeled with the letter B and the blood vessel with V.

4.2 Innate Immune Response to PVM Infection

4.2.1 Cytokine and Chemokine Gene Expression in the Lungs

To assess the local immune response to PVM in the lungs, the relative expression levels of the cytokines IFN-γ and IL-4, as well as the chemokines MIP-1α, MCP-1, and MIP-2 were measured using semi-quantitative real-time PCR. Balb/c and C57Bl/6 mice were inoculated intranasally with medium or PVM 15 at doses ranging from 30 to 3000 pfu, and lungs were collected on days 1, 3, and 5 p.i. for RNA isolation. Expression levels of the genes were expressed as normalized fold-increase over mock-infected animals collected on the same day (Fig.4.4).

No IL-4 upregulation was detected at any time following infection, and, indeed, transcript levels for this gene were so low in all animals as to be virtually undetectable (data not shown). IFN-γ, on the other hand, was highly upregulated upon infection with a lethal dose of PVM, and moderately upregulated in sublethally infected animals. Balb/c mice expressed IFN-γ earlier following infection with PVM than C57Bl/6 mice, and by day 5 even the 30 pfu dose induced greater upregulation in the Balb/c strain compared to 300 pfu in C57Bl/6. On day 3 p.i., Balb/c mice given 3000 pfu showed a 5-fold upregulation of IFN-γ over control mice, which was significantly higher than the basal expression levels measured in all other groups of infected mice ($p=0.0286$). By day 5, there was no significant difference between any of the lethally infected groups, with a median fold-increase in IFN-γ expression of 81 in 3000 pfu Balb/c, 182 in 3000 pfu C57Bl/6, and 121 in 300 pfu Balb/c mice. By contrast, the sublethal doses of 30 pfu in Balb/c and 300 pfu in C57Bl/6 mice induced significantly lower IFN-γ upregulation than any of the lethal doses, at 7.5- and 2-fold, respectively. As mentioned above, the median IFN-γ

upregulation for the 30 pfu Balb/c group was significantly higher than that of the 300 pfu C57Bl/6 group ($p=0.0286$).

The CC chemokines MCP-1 and MIP-1α were upregulated with a similar time course and pattern as IFN-γ. Both were upregulated first in 3000 pfu Balb/c mice by day 3 p.i., and then in all infected groups by day 5 p.i.. The lethal doses, 3000 pfu in Balb/c, 3000 pfu in C57Bl/6, and 300 pfu in Balb/c mice showed similar levels of CC-chemokine upregulation that were significantly higher than those in the sublethally infected groups, 300 pfu in C57Bl/6 mice and 30 pfu in Balb/c mice. The median normalized fold change of MIP-1α was measured to be 40-fold in the 3000 pfu Balb/c mice, 57-fold in the 3000 pfu C57Bl/6 mice, and 27-fold in the 300 pfu Balb/c mice, compared to just 3.2-fold in the 300 pfu C57Bl/6 mice and 4.5- fold in the 30 pfu Balb/c mice. Similarly, MCP-1 was found to be upregulated 290-fold in 3000 pfu Balb/c mice, 260-fold in 3000 pfu C57Bl/6 mice, and 240-fold in 300 pfu Balb/c mice, compared to 5-fold in 300 pfu C57Bl/6 and 27-fold in 30 pfu Balb/c. While MIP-1α upregulation was no different between sublethally infected Balb/c and C57Bl/6 mice, MCP-1 expression was significantly higher in sublethally infected Balb/c mice, despite the 10-fold lower dose ($p=0.0286$).

The CXC chemokine, MIP-2, was expressed in a different pattern compared to the CC chemokines discussed above. All three lethal doses induced upregulated expression beginning on day 3 p.i., and the level of expression was dose- and strain-dependent. Balb/c mice upregulated MIP-2 to significantly higher levels than C57Bl/6 given the same dose ($p=0.0286$). A dose-dependent upregulation was also seen on day 5 p.i., with 3000 pfu Balb/c mice at a median of 240-fold upregulation over control mice. The next highest levels were in the 3000 pfu C57Bl/6 group and the 300 pfu Balb/c group, which had a 47- and 68-fold upregulation of MIP-2 in the

lungs, respectively. These two groups were not statistically different. Similarly, the sublethal doses 300 pfu in C57Bl/6 mice and 30 pfu in Balb/c mice induced the same level of MIP-2 upregulation, at 10- and 14-fold respectively.

After determining that upregulation of proinflammatory genes was highest on day 5 p.i., we evaluated the second panel of genes on day 5 only. Analysis of the type I IFN response showed that production of IFN-α, but not IFN-β, was a prominent response to PVM infection. The Balb/c strain had enhanced IFN-α mRNA expression in response to PVM compared to the C57Bl/6 strain, as the 30 pfu dose induced higher expression of this cytokine in the Balb/c strain than either the 3000 or 300 pfu dose in the C57Bl/6. There was no significant difference in the upregulation of IFN-α between the three doses of PVM in Balb/c mice. The 3000 pfu group had the lowest IFN-α expression of the three Balb/c groups, with a median upregulation of 10-fold over the control group. The 30 pfu and 300 pfu doses induced IFN-α at a median level of 68- and 84-fold over control Balb/c mice, respectively. The 3000 pfu C57Bl/6 mice had a median upregulation of IFN-α of 7-fold over control animals, which was significantly higher than the basal expression seen in the 300 pfu C57Bl/6 group ($p=0.0286$). The 300 pfu C57Bl/6 group also had significantly lower IFN-α expression levels than either the 30 pfu or the 300 pfu Balb/c groups.

The IFN-γ response gene, IP-10, had a similar pattern of upregulation on day 5 p.i. to that of IFN-γ and the CC-chemokines described above. The lethally infected animals in both strains had strongly upregulated IP-10 expression levels, and there were no significant differences between these groups. The normalized fold-change over control animals was 625 in the 3000 pfu Balb/c group, 829 in the 3000 pfu C57Bl/6 group, and 941 in the 300 pfu Balb/c group. The sublethally infected 30 pfu Balb/c group had intermediate levels of IP-10 expression, at 83-fold

over control animals, which was significantly lower than the levels in the 300 pfu Balb/c group and significantly higher than those in the 300 pfu C57Bl/6 group ($p=0.0286$). The 300 pfu C57Bl/6 group had the lowest expression of all the infected groups, with a median upregulation of 3-fold over mock-infected animals, which was significantly lower than the 3000 pfu C57Bl/6 group, as well as the 30 and 300 pfu Balb/c groups ($p=0.0286$).

The remaining genes, IFN-β, TNF-α, RANTES, and eotaxin, were only upregulated to low levels upon infection with PVM (Fig. 4.5). In the case of TNF-α, all infected group showed upregulation of gene expression, with median levels between 4- and 11-fold over control animals. The only significant difference in TNF-α gene expression was between the sublethal doses, where the 300 pfu C57Bl/6 mice had significantly lower TNF-α expression than the 30 pfu Balb/c group ($p=0.0286$). In the case of RANTES, eotaxin, and IFN-β, all groups other than the 300 pfu C57Bl/6 group had a similar level of upregulation of less than 5-fold over control animals. For these three genes, however, the 300 pfu C57Bl/6 group showed basal transcription levels, and as such, they expressed significantly lower levels of these genes than one or more of the other infected groups. Additionally, the 300 pfu Balb/c group had a significantly higher upregulation of eotaxin transcription compared to the 3000 pfu Balb/c group, with a median upregulation of 5-fold and 2-fold, respectively.

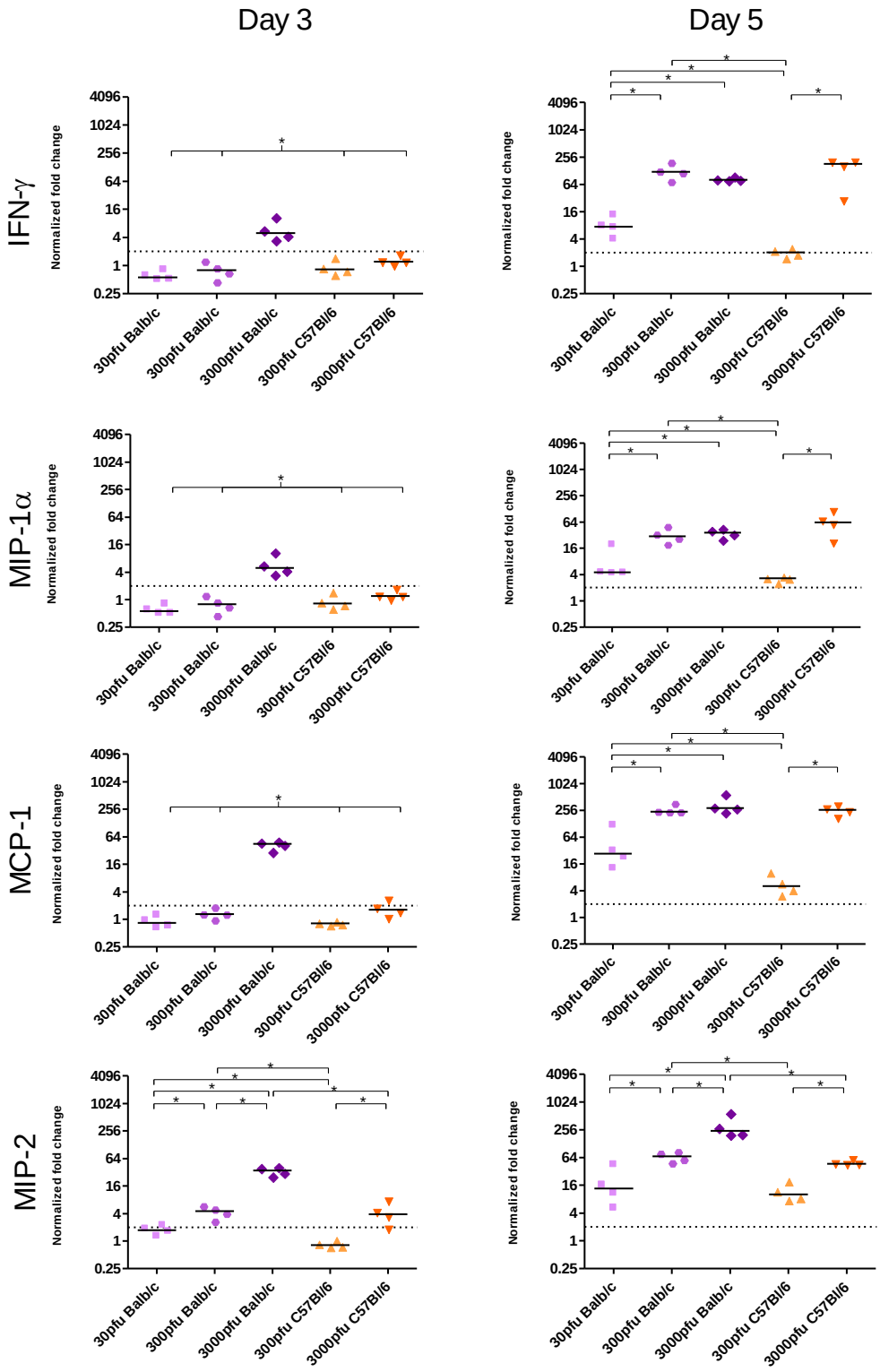
Day 3
Day 5
IFN-γ
MIP-1α
MCP-1
MIP-2
Normalized fold change
4096
1024
256
64
16
4
1
0.25
30pfu Balb/c
300pfu Balb/c
3000pfu Balb/c
30pfu C57Bl/6
300pfu C57Bl/6
3000pfu C57Bl/6

Figure 4.4

Figure 4.4: Cytokine and chemokine mRNA upregulation in response to PVM infection. 5-6 week old Balb/c and C57Bl/6 mice were inoculated with medium, 30 pfu, 300 pfu, or 3000 pfu of PVM 15 and lungs were collected from four mice/group on days 3 and 5 p.i.. The expression levels of IFN-γ, MIP-1α, MCP-1, and MIP-2 were calculated as the normalized-fold change over mock-infected mice of the same strain euthanized on the same day p.i.. The left-hand panel shows the cytokine and chemokine upregulation on day 3 p.i., and the right-hand panel on day 5 p.i.. Each data point represents a single animal and the line represents the group median. *, $p<0.05$.

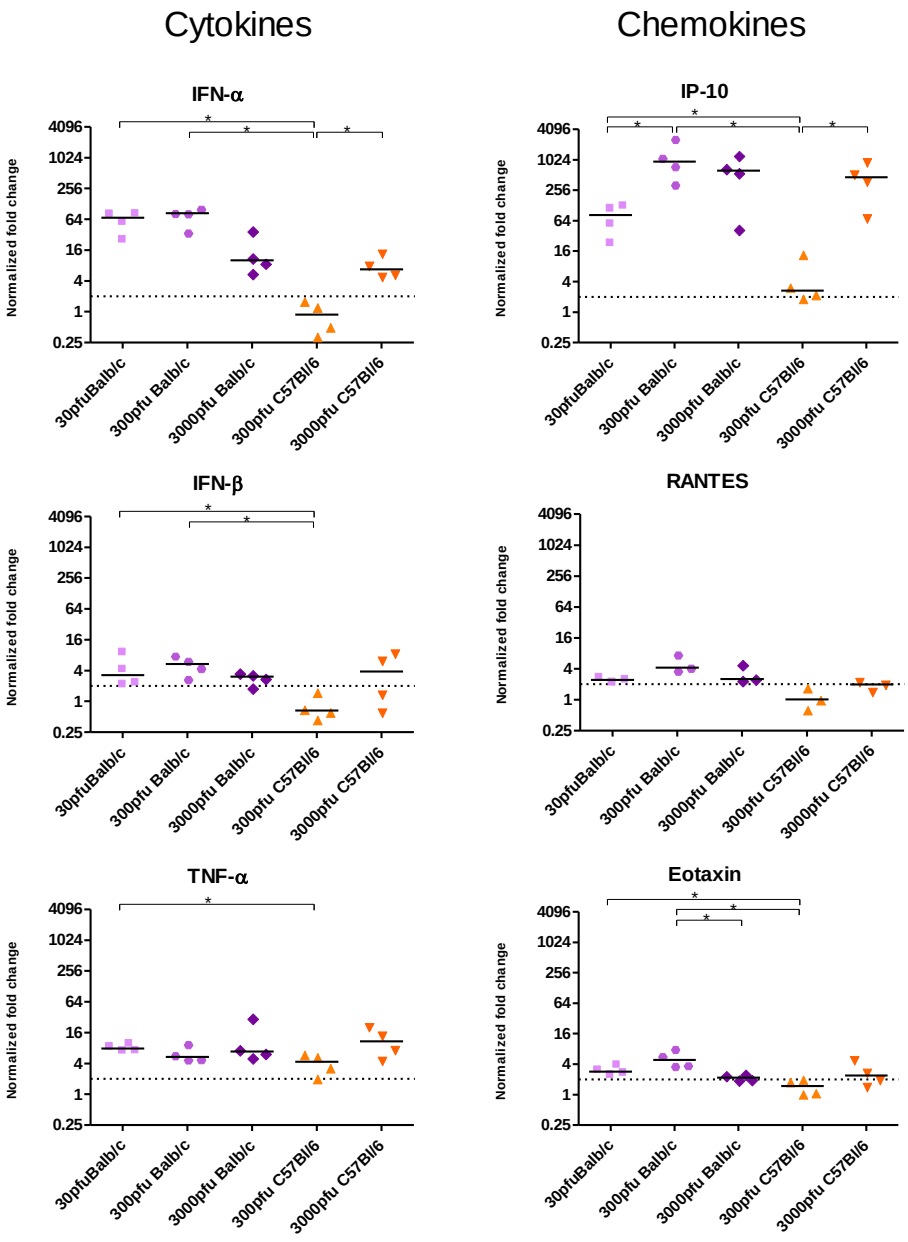
Cytokines
Chemokines
IFN-α
IP-10
IFN-β
RANTES
TNF-α
Eotaxin
Normalized fold change
4096
1024
256
64
16
4
1
0.25
30pfuBalb/c
300pfu Balb/c
3000pfu Balb/c
300pfu C57Bl/6
3000pfu C57Bl/6

Figure 4.5

Figure 4.5: Day 5 cytokine and chemokine mRNA upregulation in response to PVM infection. 5-6 week old Balb/c and C57Bl/6 mice were inoculated with medium, 30 pfu, 300 pfu, or 3000 pfu of PVM 15 and lungs were collected from four mice/group on day 5 p.i.. The expression levels of IFN-α, IFN-β, TNF-α, and IP-10 were calculated as the normalized-fold change over mock-infected mice of the same strain. Each data point represents a single animal and the line represents the group median. *, $p<0.05$.

4.2.2 Cytokine and Chemokine Protein Levels in the Lungs

To confirm that the upregulation of the cytokine and chemokine mRNA was associated with increased production of these proteins in the lungs, the levels of secreted IFN-γ, MCP-1, MIP-1α, and MIP-2 were assayed by ELISA. Balb/c and C57Bl/6 mice were inoculated with medium or a dose of PVM 15 ranging from 30 to 3000 pfu and four mice per group were euthanized daily to determine lung cytokine and chemokine levels. The cytokine and chemokine production in the lungs was measured on both days 5 and 6 p.i. in the 3000 pfu groups, since the Balb/c group had upregulated mRNA expression levels by day 3 at this dose. In the remaining groups, which showed upregulation by day 5 p.i., the chemokine and cytokine levels were only compared on day 6.

A comparison of the 3000 pfu groups on days 5 and 6 p.i., showed interesting results. The 3000 pfu dose clearly induced earlier production of at least three of the four cytokines and chemokines in Balb/c mice compared to C57Bl/6 mice (Fig.4.6). By day 5 p.i., Balb/c mice had significantly upregulated levels of IFN-γ, MCP-1, and MIP-2 over control Balb/c mice ($p=0.0286$), while the upregulation of MIP-1α was not statistically significant. Between days 5 and 6 p.i., the levels of IFN-γ and MCP-1 increased in the 3000 pfu Balb/c group, while levels of MIP-1α remained similar and MIP-2 actually dropped significantly($p<0.05$). In contrast, the C57Bl/6 group had background levels of all four cytokines and chemokines on day 5 p.i., and they all became significantly upregulated by 6 p.i. ($p=0.0286$).

Comparing all doses on day 6, it appeared that the 30 pfu Balb/c group had the same level of IFN-γ, MIP-1α, MCP-1, and MIP-2 as the 300 pfu Balb/c group, which conflicts with the apparent lower mRNA expression levels of these proteins. There was also no clear pattern

difference between the protein levels of CC and CXC chemokines, as there appeared to be at the mRNA level.

All three infected groups of Balb/c mice produced similar levels of IFN-γ by day 6 p.i., which were significantly higher than the control Balb/c group. All three infected Balb/c groups produced higher levels of IFN-γ than the C57Bl/6 mice infected with 3000 pfu or 300 pfu. The 3000 pfu C57Bl/6 group produced significantly higher levels of IFN-γ than either the control C57Bl/6 mice or the 300 pfu C57Bl/6 group, while the 300 pfu C57Bl/6 group had background levels of IFN-γ.

Similarly, at all three doses, Balb/c mice produced significantly higher levels of MCP-1 than the control group, this time with the 3000 pfu dose inducing higher levels than any other dose in Balb/c mice ($p=0.004$). The 3000 pfu Balb/c group had significantly higher MCP-1 production than either the 3000 pfu and 300 pfu doses in C57Bl/6 ($p=0.0286$). The two groups of infected C57Bl/6 mice were significantly higher than the control group ($p=0.0286$),but there was no significant difference between the two groups.

MIP-1α, another CC chemokine, was found to be significantly higher in the lungs of all groups of infected mice compared to the mock-infected controls ($p<0.05$). The only significant difference detected between groups of infected mice was higher MIP-1α production in C57Bl/6 mice infected with 3000 pfu compared to Balb/c mice infected with the same dose ($p=0.0283$).

Finally, the CXC chemokine, MIP-2, was significantly upregulated over control mice in all groups other than the 300 pfu dose in both strains ($p<0.05$). There was no statistical difference between the three doses in Balb/c mice, although the 3000 pfu group appeared to have the highest levels of MIP-2. C57Bl/6 mice, on the other hand, showed a significant dose-response,

with higher levels of MIP-2 in the lungs of 3000 pfu group compared to the 300 pfu group ($p=0.0286$). However, there was no significant difference in MIP-2 production between the two strains at a dose of either 3000 pfu or 300 pfu.

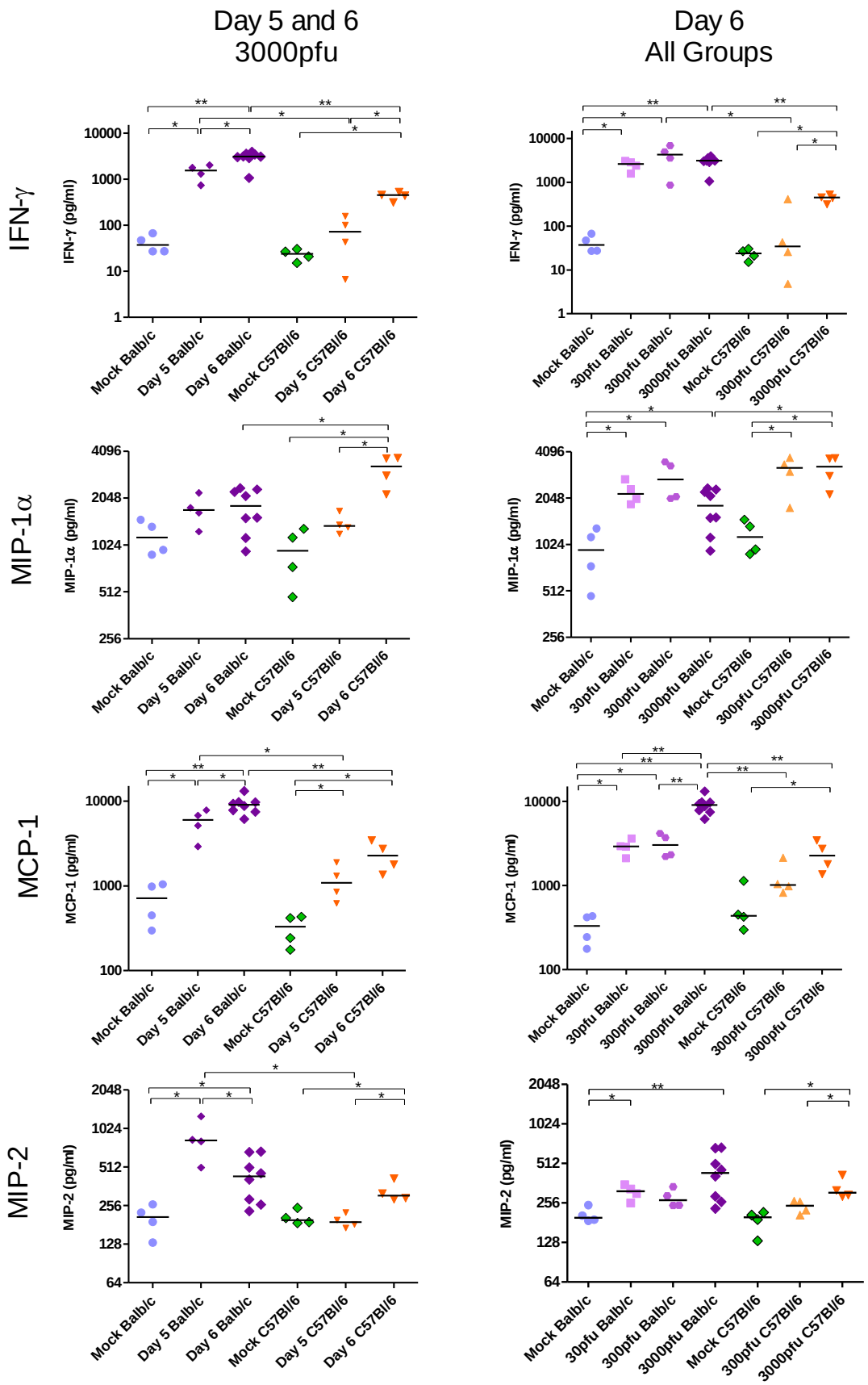
Day 5 and 6
3000pfu
Day 6
All Groups
IFN-γ
MIP-1α
MCP-1
MIP-2
IFN-γ (pg/ml)
MIP-1α (pg/ml)
MCP-1 (pg/ml)
MIP-2 (pg/ml)
Mock Balb/c
Day 5 Balb/c
Day 6 Balb/c
Mock C57Bl/6
Day 5 C57Bl/6
Day 6 C57Bl/6
30pfu Balb/c
300pfu Balb/c
3000pfu Balb/c
30pfu C57Bl/6
300pfu C57Bl/6
3000pfu C57Bl/6

Figure 4.6

Figure 4.6: Levels of cytokines and chemokines in the lungs of PVM-infected mice. 5-6 week old Balb/c and C57Bl/6 mice were inoculated with medium, 30 pfu, 300 pfu, or 3000 pfu of PVM 15, and the lungs were collected on days 5 and 6 p.i.. The levels of IFN-γ, MCP-1, MIP-1α, and MIP-2 were measured in four mice per group except for the 3000 pfu Balb/c group euthanized on day 6 p.i., which included all eight remaining animals. The left-hand panel shows the change in cytokine and chemokine levels in the highest dose animals on days 5 and 6 p.i., and the right-hand panel shows the levels in all groups on day 6 p.i.. Each data point represents a single animal and the line represents the group median. *, $p<0.05$; **, $p<0.01$.

4.2.3. Analysis of Cell Populations in Bronchioalveolar Lavages

To assess the relative contribution of different cell types to the pathogenesis of PVM in Balb/c and C57Bl/6 mice, and to examine the biological relevance of the cytokine and chemokine patterns in these mice, lung washes were collected and pooled from groups of four mice inoculated with different doses of PVM 15. The cells collected in the BAL on days 1, 3, and 5 p.i. were stained and the relative number of macrophages, neutrophils, lymphocytes, and eosinophils infiltrating the lungs was measured by differential analysis. The results of the analysis are shown in Figure 4.7.

In all mice, neutrophils infiltrated the lungs on the first day after inoculation with medium or PVM 15, but this background neutrophilia was resolved by day 3 p.i. in all groups except the 3000 pfu Balb/c (Fig. 4.7 A and B). By day 5, however, there was a clear dose-dependent increase in the total number of cells in the lungs of all infected Balb/c groups (Fig. 4.7 C). At this time point, neutrophils dominated the response in Balb/c mice, and they appeared to be increased in a dose-dependent manner. Lymphocyte numbers, on the other hand, were similar in the two lethally infected Balb/c groups, and were seen at low levels in the sublethally infected Balb/c mice by day 5 p.i.. In contrast, C57Bl/6 mice showed no increase in total cell number by day 5 p.i., although the 3000 pfu dose had increased numbers of neutrophils and lymphocytes in the lungs, in equal proportions.

A

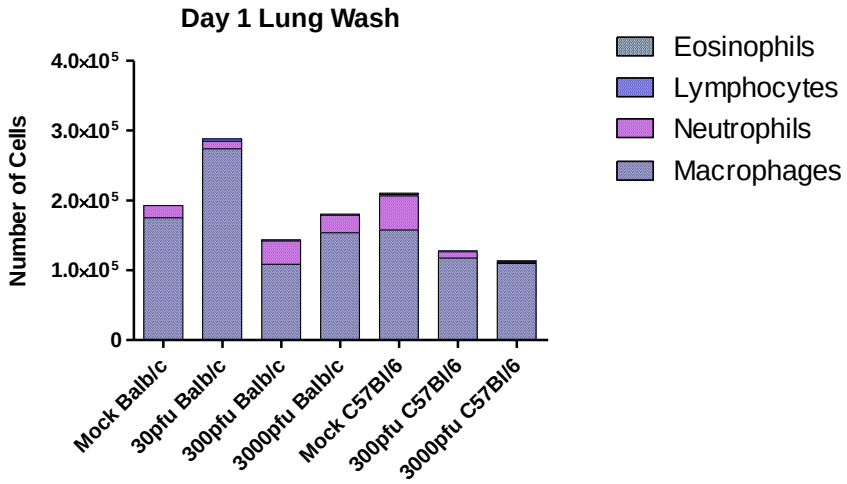

B

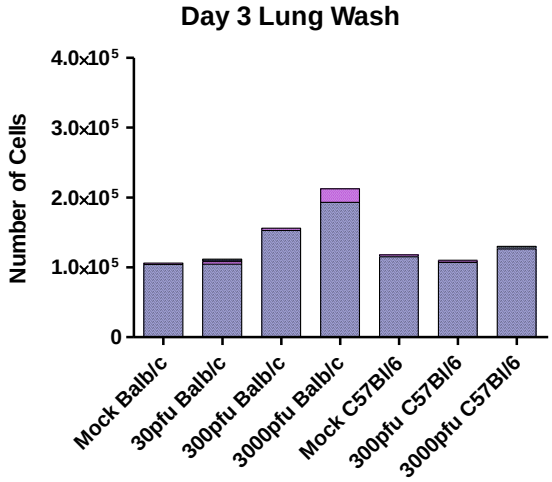

C

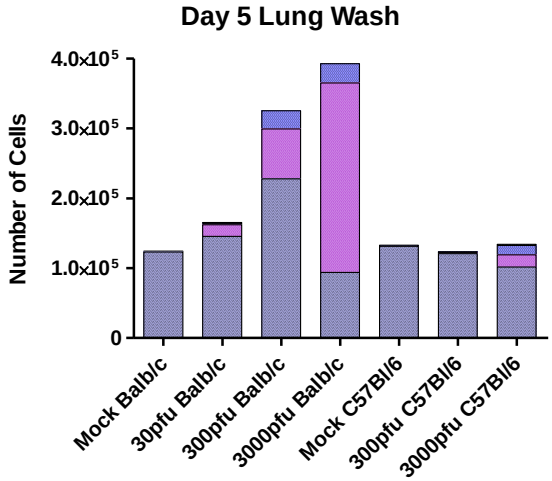

Figure 4.7

Figure 4.7: Cellular infiltration in the lungs of PVM infected Balb/c and C57Bl/6 mice. 5-6 week old Balb/c and C57Bl/6 mice were inoculated with medium, 30 pfu, or 300 pfu of PVM 15 and sacrificed on days 1, 3, and 5 p.i.. Cells collected from the pooled lung washes of 4-6 animals were stained and analyzed for the presence of macrophages, neutrophils, lymphocytes, and eosinophils. The average number of these cells is shown, calculated based on the number of total cells collected from the group and the proportion of these cell populations in the lungs.

5.0 Innate and Adaptive Responses to a Sublethal Dose of PVM in Balb/c and C57Bl/6 Mice

5.1 Clinical Response to PVM

From our preliminary studies, we observed that a dose of 30 pfu in Balb/c resulted in a survival rate of between 66 and 100%, similar to the C57Bl/6 sublethal dose of 300 pfu. Both groups began to show clinical signs of illness starting on day 8 p.i.. In addition, our short-term trials showed us that these two groups replicate PVM to similar levels *in vivo*. Based on this information, our long-term trials were designed to examine the innate and adaptive immune response to a sublethal dose of PVM during maximal lung inflammation and following recovery.

5.1.1 Body Weight Loss

Although preliminary trials suggested that PVM elicits a similar degree of illness at a dose of 30 pfu in Balb/c and 300 pfu in C57Bl/6 mice, on a larger scale the 30 pfu dose in the Balb/c strain was clinically much milder than the 300 pfu dose in C57Bl/6 mice. C57Bl/6 infected with 30 pfu, on the other hand, developed no clinical signs of infection. Throughout these trials, weight change was the only measurable sign of illness, as none of the mice developed clinical scores on the basis of appearance or behaviour.

Upon infection with 300 pfu of PVM, 87% (26/30) of C57Bl/6 mice lost weight between days 7 and 11 p.i. (Fig 5.1 B), with the group dropping from a median of 101% of their initial weight on day 7 p.i. to 93% on day 8 p.i. (Fig. 5.1 A). The median weight was significantly different from that of the control group on days 7-11 p.i., with the highest significance from days 8-10 p.i. (Fig. 5.1 A).

The sublethal dose in Balb/c mice, on the other hand, did not cause significant weight loss, although there was evidence of clinical illness in some animals. To confirm the lack of significant illness at this dose, the trial was repeated with similar results. Of the Balb/c mice infected with 30 pfu PVM, 47% (14/30) lost weight between days 7 and 11 p.i., dropping 5% of their weight, with no significant difference between the infected group as a whole compared to the control group (Fig. 5.1 C and D). This was representative of the results for the two trials. The dot-plots showing individual mouse weights (Fig. 5.1 B and D) highlight the consistency of the response to a 300 pfu dose in C57Bl/6 mice compared to the variability seen in response to a 30 pfu dose in Balb/c. The Balb/c dot plot also shows that the weight loss observed in individual Balb/c mice coincided with that of the 300 pfu C57Bl/6 group.

In each of these trials, an additional group of C57Bl/6 mice was infected with 30 pfu of PVM to confirm that this dose was not only sublethal in C57Bl/6, but had no clinical effect on the mice. As expected, the 30 pfu C57Bl/6 group continued to gain weight following infection, maintaining weights similar to or, indeed, higher than the mock-infected C57Bl/6 mice run in parallel.

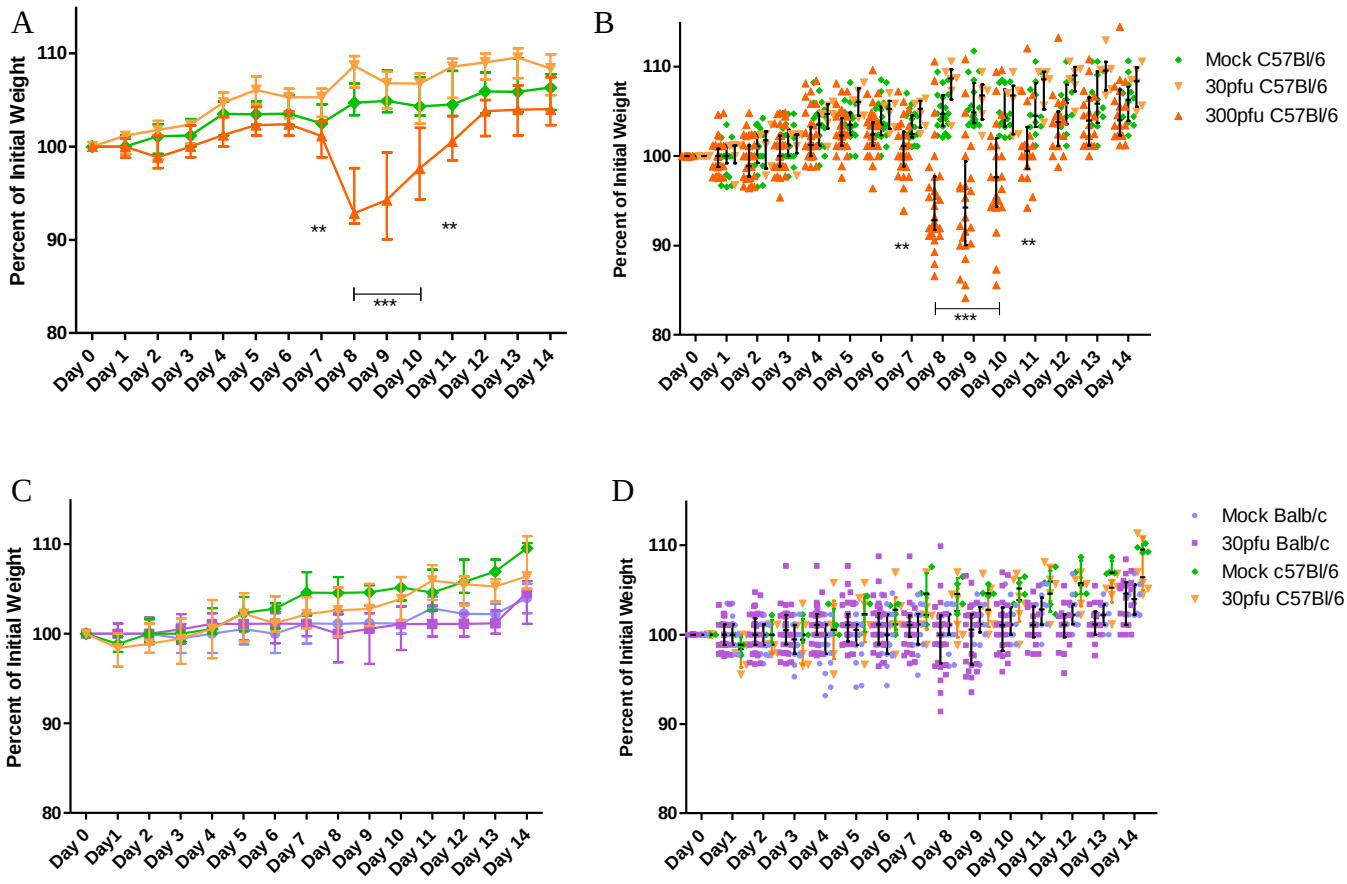
A
B
C
D
Percent of Initial Weight
110
100
90
80
Day 0
Day 1
Day 2
Day 3
Day 4
Day 5
Day 6
Day 7
Day 8
Day 9
Day 10
Day 11
Day 12
Day 13
Day 14
**
***
Mock C57Bl/6
30pfu C57Bl/6
300pfu C57Bl/6
Mock Balb/c
30pfu Balb/c
Mock c57Bl/6
30pfu C57Bl/6

Figure 5.1

Figure 5.1: Weight change associated with PVM infection. 5-6 week old Balb/c and C57Bl/6 mice were inoculated with medium, 30 pfu, or 300 pfu of PVM 15 and weighed daily for 14 days following infection. Weights are expressed as a percentage of each mouse's day 0 weight, such that a weight below 100% indicates weight loss. The panel on the left (A and C) shows the median weight for each group with error bars indicating the interquartile range. In the right-hand panel (B and D), each point represents an individual mouse, with a horizontal line indicating the median and vertical lines indicating the interquartile range. **, $p<0.01$; ***, $p<0.001$.

5.1.2 Viral Replication in the Lungs

As shown previously in the short-term time course, the sublethal dose of 30 pfu in Balb/c mice replicated to the same extent as the 10-fold higher sublethal dose in C57Bl/6 mice, with a maximum viral load on day 6 p.i.. Our long-term trials confirmed this pattern, with sublethally infected Balb/c and C57Bl/6 mice replicating the virus to similar titres on day 6 p.i. (Fig. 5.2). By day 8, Balb/c mice infected with 30 pfu had a significantly lower viral load compared to the 300 pfu C57Bl/6 group. This was in agreement with our previous findings that replication in Balb/c mice tended to have a clear peak on day 6 followed by a decline, while C57Bl/6 mice maintained their virus levels between days 6 and 7 p.i.. By day 10, however, all mice had successfully cleared the infection.

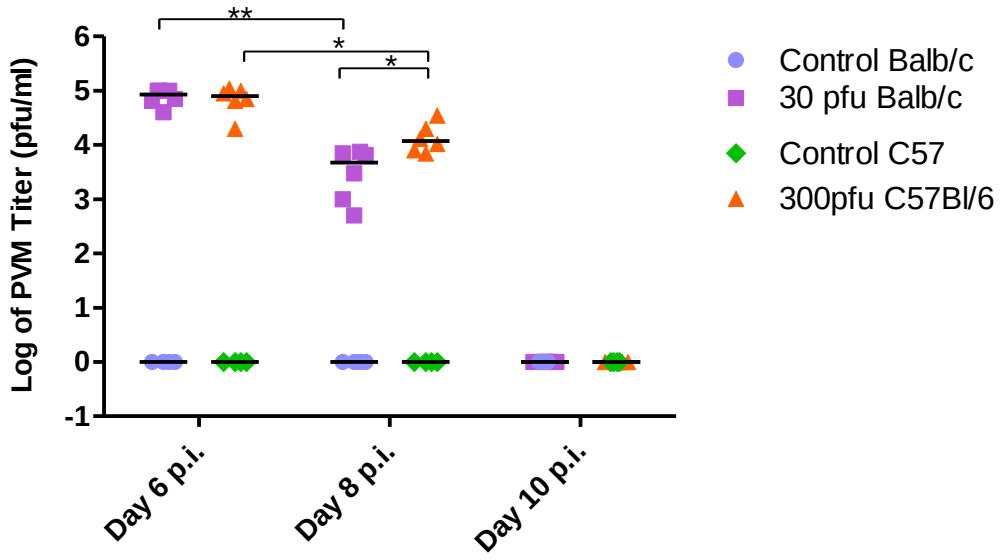
**
*
*
6
5
4
3
2
1
0
-1
Log of PVM Titer (pfu/ml)
Day 6 p.i.
Day 8 p.i.
Day 10 p.i.
Control Balb/c
30 pfu Balb/c
Control C57
300pfu C57Bl/6

Figure 5.2

Figure 5.2. Virus replication in the lungs following PVM infection. 5-6 week old Balb/c and C57Bl/6 mice were inoculated with medium, 30 pfu, or 300 pfu of PVM 15 and lungs were collected on days 6, 8, and 10 p.i.. The viral load is expressed as the log10 of the viral titre in pfu/ml, with each data point representing a single animal and the line representing the group median titre. *, $p<0.05$; **, $p<0.01$.

5.1.3 Cellular Infiltration in the Lungs

Infiltrating immune cells are critical for clearance of the virus, but they also play a role in enhancing illness. In order to assess level of cellular infiltration in the lungs, and the relative populations of inflammatory cells involved, cells collected from lung lavages of 4-6 mice per group were pooled, and differential analysis was performed on prepared cytospins of the BAL cells. The total cell numbers and numbers of macrophages, neutrophils, lymphocytes, and eosinophils in the lungs of sublethally infected and control mice are shown in Figure 5.3.

In general, the 30 pfu dose in Balb/c mice had earlier and prolonged cell infiltration compared to the 300 pfu C57Bl/6 group, although the number of cells was lower in Balb/c mice on days 8 and 10 p.i. (Fig. 5.3 B and C). In terms of total cell number after infection with PVM, both strains had normal cell numbers in the lung wash on day 6 p.i., and developed increased cellularity in the lungs from day 8-14 p.i. (Fig. 5.3 A-D). In C57Bl/6 mice infected with 300 pfu, the influx of cells into the lung followed the pattern of weight loss, with the peak of cellular infiltration on day 10 p.i., returning to normal levels by day 14 p.i.. In Balb/c mice, on the other hand, a dose of 30 pfu induced a much less drastic increase in cell number in the lungs over the course of infection and recovery, with no clear peak in cellular infiltration. By day 28 p.i., both groups of infected mice had normal lung washes (Fig. 5.3 E).

Macrophages constitute the major cell population recovered from the lungs of normal mice. Upon infection with a sublethal dose of PVM, the number of macrophages appeared to increase in the lungs of C57Bl/6 mice between days 8 and 14 p.i., while in infected Balb/c mice the number of macrophages remained the same throughout the infection.

Differential analysis showed that neutrophils peaked in infected C57Bl/6 mice on day 8 p.i. at approximately $8x10^4$ cells, accounting for 21% of the cells recovered from the lungs (Fig. 5.3 B). In spite of the increased total cell number recovered on day 10 from this group of mice, neutrophils dropped to just above half their day 8 levels, making up 7% of the total cells in the lung (Fig. 5.3 C). In infected Balb/c mice, on the other hand, neutrophils appeared earlier and were maintained at levels between $4x10^4$ and $6x10^4$ cells per mouse from days 8-14 p.i., accounting for 16 to 20% of the total cells (Fig. 5.3 B-D). Low levels of background neutrophilia developed in the control Balb/c group on days 14-42, which remains as yet unexplained.

The peak of lymphocyte infiltration was on day 10 p.i. for sublethally infected C57Bl/6 mice, at which point they made up 31% of the cells recovered, with an average of $1.8x10^5$ lymphocytes per mouse (Fig. 5.3 C). Similarly, Balb/c mice infected with a sublethal dose of PVM had 30% lymphocytes on day 10, but the variability in their total cell numbers was such that lymphocyte levels were similar on days 10 and 14 p.i., at $6.5x10^4$and $5.5x10^4$, respectively (Fig. 5.3 C and D). By day 28, a low number of lymphocytes remained in the lungs of infected Balb/c mice, making up 5% of BAL cells (Fig. 5.3 E).

Eosinophils were observed in low numbers, accounting for no more than 2% of total BAL cells. In C57Bl/6 mice they were present at 1% on day 6, increasing to 2% of BAL cells on days 8-14 p.i., such that their absolute number increased in parallel with the total cell number to a peak of $1.1x10^4$ on day 10 p.i.. However, the mock-infected group showed 1% eosinophil levels on day 14 p.i., which amounted to $1x10^3$ cells per mouse. Balb/c mice infected with 30 pfu of PVM had $3x10^3$ eosinophils in the lungs on day 14 p.i., which was also just 1% of the BAL cells, and no eosinophils were detected in the lungs of mock-infected Balb/c mice.

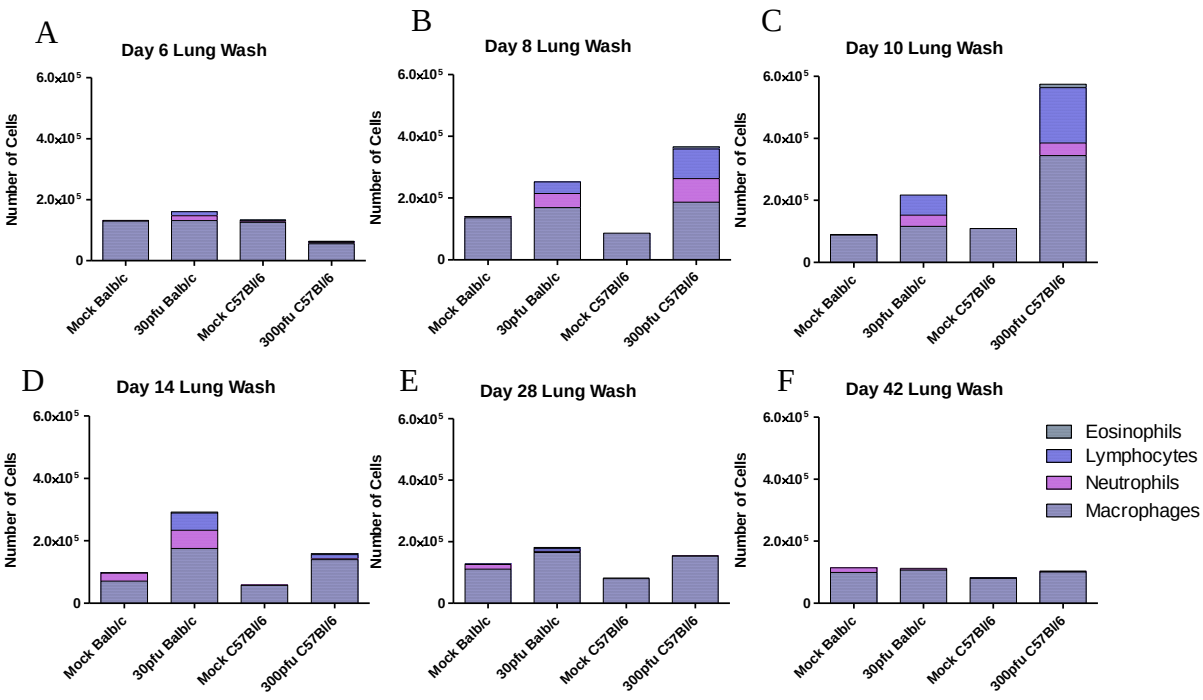
A
Day 6 Lung Wash
B
Day 8 Lung Wash
C
Day 10 Lung Wash
D
Day 14 Lung Wash
E
Day 28 Lung Wash
F
Day 42 Lung Wash
Number of Cells
6.0x10⁵
4.0x10⁵
2.0x10⁵
0
Mock Balb/c
30pfu Balb/c
Mock C57Bl/6
300pfu C57Bl/6
Eosinophils
Lymphocytes
Neutrophils
Macrophages

Figure 5.3

Figure 5.3: Cellular infiltration in the lungs of PVM infected Balb/c and C57Bl/6 mice. 5-6 week old Balb/c and C57Bl/6 mice were inoculated with medium, 30 pfu, or 300 pfu of PVM 15 and sacrificed on days 6, 8, 10, 14, 28, and 42 p.i.. Cells collected from the pooled lung washes of 4-6 animals were stained and differentially analyzed for the presence of macrophages, neutrophils, lymphocytes, and eosinophils. The average number of these cells is shown, calculated based on the number of total cells collected from the group and the proportion of these cell populations in the lungs.

5.2 Cell-mediated Immune Response

To determine the T-helper bias of the cell-mediated immune response elicited by PVM in Balb/c and C57Bl/6 mice, we performed IFN-γ and IL-5 ELISPOT assays by restimulating splenocytes with antigen from heat-inactivated PVM-infected and mock-infected cell lysates. The number of PVM-induced activated T cells was determined for each mouse by subtracting the number of spots generated in response to mock-infected cell lysate from those generated by PVM-infected cell lysate.

The response to PVM was Th1-biased in both strains of mice. All infected mice generated significantly higher numbers of PVM-specific IFN-γ-secreting cells compared to mock-infected animals of the same strain ($p=0.0022$ for all comparisons) (Fig. 5.4A). IL-5-secreting cells, on the other hand, remained low at all time points, although Balb/c mice did have a significantly higher number of IL-5-secreting cells than the mock-infected Balb/c mice analyzed in parallel (Fig. 5.4 B). The two strains showed a clear difference in the pattern of T-cell response, with infected Balb/c mice generating a similar number of IFN-γ spots between days 14 and 42 p.i., while C57Bl/6 mice showed high IFN-γ production on day 14 p.i. which dropped significantly by day 28 p.i. ($p=0.0022$). The two strains had significantly different numbers of IFN-γ secreting cells at all three time points, with C57Bl/6 mice showing higher levels than Balb/c mice on day 14 p.i. and lower levels on days 28 and 42 p.i. ($p<0.01$).

On day 28 p.i., the T cell response in C57Bl/6 mice inoculated with 30 pfu of PVM was evaluated as a control for the ten-fold difference in initial PVM dose between the sublethal doses in the two strains. In the first trial, comparing a dose of 300 pfu and 30 pfu in C57Bl/6 mice on day 28 p.i., the 300 pfu C57Bl/6 group had fewer IFN-γ secreting splenocytes than expected

based on preliminary results. The 30 pfu C57Bl/6 group had significantly lower PVM-specific IFN-γ response than the 300 pfu C57Bl/6 group run in parallel. When this dose was repeated in the Balb/c trial, the 30 pfu C57Bl/6 group showed an enhanced IFN-γ response compared to the previous trial (Fig. 5.4C). However, the difference in the IFN-γ response between the two 30 pfu C57Bl/6 groups parallels the mock-infected mice assayed on the same day, with a lower background response in the C57Bl/6 trial. A direct comparison of a 30 pfu dose in Balb/c and C57Bl/6 mice showed that the C57Bl/6 mice had a significantly lower number of PVM-specific IFN-γ-secreting splenocytes than the Balb/c mice ($p=0.0043$). The response measured in the Balb/c trial was representative of two trials. Although the two sublethal doses were not compared directly in this experiment, our preliminary results showed, similarly, that 30 pfu induced a stronger IFN-γ cell-mediated response in Balb/c mice than a 300 pfu dose in C57Bl/6 mice.

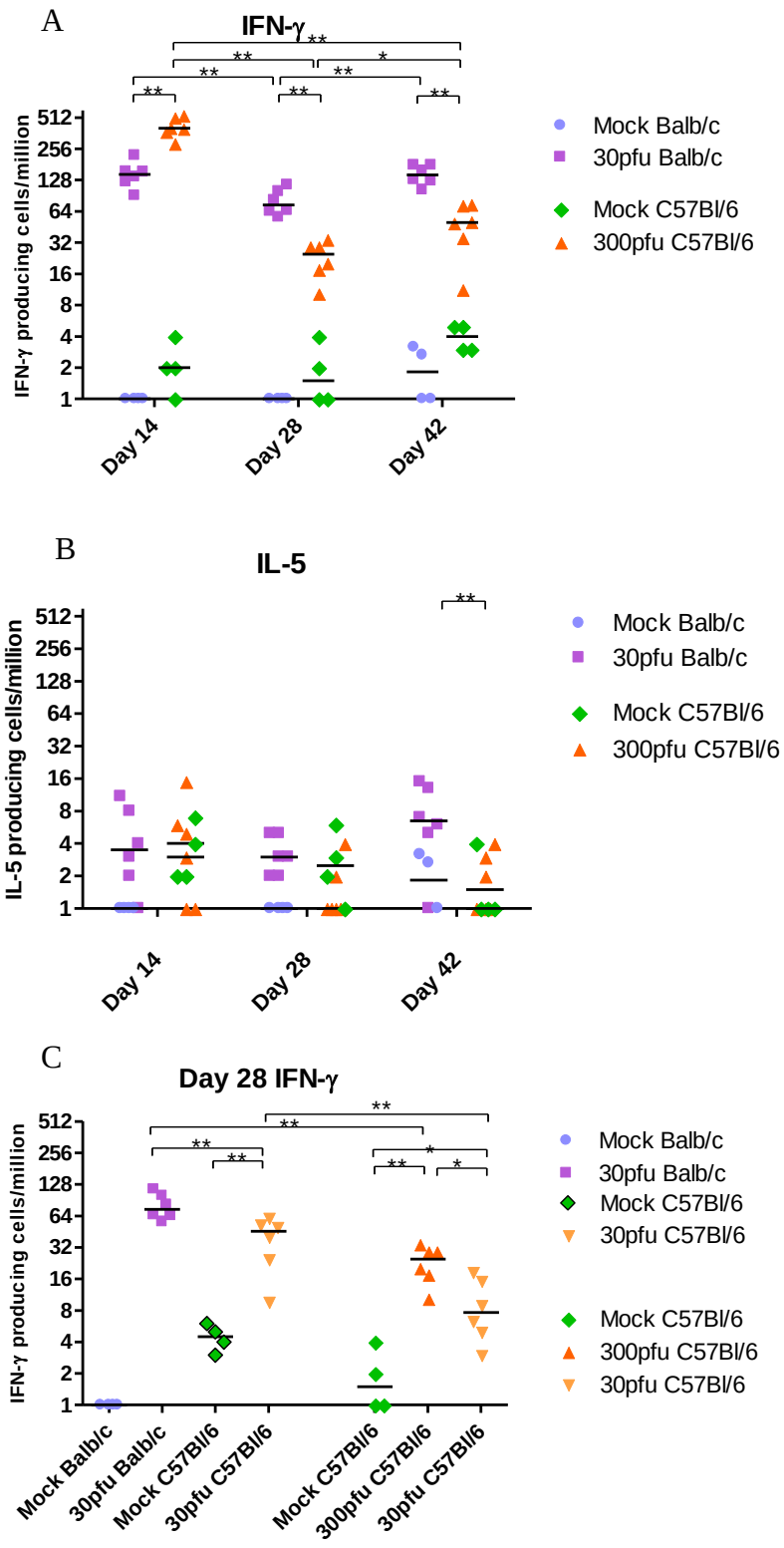
A
IFN-γ
IFN-γ producing cells/million
512
256
128
64
32
16
8
4
2
1
Day 14
Day 28
Day 42
Mock Balb/c
30pfu Balb/c
Mock C57Bl/6
300pfu C57Bl/6
B
IL-5
IL-5 producing cells/million
C
Day 28 IFN-γ
30pfu C57Bl/6
Mock Balb/c
30pfu Balb/c
Mock C57Bl/6
30pfu C57Bl/6

Figure 5.4

Figure 5.4: Time course of PVM-specific IFN-γ-secreting (A) and IL-5-secreting (B) splenocytes following *in vitro* restimulation with PVM-infected cell lysates. (C) IFN-γ-secreting splenocytes in 30 pfu C57Bl/6 mice compared to the sublethal dose run in parallel on day 28 p.i.. 5-6 week old Balb/c and C57Bl/6 mice were inoculated with medium, 30 pfu, or 300 pfu of PVM 15 and sacrificed on days 14, 28, and 42 p.i.. The PVM-specific response is calculated by subtracting the number of cytokine-secreting cells restimulated with mock-infected cell lysates from those restimulated with PVM-infected lysates. The data points represent individual animals, with the median indicated by a line. *,$p<0.05$; *,$p<0.01$.

5.3 Humoral Immune Response

To examine the PVM-specific humoral response induced by a sublethal infection, production of IgA, IgE, and IgG in the lungs and sera of Balb/c and C57Bl/6 mice was measured by ELISA. We found that neither strain produced IgE in the sera or lungs. IgA was detected in the lungs of both strains by day 14 p.i., while IgG was detected in the lungs and sera of both strains by day 14 p.i..

Balb/c mice showed increasing levels of IgG and IgA in the lungs, as well as increasing IgG in the serum between days 14 and 42 p.i.. Although they generally had the same, or lower levels of antibodies as Balb/c mice, the response of the C57Bl/6 mice had already reached a maximum by day 14 p.i.. The C57Bl/6 mice maintained their day 14 antibody levels to day 42.

5.3.1 Serum IgG

The IgG production in the serum of sublethally infected Balb/c and C57Bl/6 mice was compared on days 14, 28, and 42 p.i.. All infected animals had significantly higher serum IgG than mock-infected animals sacrificed in parallel ($p=0.0095$ for all comparisons). In general, Balb/c mice produced increasing amounts of IgG throughout this time period, while C57Bl/6 mice showed no increase. The data shown in Figure 5.5 are representative of both Balb/c trials.

Between days 14 and 28, serum IgG significantly increased in Balb/c mice infected with 30 pfu ($p=0.0022$), and continued to rise between days 28 and 42 ($p=0.026$), such that the day 14 levels were also significantly lower than day 42 serum IgG ($p=0.0022$) (Fig. 5.5 A). C57Bl/6 mice on the other hand, had significantly higher levels of serum IgG than Balb/c mice on day 14

p.i. (p=0.026), and they maintained their serum IgG at a similar level on days 28 and 42 p.i. (Fig 5.5 A).

Serum IgG in the 30 pfu C57Bl/6 mice was assessed on day 28 p.i., and the levels of PVM-specific IgG were similar to that of both the 30 pfu Balb/c mice and the 300 pfu C57Bl/6 mice (Fig. 5.5 B).

5.3.2 Neutralizing Antibody in Serum

To determine the biological effectiveness of the antibodies produced in these two strains of mice, a virus neutralization assay, which assesses the capacity of serum to neutralize PVM *in vitro*, was performed on day 28 p.i.. The dilution of serum at which the virus was completely neutralized is shown in Figure 5.5 C.

All infected mice developed neutralizing antibodies in the serum, while the serum of mock-infected animals was non-neutralizing. Despite having similar levels of PVM-specific IgG in the serum, the 300 pfu C57Bl/6 mice had significantly higher neutralizing antibody titres compared to the 30 pfu Balb/c mice (p=0.0198) (Fig. 5.5 C). Similarly, the 300 pfu C57Bl/6 mice also had higher neutralizing antibody titres compared to those inoculated with 30 pfu (p=0.0242) (Fig. 5.5 C).

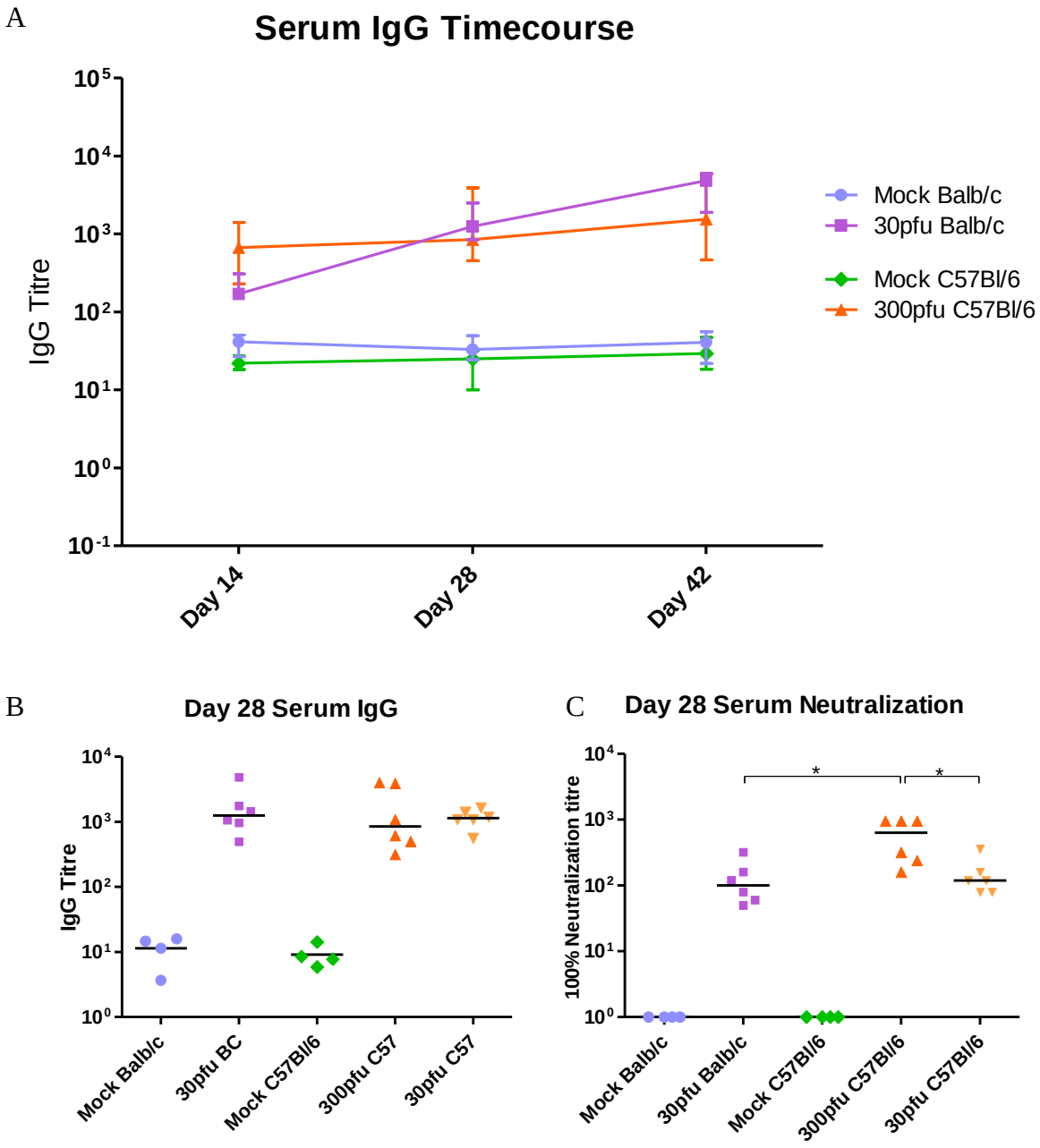
A
Serum IgG Timecourse
IgG Titre
Day 14
Day 28
Day 42
Mock Balb/c
30pfu Balb/c
Mock C57Bl/6
300pfu C57Bl/6
B
Day 28 Serum IgG
IgG Titre
Mock Balb/c
30pfu BC
Mock C57Bl/6
300pfu C57
30pfu C57
C
Day 28 Serum Neutralization
100% Neutralization titre
Mock Balb/c
30pfu Balb/c
Mock C57Bl/6
300pfu C57Bl/6
30pfu C57Bl/6

Figure 5.5

Figure 5.5: PVM-specific antibody response in the serum. 5-6 week old Balb/c and C57Bl/6 mice were inoculated with medium, 30 pfu, or 300 pfu of PVM 15 and sacrificed on days 14, 28, and 42 p.i.. (A) shows the timeline of serum IgG production, and (B) shows the day 28 serum IgG on the left and neutralizing titres on the right. In (A), the symbols represent the group median, with error bars indicating the interquartile range. In (C) the neutralization titre is measured by the dilution of serum at which 100% of the virus was neutralized, and in (B) and (C) each data point represents an individual animal, with the group median indicated by a line. *, $p<0.05$.

5.3.3 Lung IgG

The IgG levels were lower in the lungs than in the serum, though its production followed a similar pattern (Fig. 5.6 A). All infected groups had significantly higher levels of lung IgG than the mock-infected groups run in parallel. Infected C57Bl/6 mice showed no change in lung IgG levels from days 14 to 42 p.i., while lung IgG increased in infected Balb/c mice during this time (Fig. 5.6 A). The Balb/c mice had similar levels of lung IgG on days 14 and 28, which increased to a statistically higher level by day 42 than either of the earlier time points ($p=0.0022$ compared to day 14, and $p=0.0087$ compared to day 28). There was no significant difference in lung IgG levels between the sublethally infected Balb/c and C57Bl/6 mice at any of these time points.

The 30 pfu C57Bl/6 mice were assessed for lung IgG levels on day 28 p.i., and they had similar levels to the 300 pfu C57Bl/6 group, and significantly lower levels than the 30 pfu Balb/c group (Fig. 5.6 C).

5.3.4 Lung IgA

The levels of mucosally-derived IgA were measured in the supernatants of lung fragment cultures collected on days 14-42 p.i. (Fig. 5.6 B). C57Bl/6 had low levels of IgA that peaked on day 28 p.i., at a significantly higher level than either day 14 or day 42 ($p=0.0260$). The Balb/c mice had low levels of IgA on day 14 p.i., rising to significantly higher levels by days 28 and 42 ($p=0.0260$ in both cases). There was no difference between day 28 and day 42 levels in Balb/c mice. Comparing between C57Bl/6 and Balb/c mice, the two strains had similar levels of lung IgA on day 14 p.i., while on days 28 and 42, Balb/c mice had significantly higher levels ($p=0.0043$ and $p=0.0022$, respectively).

On day 28 p.i., the 30 pfu C57Bl/6 mice were also assessed for levels of lung IgA (Fig. 5.6 D). They had lung IgA levels similar to those in the 300 pfu C57Bl/6 mice, but significantly lower than those in the Balb/c group ($p=0.0022$).

5.3.5 Neutralizing Antibody in Lungs

The neutralizing capacity of the antibodies produced in the lung was determined using a virus neutralization assay, as previously described for the serum. The results were similar to those for neutralizing antibodies in the serum, though the lung fragment culture supernatants had a lower neutralizing capacity overall, and there was more overlap between the different groups of mice (Fig. 5.6 E). The 300 pfu C57Bl/6 group had significantly higher neutralizing titres on day 28 p.i. compared to the 30 pfu Balb/c group ($p=0.0484$). Similarly, the Balb/c mice had significantly lower neutralizing titres compared to C57Bl/6 mice inoculated with the same dose ($p=0.0222$).

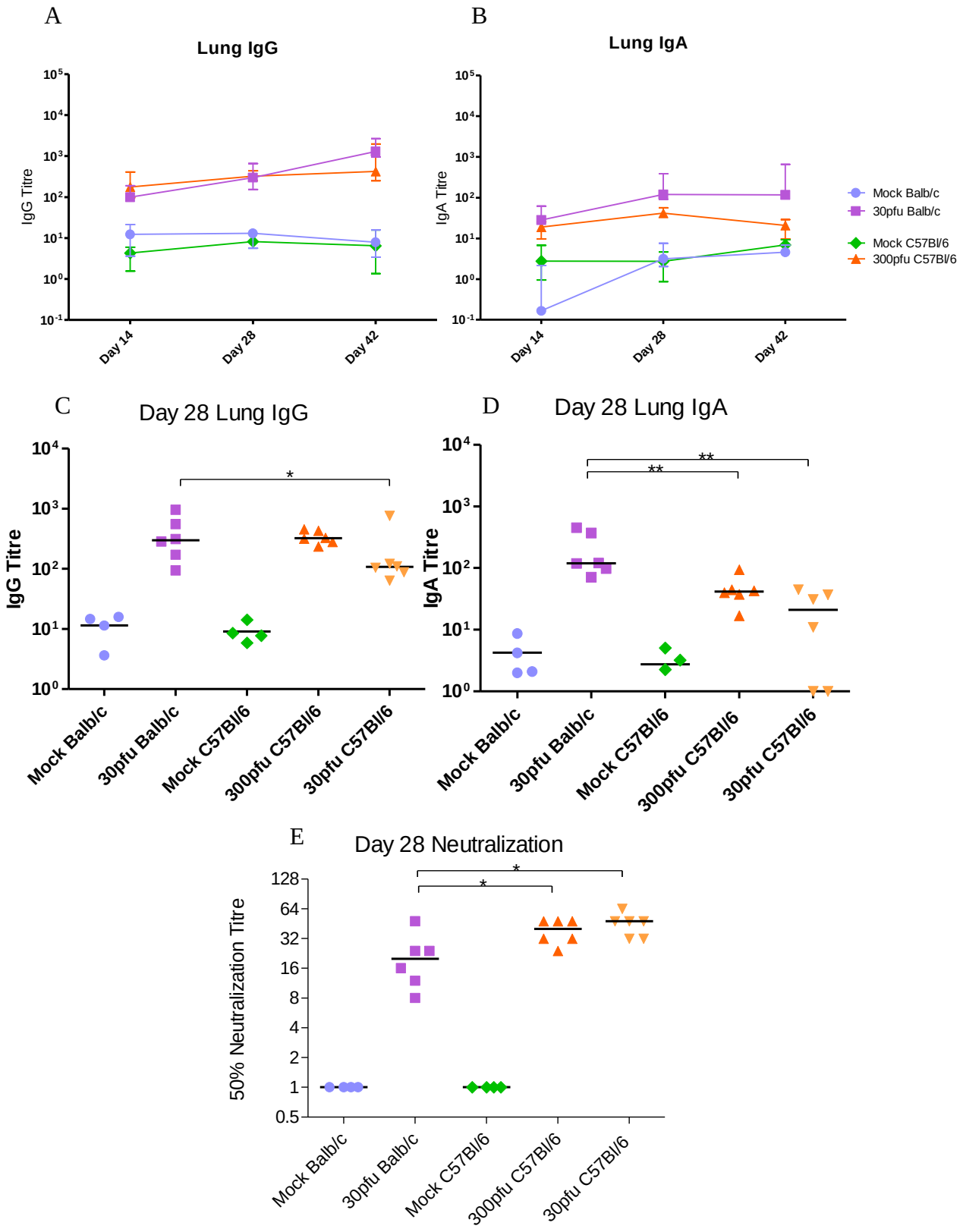
A
Lung IgG
IgG Titre
Day 14
Day 28
Day 42
B
Lung IgA
IgA Titre
Mock Balb/c
30pfu Balb/c
Mock C57Bl/6
300pfu C57Bl/6
C
Day 28 Lung IgG
IgG Titre
D
Day 28 Lung IgA
IgA Titre
E
Day 28 Neutralization
50% Neutralization Titre
Mock Balb/c
30pfu Balb/c
Mock C57Bl/6
300pfu C57Bl/6
30pfu C57Bl/6

Figure 5.6

Figure 5.6: PVM-specific antibody response in the lungs. 5-6 week old Balb/c and C57Bl/6 mice were inoculated with medium, 30 pfu, or 300 pfu of PVM 15 and sacrificed on days 14, 28, and 42 p.i. to determine the time course of lung IgG (A) and IgA (B) production. The top panel, (A) and (B), shows the time course of antibody production in the lungs, with symbols representing the group median and vertical lines indicating the interquartile range. In the lower panels, each data point represents an individual animal, with the group median indicated by a line. The day 28 IgG and IgA titres in the lungs are depicted in (C) and (D), respectively, and the neutralizing antibody titre is shown in (E). Neutralizing antibody titres were measured as the dilution of lung fragment culture supernatant at which 50% of the virus was neutralized. *, $p<0.05$; **, $p<0.01$

6.0 Discussion and Conclusions

6.1 Pathogenesis of PVM *in vivo*

In recent years, much work has been done evaluating the rodent Pneumovirus, PVM, as a model of severe infection with RSV in infants. In the majority of studies, the mouse-passaged J3666 strain of PVM is used, although PVM 15, available from the American Type Culture Collection, is now also recognized as a pathogenic strain. Originally, strain 15 was believed to be attenuated in mice, but subsequent analysis showed that it is in fact quite pathogenic, though it appears to be less so than the J3666 strain [181, 182].

The difference in pathogenicity is evident from independent studies where inoculation with as few as 20 particles of PVMJ3666 was found to be lethal in C57Bl/6 by day 8-9 p.i., while C57Bl/6 mice given a 10-fold higher dose of PVM 15 recovered by day 14 p.i. [160, 165]. Our study showed that PVM 15 had a similar pathogenicity to that reported by Frey et al., with the 300 pfu dose in C57Bl/6 mice inducing a clinically relevant but sublethal infection [165]. The onset of illness and the nature of the immune response were also similar to that reported for C57Bl/6 given 200 pfu of PVM 15 [165].

In agreement with the difference in pathogenicity, the progression of PVM J3666 infection appears to be slightly different from strain 15. While both strains of virus effect a heavy influx of leukocytes, especially granulocytes, into the lungs, there are substantial differences in the nature of this response between the two viral strains. In response to PVM J3666, Balb/c and C57Bl/6 mice experience neutrophilia beginning on day 3 p.i. that increases over the course of infection [159, 183]. Our results suggest that neutrophilia commences later upon infection with PVM 15, although the highest dose, 3000 pfu, induced moderate levels of neutrophils in Balb/c

mice by day 3 p.i.. The degree of neutrophilia induced by PVM J3666 did not appear to be dose-dependent in Balb/c mice [159], unlike what we saw in our trials with PVM 15. In C57Bl/6 mice sublethally infected with PVM J3666, the peak of neutrophil influx occurred on day 7 p.i. [159], which was similar to our findings, where neutrophils peaked on day 8 p.i. in response to a sublethal dose of PVM 15. However, the onset of neutrophilia was earlier in J3666 infection, with day 3 levels exceeding day 10 levels [183], while we found that neutrophils were undetectable until day 7 p.i. and remained high up to day 10 p.i..

In addition to neutrophils, eosinophils appear to play a role in PVM J3666 pathogenesis, while they were largely absent in the lungs of mice infected with PVM 15. Like neutrophils, eosinophils were recruited to the lungs of PVM J3666-infected Balb/c and C57Bl/6 mice on day 3 p.i., though at levels around 10-fold lower than neutrophils [159, 183]. The peak of eosinophilia occurred on day 3, with levels dropping thereafter [159, 183]. In Balb/c mice, eosinophils appeared to be recruited in a dose-dependent manner [159]. By contrast, we found that eosinophils were increased in the lungs of C57Bl/6 mice on days 6-10 following a 300 pfu dose of PVM 15, but never rose over 2% of the total cells in the lung. In addition, they appeared in low numbers on day 6 p.i. in 3000 pfu Balb/c mice, at which point the mice were moribund. Otherwise, eosinophils were not detected in response to PVM 15, which is quite different from what is reported for PVM J3666.

It is well documented that Balb/c mice are more susceptible to PVM infection than C57Bl/6 mice despite these differences in the pathogenesis of PVM J3666 and PVM 15 [35, 160]. The Balb/c strain develops earlier and stronger responses to PVM, with enhanced production of proinflammatory cytokines and chemokines and earlier influx of immune cells compared to C57Bl/6 mice [160, 161]. Therefore, our goal was to explore the basis of this

difference by directly comparing their immune response to lethal and sublethal doses of PVM 15.

6.2 Initiation of the Immune Response and Viral Replication

In the more susceptible Balb/c strain, PVM replication was enhanced, with earlier onset of detectible virus in the lungs, replicating to an earlier and higher peak, compared to C57Bl/6 mice given the same dose. The different pattern of replication in the two strains, characterized by the slower, steadier increase of PVM in the lungs of C57Bl/6 strain rather than the rapid increase followed by a decline seen in Balb/c mice may indicate different mechanisms of fighting PVM infection. There are several possibilities that could lead to the difference in susceptibility between these two strains, at the level of infection, replication, cell-to-cell spread, or immune-mediated viral clearance. Since C57Bl/6 mice can suppress not only PVM replication, but the inflammatory response as well, the difference may be due to the presence of one or more factors in the lung that lowers the capacity of PVM to infect or replicate *in vivo*.

One of the first sites to examine is the respiratory epithelium itself, since it is the primary target of pneumovirus infection and therefore initiates the immune response. Even before infection begins, the lungs can be partially protected by the immunomodulatory effects of surfactant proteins (SP) secreted by type II pneumocytes in the lower airways. Two of these proteins, SP-A and SP-D, act as PRRs in the lung and interact with pathogens including RSV, aiding in opsonization [184-186]. SP-A binding to RSV has been shown to enhance the phagocytosis of RSV by human macrophages and cultured monocytes [184]. In addition, SP-A binds directly to TLR4 present on macrophages and downregulates receptor signalling, thereby acting as an anti-inflammatory molecule [187]. Infection of cultured type II pneumocytes with

RSV upregulates expression of SP-A mRNA but decreases its secretion *in vitro* [188]. This finding is supported by a study of infants hospitalized with severe RSV bronchiolitis, which found decreased levels of SP-A and SP-D in BALs compared to control infants [189].

Not only has the role of surfactant proteins in RSV pathogenesis been studied in infants and human cells, several studies using the murine model of RSV infection have also been carried out. RSV infection in SP-A knock-out mice is more severe than in wild-type mice, replicating to higher titres and inducing a stronger influx of neutrophils to the lungs [190]. RSV infection *in vivo* also causes wild-type Balb/c mice to produce surfactant inhibitors, as demonstrated both by the reduced function of surfactant collected in the BAL of infected mice as well as the inhibition of calf surfactant that was incubated with these BAL samples [191]. Intriguingly, a paper examining the role of surfactant proteins in the susceptibility of Balb/c and C57Bl/6 to airway hyperresponsiveness found that the basal levels of surfactant A and D proteins are different in the lungs of naive Balb/c and C57Bl/6 mice, and are differentially upregulated upon sensitization with antigens [192]. Somewhat counterintuitively, Balb/c mice actually have higher levels of SP-A and lower levels of SP-D than the C57Bl/6 strain. SP-D is upregulated in both strains upon sensitization with *Aspergillus fumigatus* antigen, but to a higher degree in the C57Bl/6 mice. These findings could point to a more prominent role for SP-D than SP-A in protection from PVM, although this remains to be investigated.

Given the immunomodulatory effects of surfactant proteins, their impact on RSV infection *in vivo* and *in vitro*, as well as RSV's impact on their expression, secretion, and functional activity, there is a strong possibility that they play a role in the differential susceptibility of Balb/c and C57Bl/6 mice during pneumovirus infection *in vivo*.

Another factor that could allow C57Bl/6 mice to suppress the replication of PVM without activating the immune system could be the surface expression of key TLRs, both in naïve mice and after infection. TLR4 is expressed on the surface of human and murine alveolar macrophages and DCs, and the response to RSV infection in mice relies on TLR4 and CD14 [74, 79, 187, 193-196]. Naïve Balb/c mice have higher TLR4 mRNA expression in the lungs than C57Bl/6 mice, which may indicate a difference in TLR surface expression on resident macrophages or the respiratory epithelium [197]. If Balb/c macrophages have higher levels of surface TLR4, this could trigger a stronger and earlier immune response to PVM infection than that in C57Bl/6 mice. Similarly, the interaction of RSV with TLR2/TLR6 dimers is important for the activation of innate responses *in vivo*, and while both strains expressed high levels of TLR2, Balb/c mice had higher levels of TLR6 mRNA in the lung than C57Bl/6 [75, 197].

TLR3 signalling has been shown to play a role in the response of the airway epithelium to RSV, and this PRR was not expressed in the lungs of naïve Balb/c mice [47, 197]. Its expression is upregulated in cultured human respiratory epithelial cells upon infection with RSV, as well as following infection of mice with RSV [198]. Knock-out of TLR3 in the C57Bl/6 genetic background did not affect RSV replication, but caused the mice to produce higher quantities of Th2 biased cytokines and eosinophilia [198]. Since Balb/c mice lack TLR3 expression in the lungs prior to infection, while C57Bl/6 mice express this PRR, this may also influence the nature of the response to PVM infection *in vivo* [197]. Given the difference in TLR expression between these two strains, an analysis of the capacity of primary respiratory epithelial cells and alveolar macrophages isolated from Balb/c and C57Bl/6 to support and respond to PVM infection would give important information about the mechanisms they use to suppress viral replication *in vivo*.

6.3 Cellular Influx and Inflammatory Mediators

The interplay of inflammatory mediators and pneumovirus infection in mice has long been recognized as a critical pathway leading to lung pathology. The lesions caused by RSV and PVM *in vivo* are due in part to the virus itself, but largely to inflammatory responses that cause excessive damage to the lung tissue. Control of lung inflammation generally inhibits viral clearance, despite improving outward signs of clinical infection. Similarly, the application of antiviral compounds after the onset of viral replication has little effect on disease progression, likely because the wave of inflammation has already been set in motion.

The most thoroughly researched chemokine in pneumovirus pathogenesis is MIP-1α, the role of which has been examined during RSV infection in infants and mice, as well as during PVM infection in mice. Although some parallels are evident in the role of MIP-1α in PVM and RSV infection, there are also striking differences in the role of this chemokine in the murine model of pneumovirus pathogenesis. MIP-1α is upregulated in lung washes and nasopharangeal aspirates of RSV-infected infants and is associated with disease severity [199, 200]. Likewise, it is also upregulated upon infection of mice with RSV and PVM [87, 160].

During murine RSV infection, MIP-1α depletion using antibodies had no effect on viral replication or NK responses, but reduced T cell recruitment to the lungs by day 7 p.i. [67]. Paradoxically, while total T cell numbers were reduced, there was an increase in the number of activated RSV-specific CD8 T cells secreting IFN-γ and TNF-α, which led to enhanced pathology and weight loss in these mice [67]. However, in another study, blockade of MIP-1α signalling by deletion of CCR1 had no effect on viral replication, cellular influx, or morbidity associated with RSV infection [87].

PVM pathogenesis, by contrast, is strongly governed by MIP-1α production *in vivo*. Transgenic mice in the C57Bl/6 background that lack functional MIP-1α or CCR1 are more susceptible to infection with PVM J3666, and had drastically reduced levels of neutrophil infiltration, with no eosinophils and very low levels of lymphocytes in the lungs upon infection with PVM [160, 201]. The virus also replicated to a higher titre in these mice and they succumbed to infection earlier than non-transgenic littermates, suggesting that cells responding to MIP-1α are important for controlling PVM infection. However, blockade of MIP-1α signalling by the CCR1/CCR5 receptor antagonist, Met-RANTES, resulted in decreased lung inflammation without affecting PVM replication in the lungs [201]. The group found that reducing disease severity in MIP-1α-deficient mice required the application of the antiviral Ribavirin to control viral replication, as MIP-1α blockade or Ribavirin alone did not reduce disease severity *in vivo* [201, 202].

Our results showed that MIP-1α was upregulated earlier in Balb/c mice infected with PVM 15, as evidenced by transcript upregulation in high dose animals by day 3 p.i., and higher levels of MIP-1α mRNA upregulation in 300 pfu Balb/c mice on day 5 p.i. compared to C57Bl/6 mice inoculated with the same dose. Indeed, a 30 pfu dose in Balb/c mice induced similar levels of MIP-1α mRNA upregulation as the 300 pfu dose in C57Bl/6. By day 6, however, the 3000 pfu C57Bl/6 mice were producing higher levels of MIP-1α protein than 3000 pfu Balb/c mice, and these levels were similar to the 300 pfu C57Bl/6 mice assayed on the same day. Strikingly, other than the difference between the 3000 pfu dose in Balb/c and C57Bl/6 mice, MIP-1α was produced at a similar level in all infected mice by day 6 p.i..

Similarly, Domachowske et al. compared the production of MIP-1α in Balb/c mice inoculated with 60 pfu of PVM J3666 with another study by the group using C57Bl/6 mice

inoculated with 200 pfu. The Balb/c mice given a lower dose had earlier and higher production of MIP-1α than C57Bl/6 mice inoculated with 200 pfu [203]. In their study, MIP-1α production in Balb/c mice peaked on day 4 p.i., while the other study showed that it continued to rise in C57Bl/6 mice. By day 5 p.i. the levels in C57Bl/6 were still below the peak levels reached in Balb/c mice, but they may have continued to rise to higher levels after day 5, as Bonville et al. saw an increase in proinflammatory mediators between days 3 and 7 p.i., with a peak on day 7 [183]. Based on these results and our own, the production of MIP-1α was delayed in Balb/c infected with PVM 15 relative to Balb/c mice infected with PVM J3666, while C57Bl/6 mice appeared to have a similar time-course of MIP-1α production in response to the two strains of PVM.

Interestingly, in examining the contribution of IFN-γ to PVM-induced illness, Bonville et al. found that the combination of IFN-γ and MIP-1α was necessary to induce neutrophil influx in response to PVM [161]. Indeed, neutrophil infiltration, lung pathology, and weight loss could be induced simply by overexpression of MIP-1α in the lungs of Balb/c mice given exogenous IFN-γ *in vivo* [161]. This result is interesting, given our findings that Balb/c mice respond to PVM 15 infection with earlier and enhanced production of both IFN-γ and MIP-1α compared to C57Bl/6 mice. Since neutrophils dominated the response to PVM 15 infection in Balb/c mice, the combined effect of MIP-1α and IFN-γ may be important for the difference in the response between these strains.

Further support for their hypothesis stems from a comparison between the high and low dose C57Bl/6 mice in our trials. The high dose group expressed higher levels of IFN-γ and MIP-1α transcripts on day 5 p.i. and both proteins were first detectible in the lungs by day 6 p.i.. Accordingly, these animals displayed a marked increased in both neutrophil and lymphocyte

levels in the lungs between day 5 and 7 p.i.. Examination of the low dose animals, however, showed that despite lower upregulation at the mRNA level on day 5, the 300 pfu C57Bl/6 group was secreting levels of MIP-1α that were similar to those produced by the 3000 pfu group by day 6. However, as would be expected given the results of the Bonville study, the lack of IFN-γ production in low dose C57Bl/6 mice was associated with little to no cellular infiltration on day 6 p.i., despite high levels of MIP-1α in lung tissues. Examination of the IFN-γ and MIP-1α production in these mice between days 6 and 14 p.i. will further elucidate the mechanism of neutrophil recruitment in this strain.

In addition to its apparent role in neutrophil infiltration, IFN-γ production is a hallmark of Th1 bias, which is critical for directing the nature of the long-term response to sublethal doses. A study of Balb/c mice inoculated with 10 pfu of PVM J3666 showed that IFN-γ production in the lungs on day 6 p.i. was due to the combined effects of NK cells and CD8 T cells [161]. In terms of total number of cells in the lung, CD4 and CD8 T cells were present in similar numbers, but only 1.4% of CD4 T cells were secreting IFN-γ compared to 11% of CD8 T cells. Despite lower total numbers of NK cells in the lungs, 23% of them were secreting IFN-γ on day 6 p.i.. As such, the number of CD8 T cells secreting IFN-γ in the lungs was around three times the number of IFN-γ-secreting NK cells [161].

Similarly, in a study on the role of T cells in clearance of PVM 15 from the lungs of C57Bl/6 mice, the authors found that neutrophils and macrophages were the predominant cell type in lung lavages up to day 6 p.i., but CD8 T cells dominated the response between days 8 and 10 [165]. This time period coincides with the clearance of PVM from the lungs and weight loss, suggesting that CD8 T cells might play a role in these events. The role of CD8 and CD4 T cells was further elucidated by depletion and knock-out experiments, which showed that the combined

effect of CD4 and CD8 T cells are important for clearance of PVM 15. Mice lacking functional T cell receptors displayed no weight loss in response to PVM 15, but maintained high titres of PVM in the lungs for more than a month following infection [165]. Knock-out of individual CD4 or CD8 T cell populations, however, had little effect on weight loss and no effect on viral clearance. Mice depleted of both T cell subsets with monoclonal antibodies for CD4 and CD8 responded similar to the T cell receptor knock-out mice with asymptomatic infection and poor viral clearance. Interestingly, the presence or absence of T cells had little effect on the response to a lethal dose of PVM 15 [165].

Tying these results in with the previous findings on IFN-γ in PVM pathogenesis, as well with as our own studies, it is likely that early production of IFN-γ relies on the contribution of NK cells and drives inflammatory processes leading to immune cell influx. In sublethally infected mice, IFN-γ production by CD8 T cells and supported by T helper cells plays a role in clearance of the virus from the lungs and is likely associated with weight loss. This may be similar to the role that IFN-γ plays in RSV pathogenesis in infants, as IFN-γ appears to be produced in the airways upon infection with RSV, and weak cell-mediated IFN-γ responses or the absence of CD8 T cells in the respiratory tract has been associated with severe lower respiratory tract infection that leads to mechanical ventilation and death [103, 121, 204, 205]. This supports the notion that while IFN-γ may mediate RSV-induced pathology, it likely also plays a role in protection from severe RSV bronchiolitis.

Although neutrophil recruitment in response to PVM infection has been shown to be partially dependent on MIP-1α and IFN-γ secretion *in vivo*, low levels of neutrophils are still recruited in the absence of either of these two molecules [160, 161]. The action of MIP-2, a chemokine that signals through CXCR2 on neutrophils, may be an alternate route of neutrophil

activation and chemotaxis in mice lacking MIP-1α signalling. The human functional homologue of MIP-2 is IL-8, which likewise signals through human CXCR2 and CXCR1. IL-8 is produced in response to RSV infection of infants and is associated with disease severity and neutrophil degranulation products [61, 121, 199, 200]. Similar to our findings for MIP-1α, MIP-2 was produced earlier and reached higher levels in Balb/c mice compared to the C57Bl/6 strain. The 3000 pfu Balb/c mice had higher levels of MIP-2 on day 5 than on day 6 p.i., suggesting an earlier peak in these mice. MIP-2 mRNA was upregulated in a dose-dependent manner in both strains, and C57Bl/6 mice required a 10-fold higher dose to induce a similar response to Balb/c mice inoculated with PVM 15. Strikingly, the relative level of MIP-2 paralleled the relative level of virus in lung homogenates for all dose groups. This could indicate that the level of viral replication or PVM antigen in the lung leads to activation of MIP-2 transcription, although further studies would be needed to examine whether this is a direct effect or simply coincidence. Despite reports that MIP-2 is one of the predominant chemokines upregulated during PVM infection, the majority of studies have not examined its role in PVM pathogenesis [35].

Expression of the IP-10 gene was induced upon infection with PVM in a similar pattern to IFN-γ, which would be expected based on its role as an interferon response gene. Its mRNA upregulation was also similar to that of the CC chemokines, MIP-1α and MCP-1, with the three lethal doses showing a similar level of gene upregulation on day 5 p.i.. The CXC chemokine, MIP-2, on the other hand, was upregulated in a dose-dependent manner, such that a 10-fold higher dose of PVM induced between 3 and 5-fold higher levels of mRNA upregulation in the Balb/c strain, and roughly 7-fold higher upregulation in the C57Bl/6 strain. The different pattern of upregulation between these genses suggests that MIP-2 expression is dependent on a different pathway than the chemokines MIP-1α, MCP-1, and IP-10. Similar results were obtained when

comparing the chemokine response of cultured human airway epithelial cells to RSV, whereby the MIP-2 homologue, IL-8, was upregulated in a MyD88 dependent manner, while IP-10 and RANTES were unaffected by the blockade of MyD88 signalling[60]. Another study showed that the production of IP-10 and RANTES by RSV-infected epithelial cells was dependent on RIG-I-mediated signalling[47]. Thus, these results suggest that a similar difference in the regulation of chemokine expression could exist in PVM-infected mice.

MCP-1 has been examined in many studies on PVM infection, although usually as a measure of the response to PVM infection during the blockade of another pathway. Blockade of MIP-1α, for example, had no effect on the production of MCP-1 in PVM-infected mice, while this chemokine was significantly decreased by use of the antiviral ribavirin, suggesting that PVM replication stimulates its production *in vivo* [202]. Interestingly, another study examining age-related changes in susceptibility found that older mice had decreased MCP-1 production in response to PVM, which was associated with reduced disease presentation, despite similar viral replication [183]. Our study showed that MCP-1 production, as with the other chemokines examined, was earlier in Balb/c mice compared to C57Bl/6. The lethal doses induced a strong upregulation of MCP-1 RNA by day 5, and by day 6, MCP-1 was produced at high levels in all mice other than the 300 pfu C57Bl/6 mice. Again, the two lower doses of PVM in the Balb/c strain produced the same amount of MCP-1 protein as the 10- and 100-fold higher dose C57Bl/6 group. Further evidence of the role of MCP-1 in severe disease is highlighted by the drastic increase in MCP-1 levels between days 5 and 6 p.i., when the 3000 pfu Balb/c mice dropped the majority of their weight and began to succumb to infection.

Since the precise roles of the chemokines, IP-10, MCP-1, and MIP-2 have not yet been elucidated in PVM pathogenesis, nor have they been widely researched in RSV pathogenesis in infants, other than noting their association with disease severity, these chemokines are good candidates for further evaluation in our model system. In addition, since there are slight differences between the PVM J3666 model and strain 15, the comparison of IFN-γ and MIP-1α in the PVM 15 pathogenesis model would enhance our understanding of these mechanisms *in vivo*.

6.4 Linking the Innate and Cell-Mediated Responses in Sublethally Infected Mice

The innate immune system is critical for directing the adaptive response to pathogens. As previously mentioned, the cell-mediated immune response is critical for clearance of pneumoviruses, and the memory T cell response later plays a role in protection. There is also evidence that a threshold level of neutralizing antibodies is at least partially protective. Since RSV reinfection is common throughout life, despite measurable cell-mediated and humoral responses to the virus, our study of PVM infection in mice will help to determine whether this is a common feature of the pneumovirus subfamily. Long-term trials to examine correlates of protection and responses to reinfection in sublethally infected Balb/c and C57Bl/6 mice have already been initiated. Here, we examined the long-term adaptive responses to sublethal doses in the two strains, and how these data relate to the innate response.

Balb/c and C57Bl/6 mice replicate their respective sublethal doses of PVM 15 to the same peak titre. Thus, an examination of the clearance mechanisms and long-term responses in these strains may lead to a better understanding of the difference between them and their use in the mouse model of RSV pathogenesis. They showed clear differences in the clinical severity of

the infection and displayed a difference in the relative contribution of lymphocytes and neutrophils to lung inflammation.

The early infiltration of immune cells in the Balb/c mice, which started as early as day 5 p.i., was associated with earlier IFN-α and IFN-γ expression in the lungs. Plasmacytoid DCs and NK cells are attractive candidates as the respective sources of these cytokines. Cells responding to IFN stimulation could be a source of chemokines in Balb/c mice, and may play a role in their susceptibility to earlier infiltration of immune cells. Infection of Balb/c mice with 10 pfu of PVM J3666 led to infiltration of NK cells and CD4 and CD8 T cells by day 6 p.i., and functional pDCs have been associated with neonatal survival of PVM infection in the Balb/c strain [161, 206].

Direct analysis of the role of type I IFN in PVM infection has only been carried out in C57Bl/6 mice with a deletion in the IFN-α/β receptor gene. Abrogation of type I IFN signalling during PVM J3666 infection led to decreased expression of IFN response genes, lower levels of IFN-α and IFN-β, and, intriguingly, a slightly enhanced survival time in C57Bl/6 mice given a lethal dose of 60 pfu [162]. The study also showed that there was no difference in the expression of the chemokines MIP-1α and MIP-2 in wildtype and gene-deleted mice, suggesting that they are upregulated independent of IFN signalling [162]. Whether these results hold true in the Balb/c strain is not yet clear, and the use of antibodies for depletion of these factors would enable a direct comparison between these strains and the role of type I IFN in response to both lethal and sublethal doses of PVM 15.

Since pDC-derived IFN-α and NK cell-derived IFN-γ production has been reported to enhance the CTL response both in pneumovirus infection and in other models, a comparison of the contribution of CD8 T cells to the cell-mediated response in Balb/c and C57Bl/6 would be

interesting. The role of T cells in clearance at early time points and long-term memory responses may be quite different, given the difference in early levels of type I and II IFNs in these mice. The results of Frey et al. suggest that CD8 T cells are likely to be a strong contributor to weight loss and IFN-γ production in the lungs of C57Bl/6 mice at a dose of 200 pfu of PVM 15 [165]. It is interesting to note that in our study the two mouse strains replicated the virus to the same level by day 6, at which point the Balb/c mice began to clear the virus, while clearance was delayed by at least one day in C57Bl/6 mice. Since viral clearance began earlier and was not associated with weight loss in Balb/c mice, the contribution of the CTL response to pathogenesis in sublethally infected Balb/c mice may be less important than in C57Bl/6 mice.

Similar to our findings for the innate response to a sublethal PVM infection, the cell-mediated immune response in both strains was highly Th1-biased. The sublethal dose induced a median of less than 10 PVM-specific cells secreting IL-5 out of one million splenocytes in both strains. These levels were similar to the mock-infected C57Bl/6 mice, which suggests the cells could have been activated by factors in the PVM-infected lysate or inactivated virus alone. Mock-infected Balb/c mice had virtually no PVM-specific IL-5 spots, making the infected Balb/c group statistically higher than the control group at all time points, and higher than the infected C57Bl/6 mice on day 42 p.i.. Whether these cells are biologically relevant in the response to PVM remains to be seen. As discussed below, the induction of the antibody response depends on T helper cell-derived cytokines, including IL-5 and IFN-γ, and the Balb/c mice showed a greater Th2 bias than the C57Bl/6 mice.

In agreement with the high levels of IFN-γ in the lungs of Balb/c mice at early time points, restimulated splenocytes from these mice had a high number of PVM-specific IFN-γ-producing cells, that exceeded the C57Bl/6 response on day 28 and 42 p.i.. They maintained a

similar response between days 14 and 42 p.i., in contrast to the C57Bl/6 mice that showed strong IFN-γ responses on day 14, which were drastically reduced by day 28 p.i..

Not only was the PVM-specific IFN-γ production in the spleen higher in C57Bl/6 than in Balb/c mice on day 14 p.i., the splenocytes isolated from these animals also had a strong IFN-γ response to culture medium and mock-infected cell lysate. In fact, they had as many IFN-γ secreting cells in control wells as the Balb/c mice did in response to PVM-infected cell lysate (data not shown). The high number of PVM-specific IFN-γ-secreting cells in C57Bl/6 mice, which takes into account the background, highlights the level of activation seen in these mice. This may be related to the clinical severity of their illness. As discussed previously, the weight loss observed in C57Bl/6 mice infected with a sublethal dose of PVM 15 is likely due to the activity of CD8 T cells. Although there were few lymphocytes remaining in the lungs on day 14 p.i., the peripheral lymphoid tissue clearly contained high levels of primed and activated T cells that were secreting IFN-γ. We have yet to confirm whether the lymphocytes in the BAL of C57Bl/6 mice between days 8 and 10 were CD8 T cells, but given the results of Frey et al., who also used strain 15, this seems likely [165]. By day 28 p.i., however, the C57Bl/6 mice had lower levels of IFN-γ secreting cells in the spleen than sublethally infected Balb/c mice.

6.5 Humoral Response to PVM Infection

The interplay between the innate response and later adaptive responses is also seen in the development of humoral immunity. DCs activated during infection, along with T-helper cells primed by activated DCs, are critical for determining the type of antibody produced against a pathogen. B-cell isotype switching is regulated by the cytokines produced by activated T-helper cells that recognize viral MHC-bound peptides displayed on the surface of mature B-cells. When T-helper cells are activated by DCs in secondary lymphoid organs like the lymph nodes or

spleen, the production of regulatory cytokines like IL-12 and IL-10 drive the T-helper cells towards the production of IFN-γ and IL-4, respectively. In both humans and mice, the Th-2 cytokines IL-4 and IL-5 produced by T-helper cells are associated with the production of IgE and IgA, respectively [97, 147]. In mice, IL-5 is also associated with IgG_1 production, while Th1 biased cytokine IFN-γ regulates switching to IgG_{2a} production in Balb/c mice [147]. C57Bl/6 mice are often assessed for IgG_{2a} production, with positive results, but this is due to cross-reactivity of the IgG_{2a} and IgG_{2c} isotypes, the latter of which the C57Bl/6 produces in place of IgG_{2a} [207, 208]. Assessment of the antibody isotype produced upon infection should give further evidence of the T-helper bias observed in the cell-mediated response.

In agreement with the cytokine production by restimulated splenocytes, we observed higher levels of IgA in Balb/c mice than in the C57Bl/6 strain, which could be indicative of the biological relevance of the low number of PVM-specific IL-5 secreting splenoctyes that were detected consistently above the mock-infected control mice between days 14 and 42 p.i.. Although C57Bl/6 mice had similar numbers of IL-5 secreting cells on days 14 and 28, their response was similar to the mock-infected mice at all time points. However, the infected C57Bl/6 also produced low levels of PVM-specific IgA in the lungs, which peaked on day 28. By day 42, both IL-5 secreting cells and IgA levels were reduced compared to day 28 levels in the C57Bl/6 mice. Again, the mock-infected C57Bl/6 mice had similar levels of IL-5 secreting cells at this time point, which brings into question the physiological relevance of the low number of cells responding to PVM antigen.

IgG isotyping has not yet been performed on these groups of mice. Given the higher "quality" of the antibody response in C57Bl/6 mice, as evidenced by the higher neutralization capacity of their sera and lung secretions, it is likely that the strains are secreting different IgG

isotypes. Also, since their T-helper responses are both highly Th1-biased, there is further likelihood that the strains are secreting different isotypes of the IgG_2 antibody, although the level of IgG_1 could also differ between these strains.

Interestingly, the C57Bl/6 mice inoculated with 30 pfu had the same amount of IgG in the serum, but it had a lower capacity to neutralize the virus than serum from the 300 pfu C57Bl/6 group. The neutralization capacity of the lung fragment culture supernatant was not, however, decreased in the lungs of 30 pfu C57Bl/6 mice compared to the 300 pfu dose group. This may indicate that different IgG isotypes are secreted at the mucosal surface, perhaps based on the level of antigen present or due to the effects of the virus and the local immune response to it. Since the 30 pfu C57Bl/6 mice had fewer Th1-biased splenocytes and similar levels of Th2-biased splenocytes relative to the 300 pfu C57Bl/6 group, they may have a different IgG isotype profile, which, given their similar production of total IgG would help point to the role of different IgG isotypes in enhancing the neutralization of PVM in vitro.

Our examination of the adaptive response to a sublethal dose of PVM in Balb/c and C57Bl/6 mice showed that by day 42 p.i., the Balb/c strain had a stronger cell-mediated response to PVM, along with enhanced production of mucosal and serum antibodies. However, their humoral response was less effective than the C57Bl/6 strain, and its slower production suggests that the C57Bl/6 mice produce more effective antibodies earlier in the infection. In terms of comparing their usefulness as a model of RSV, the next critical step will be determining the effectiveness of these responses in reducing illness upon reinfection. The C57Bl/6 strain infected with 300 pfu shows a rapid decline in activated peripheral T cells similar to that reported in infants monitored at the height of severe infection and 4 weeks later. Since humoral responses in children are also known to decline following infection with RSV, the duration of the antibody

response to PVM in these two strains of mice will give further insight into their use as a model of RSV.

6.6 General Conclusions and Future Directions

In the current study, we examined the immune response to PVM in two mouse strains with differential susceptibility to this pathogen as a means of understanding their usefulness as a model of RSV pathogenesis in infants. The specific aims were to compare the innate and adaptive responses displayed upon infection of Balb/c and C57Bl/6 mice with PVM, and to examine the difference in their susceptibility to this pathogen. Our results showed that the Balb/c strain had earlier detectible virus that reached an earlier peak compared to C57Bl/6 mice infected with the same dose. Chemokines and the proinflammatory Th1 cytokine, IFN-γ, were also produced earlier in Balb/c, and the strain experienced enhanced neutrophilic inflammation in the lungs. Even at a dose as low as 30 pfu, Balb/c mice experienced an earlier influx of neutrophils and lymphocytes beginning on day 5 p.i., at which point they had high levels of proinflammatory mediators, as well as IFN-α and IP-10 transcripts, in the lungs.

Further examination of the cell types involved in these responses would help us to understand whether the NK and pDC populations that are suggested by the profile of inflammation seen in the lungs are actually responsible for these cytokines. FACS analysis of stained cells collected from the BAL or digested lungs of infected mice would be the best method to examine which populations of leukocytes are responsible for the production of IFN-α and IFN-γ in this strain. In addition, an examination of the production of surfactants and TLR expression on the surface of key immune cells in these two strains over the course of infection would give insight into the role of these molecules in the relative susceptibility of Balb/c and

C57Bl/6 mice to PVM. We also hope to examine the maturation level and cytokine profile of DCs in the lungs during and after infection with PVM as a means of understanding their contribution to the T-helper response in these mice.

The more resistant C57Bl/6 strain requires a 10-fold higher dose to display the same degree of illness and inflammatory responses in Balb/c mice. Upon infection with a sublethal dose of 300 pfu they experience illness with a rapid onset on day 7-8 and subsequent recovery by day 14. There was a dramatic influx of cells, predominantly lymphocytes, which peaked on day 10 and dropped to normal levels on day 14. By then, the mice had returned to a normal weight and had only a few lymphocytes remaining in the lungs. However, these mice had exceptionally strong cell-mediated IFN-γ production in the spleen on day 14, even in response to culture medium alone. The number of IFN-γ producing cells in the spleen of sublethally infected C57Bl/6 mice dropped drastically by day 28 and remained relatively low on day 42 p.i.. The Balb/c mice, on the other hand, had intermediate levels of IFN-γ production by splenocytes that were similar between days 14 and 42, and these levels were higher than the C57Bl/6 mice on day 28 and 42.

Our attempts to examine the relative contribution of CD4 and CD8 T cells to the IFN-γ response in the spleen were not successful. It appeared that both cell types likely contributed, but without a FACS-based assessment, whereby the production of IFN-γ can be directly attributed to individual cells, the interplay between these cells and APCs in the spleen makes it difficult to interpret their role as supportive or in IFN-γ production itself. Further assessment of this response and the relative contribution of CD4 and CD8 T cells will help us to understand the difference in the cell-mediated response to PVM between these two strains.

The antibody response in C57Bl/6 mice had reached maximal levels by day 14 in the lung and the serum, while in Balb/c mice it continued to increase over the 42 day period. Despite similar antibody levels, the 30 pfu Balb/c mice had reduced neutralizing antibody in both lungs and serum on day 28. Thus, they likely produce different antibody isotypes in response to PVM, so IgG isotype profiling will add greatly to our understanding of how the response of these mice differs. Similarly, the 30 pfu C57Bl/6 group had lower neutralizing antibody levels in the serum compared to the 300 pfu group, despite similar IgG, while their mucosal antibody response was as capable of neutralizing PVM as the high dose group. Again, IgG isotyping will help to understand what role the different isotypes play in protection and how they are distributed between the mucosal and peripheral areas.

In future, this research will be continued by examining the responses of sublethally infected Balb/c and C57Bl/6 mice upon reinfection with PVM 15. As the two strains show alternative modes of protection, with Balb/c mice showing enhanced cell-mediated responses by day 42 p.i. compared to the C57Bl/6 mice and C57Bl/6 mice showing enhanced neutralizing antibody in the serum and lungs compared to Balb/c mice, we can examine the relative contribution of these two responses in protection from reinfection and the development of severe illness during secondary infection.

Our examination of the responses to pneumovirus infection in a susceptible and a resistant mouse strain has led to a number of interesting possibilities for further research. The innate immune response is critical during PVM pathogenesis in Balb/c mice. C57Bl/6 mice, on the other hand, have little upregulation of innate inflammatory mediators, and the onset of illness coincided with the initiation of the cell-mediated immune response. Although the profile of upregulated inflammatory mediators was similar between the two strains, they displayed quite

different immune responses, both in the short- and long-term. There is still much to be learned about the basis of this difference, and it will help to clarify studies where deletion of the same gene in two different strains yields conflicting results or indeed any study where knock-out mice are available only in one genetic background. Whether one of these two strains represents a "better" model of RSV pathogenesis is unclear. Since RSV can cause a spectrum of disease depending on the age and immune history of the child in question, they may be useful in examining a number of aspects of pneumovirus pathogenesis.

7.0 References

1. El-Hajje, M.J., et al., *The burden of respiratory viral disease in hospitalized children in Paris.* Eur J Pediatr, 2008. **167**(4): p. 435-6.
2. Deshpande, S.A. and V. Northern, *The clinical and health economic burden of respiratory syncytial virus disease among children under 2 years of age in a defined geographical area.* Arch Dis Child, 2003. **88**(12): p. 1065-9.
3. Iwane, M.K., et al., *Population-based surveillance for hospitalizations associated with respiratory syncytial virus, influenza virus, and parainfluenza viruses among young children.* Pediatrics, 2004. **113**(6): p. 1758-64.
4. Van der Poel, W.H., et al., *Respiratory syncytial virus infections in human beings and in cattle.* J Infect, 1994. **29**(2): p. 215-28.
5. Moineddin, R., et al., *Seasonality of primary care utilization for respiratory diseases in Ontario: a time-series analysis.* BMC Health Serv Res, 2008. **8**: p. 160.
6. Mlinaric-Galinovic, G., et al., *The biennial cycle of respiratory syncytial virus outbreaks in Croatia.* Virol J, 2008. **5**: p. 18.
7. Djelantik, I.G., et al., *Incidence and clinical features of hospitalization because of respiratory syncytial virus lower respiratory illness among children less than two years of age in a rural Asian setting.* Pediatr Infect Dis J, 2003. **22**(2): p. 150-7.
8. Glezen, W.P., et al., *Risk of primary infection and reinfection with respiratory syncytial virus.* Am J Dis Child, 1986. **140**(6): p. 543-6.
9. Hall, C.B., et al., *Control of nosocomial respiratory syncytial viral infections.* Pediatrics, 1978. **62**(5): p. 728-32.
10. Hall, C.B., R.G. Douglas, Jr., and J.M. Geiman, *Possible transmission by fomites of respiratory syncytial virus.* J Infect Dis, 1980. **141**(1): p. 98-102.
11. Hall, C.B., *Respiratory syncytial virus: its transmission in the hospital environment.* Yale J Biol Med, 1982. **55**(3-4): p. 219-23.
12. Hall, C.B., et al., *Immunity to and Frequency of Reinfection with Respiratory Syncytial Virus.* Journal of Infectious Diseases, 1991. **163**(4): p. 693-698.
13. Hall, C.B., J.R.G. Douglas, and J.M. Geiman, *Respiratory syncytial virus infections in infants: Quantitation and duration of shedding.* The Journal of Pediatrics, 1976. **89**(1): p. 11-15.
14. Fodha, I., et al., *Respiratory syncytial virus infections in hospitalized infants: Association between viral load, virus subgroup, and disease severity.* Journal of Medical Virology, 2007. **79**(12): p. 1951-1958.
15. Hall, C.B. and R.G. Douglas, *Modes of transmission of respiratory syncytial virus.* The Journal of Pediatrics, 1981. **99**(1): p. 100-103.
16. Hall, C.B. and R.G. Douglas, Jr., *Nosocomial respiratory syncytial viral infections. Should gowns and masks be used?* Am J Dis Child, 1981. **135**(6): p. 512-5.
17. Boyce, T.G., et al., *Rates of hospitalization for respiratory syncytial virus infection among children in Medicaid.* The Journal of Pediatrics, 2000. **137**(6): p. 865-870.
18. Lowther, S.A., et al., *Bronchiolitis-associated hospitalizations among American Indian and Alaska Native children.* Pediatr Infect Dis J, 2000. **19**(1): p. 11-7.
19. Shay, D.K., et al., *Bronchiolitis-associated hospitalizations among US children, 1980-1996.* JAMA, 1999. **282**(15): p. 1440-6.
20. Sampalis, J.S., *Morbidity and mortality after RSV-associated hospitalizations among premature Canadian infants.* The Journal of Pediatrics, 2003. **143**(5, Supplement 1): p. 150-156.
21. Shay, D.K., et al., *Bronchiolitis-associated mortality and estimates of respiratory syncytial virus-associated deaths among US children, 1979-1997.* J Infect Dis, 2001. **183**(1): p. 16-22.
22. Welliver, R.C., *Review of epidemiology and clinical risk factors for severe respiratory syncytial virus (RSV) infection.* The Journal of Pediatrics, 2003. **143**(5, Supplement 1): p. 112-117.

23. Wang, E.E., et al., *Pediatric Investigators Collaborative Network on Infections in Canada (PICNIC) study of admission and management variation in patients hospitalized with respiratory syncytial viral lower respiratory tract infection.* J Pediatr, 1996. **129**(3): p. 390-5.
24. Langley, J.M., et al., *Increasing Incidence of Hospitalization for Bronchiolitis among Canadian Children, 1980-2000.* The Journal of Infectious Diseases, 2003. **188**(11): p. 1764-1767.
25. Ehlken, B., et al., *Economic impact of community-acquired and nosocomial lower respiratory tract infections in young children in Germany.* Eur J Pediatr, 2005. **164**(10): p. 607-15.
26. Thompson, W.W., et al., *Mortality associated with influenza and respiratory syncytial virus in the United States.* JAMA, 2003. **289**(2): p. 179-86.
27. Karron, RuthÂ A., et al., *Severe Respiratory Syncytial Virus Disease in Alaska Native Children.* The Journal of Infectious Diseases, 1999. **180**(1): p. 41-49.
28. Karron, R.A., et al., *Severe respiratory syncytial virus disease in Alaska native children. RSV Alaska Study Group.* J Infect Dis, 1999. **180**(1): p. 41 - 49.
29. Nair, H., et al., *Global burden of acute lower respiratory infections due to respiratory syncytial virus in young children: a systematic review and meta-analysis.* Lancet, 2010. **375**(9725): p. 1545-55.
30. Kumar, M., *Childhood mortality due to respiratory syncytial virus.* The Lancet, 2010. **376**(9744): p. 872-872.
31. Manjarrez, M.E., et al., *Comparative viral frequency in Mexican children under 5 years of age with and without upper respiratory symptoms.* J Med Microbiol, 2003. **52**(Pt 7): p. 579-83.
32. Rohwedder, A., et al., *Detection of respiratory syncytial virus RNA in blood of neonates by polymerase chain reaction.* J Med Virol, 1998. **54**(4): p. 320-7.
33. Moore, M.L. and R.S. Peebles, Jr., *Respiratory syncytial virus disease mechanisms implicated by human, animal model, and in vitro data facilitate vaccine strategies and new therapeutics.* Pharmacol Ther, 2006. **112**(2): p. 405-24.
34. Byrd, LindaÂ G. and GregoryÂ A. Prince, *Animal Models of Respiratory Syncytial Virus Infection.* Clinical Infectious Diseases, 1997. **25**(6): p. 1363-1368.
35. Bonville, C.A., et al., *Respiratory dysfunction and proinflammatory chemokines in the pneumonia virus of mice (PVM) model of viral bronchiolitis.* Virology, 2006. **349**(1): p. 87-95.
36. Rosenberg, H.F. and J.B. Domachowske, *Pneumonia virus of mice: severe respiratory infection in a natural host.* Immunology Letters, 2008. **118**(1): p. 6-12.
37. Horsfall, F.L. and R.G. Hahn, *A Latent Virus in Normal Mice Capable of Producing Pneumonia in Its Natural Host.* J Exp Med, 1940. **71**(3): p. 391-408.
38. Cook, P.M., R.P. Eglin, and A.J. Easton, *Pathogenesis of pneumovirus infections in mice: detection of pneumonia virus of mice and human respiratory syncytial virus mRNA in lungs of infected mice by in situ hybridization.* Journal of General Virology, 1998. **79**(10): p. 2411-7.
39. Anh, D.B., P. Faisca, and D.J. Desmecht, *Differential resistance/susceptibility patterns to pneumovirus infection among inbred mouse strains.* Am J Physiol Lung Cell Mol Physiol, 2006. **291**(3): p. L426-35.
40. Arsic, N., *Pneumovirus Infections and Effects on Dendritic Cells of Mice*, in *Veterinary Microbiology*2008, University of Saskatchewan: Saskatoon. p. 136.
41. Easton, A.J., J.B. Domachowske, and H.F. Rosenberg, *Animal Pneumoviruses: Molecular Genetics and Pathogenesis.* Clin. Microbiol. Rev., 2004. **17**(2): p. 390-412.
42. Zhang, Y., et al., *Expression of respiratory syncytial virus-induced chemokine gene networks in lower airway epithelial cells revealed by cDNA microarrays.* J Virol, 2001. **75**(19): p. 9044-58.
43. Cirino, N.M., et al., *Restricted replication of respiratory syncytial virus in human alveolar macrophages.* J Gen Virol, 1993. **74 (Pt 8)**: p. 1527-37.
44. Bataki, E.L., G.S. Evans, and M.L. Everard, *Respiratory syncytial virus and neutrophil activation.* Clin Exp Immunol, 2005. **140**(3): p. 470-7.

45. Konig, B., et al., *IL-8 release from human neutrophils by the respiratory syncytial virus is independent of viral replication.* J Leukoc Biol, 1996. **60**(2): p. 253-60.
46. Becker, S., J. Quay, and J. Soukup, *Cytokine (tumor necrosis factor, IL-6, and IL-8) production by respiratory syncytial virus-infected human alveolar macrophages.* J Immunol, 1991. **147**(12): p. 4307-12.
47. Liu, P., et al., *Retinoic acid-inducible gene I mediates early antiviral response and Toll-like receptor 3 expression in respiratory syncytial virus-infected airway epithelial cells.* J Virol, 2007. **81**(3): p. 1401-11.
48. Mellow, T.E., et al., *The effect of respiratory synctial virus on chemokine release by differentiated airway epithelium.* Exp Lung Res, 2004. **30**(1): p. 43-57.
49. Olszewska-Pazdrak, B., et al., *Cell-specific expression of RANTES, MCP-1, and MIP-1alpha by lower airway epithelial cells and eosinophils infected with respiratory syncytial virus.* J Virol, 1998. **72**(6): p. 4756-64.
50. Rezaee, F., et al., *Respiratory syncytial virus infection in human bone marrow stromal cells.* Am J Respir Cell Mol Biol, 2011. **45**(2): p. 277-86.
51. Dyer, K.D., et al., *Pneumoviruses infect eosinophils and elicit MyD88-dependent release of chemoattractant cytokines and interleukin-6.* Blood, 2009. **114**(13): p. 2649-2656.
52. Morrison, P.T., et al., *RSV-infected airway epithelial cells cause biphasic up-regulation of CCR1 expression on human monocytes.* J Leukoc Biol, 2007. **81**(6): p. 1487-1495.
53. Soukup, J.M. and S. Becker, *Role of monocytes and eosinophils in human respiratory syncytial virus infection in vitro.* Clin Immunol, 2003. **107**(3): p. 178-85.
54. Wang, H., Z. Su, and J. Schwarze, *Healthy but not RSV-infected lung epithelial cells profoundly inhibit T cell activation.* Thorax, 2009. **64**(4): p. 283-90.
55. Bitko, V., et al., *Activation of cytokines and NF-kappa B in corneal epithelial cells infected by respiratory syncytial virus: potential relevance in ocular inflammation and respiratory infection.* BMC Microbiol, 2004. **4**(1): p. 28.
56. Johnson, J.E., et al., *The histopathology of fatal untreated human respiratory syncytial virus infection.* Mod Pathol, 2007. **20**(1): p. 108-19.
57. Fiedler, M.A., K. Wernke-Dollries, and J.M. Stark, *Mechanism of RSV-induced IL-8 gene expression in A549 cells before viral replication.* American Journal of Physiology - Lung Cellular and Molecular Physiology, 1996. **271**(6): p. L963-L971.
58. Jewell, N.A., et al., *Differential type I interferon induction by respiratory syncytial virus and influenza a virus in vivo.* J Virol, 2007. **81**(18): p. 9790-800.
59. Saito, T., et al., *Respiratory Syncytial Virus Induces Selective Production of the Chemokine RANTES by Upper Airway Epithelial Cells.* The Journal of Infectious Diseases, 1997. **175**(3): p. 497-504.
60. Rudd, B.D., et al., *Differential Role for TLR3 in Respiratory Syncytial Virus-Induced Chemokine Expression.* Journal of Virology, 2005. **79**(6): p. 3350-3357.
61. Abu-Harb, M., et al., *IL-8 and neutrophil elastase levels in the respiratory tract of infants with RSV bronchiolitis.* European Respiratory Journal, 1999. **14**(1): p. 139-143.
62. Garofalo, R.P., et al., *Macrophage inflammatory protein-1alpha (not T helper type 2 cytokines) is associated with severe forms of respiratory syncytial virus bronchiolitis.* J Infect Dis, 2001. **184**(4): p. 393 - 399.
63. Hornsleth, A., L. Loland, and L.B. Larsen, *Cytokines and chemokines in respiratory secretion and severity of disease in infants with respiratory syncytial virus (RSV) infection.* Journal of Clinical Virology, 2001. **21**(2): p. 163-170.
64. Murai, H., et al., *IL-10 and RANTES are elevated in nasopharyngeal secretions of children with respiratory syncytial virus infection.* Allergol Int, 2007. **56**(2): p. 157-63.
65. Culley, F.J., et al., *Role of CCL5 (RANTES) in viral lung disease.* J Virol, 2006. **80**(16): p. 8151-7.

66. Culley, F.J., et al., *Differential chemokine expression following respiratory virus infection reflects Th1- or Th2-biased immunopathology.* J Virol, 2006. **80**(9): p. 4521-7.
67. Tregoning, J.S., et al., *The chemokine MIP1alpha/CCL3 determines pathology in primary RSV infection by regulating the balance of T cell populations in the murine lung.* PLoS One. **5**(2): p. e9381.
68. Patel, J.A., et al., *Interleukin-1 alpha mediates the enhanced expression of intercellular adhesion molecule-1 in pulmonary epithelial cells infected with respiratory syncytial virus.* Am J Respir Cell Mol Biol, 1995. **13**(5): p. 602-9.
69. Noah, T.L. and S. Becker, *Respiratory syncytial virus-induced cytokine production by a human bronchial epithelial cell line.* American Journal of Physiology - Lung Cellular and Molecular Physiology, 1993. **265**(5): p. L472-L478.
70. Arnold, R., et al., *Interleukin-8, interleukin-6, and soluble tumour necrosis factor receptor type I release from a human pulmonary epithelial cell line (A549) exposed to respiratory syncytial virus.* Immunology, 1994. **82**(1): p. 126-33.
71. Garofalo, R., et al., *Respiratory syncytial virus infection of human respiratory epithelial cells up-regulates class I MHC expression through the induction of IFN- beta and IL-1 alpha.* The Journal of Immunology, 1996. **157**(6): p. 2506-2513.
72. Jiang, Z., M. Kunimoto, and J.A. Patel, *Autocrine Regulation and Experimental Modulation of Interleukin-6 Expression by Human Pulmonary Epithelial Cells Infected with Respiratory Syncytial Virus.* Journal of Virology, 1998. **72**(3): p. 2496-2499.
73. Monick, M.M., et al., *Respiratory syncytial virus up-regulates TLR4 and sensitizes airway epithelial cells to endotoxin.* J Biol Chem, 2003. **278**(52): p. 53035-44.
74. Kurt-Jones, E.A., et al., *Pattern recognition receptors TLR4 and CD14 mediate response to respiratory syncytial virus.* Nat Immunol, 2000. **1**(5): p. 398-401.
75. Murawski, M.R., et al., *Respiratory Syncytial Virus Activates Innate Immunity through Toll-Like Receptor 2.* Journal of Virology, 2009. **83**(3): p. 1492-1500.
76. Puthothu, B., et al., *TLR-4 and CD14 polymorphisms in respiratory syncytial virus associated disease.* Dis Markers, 2006. **22**(5-6): p. 303-8.
77. Xie, X.H., et al., *[Toll-like receptor 4 expression and function of respiratory syncytial virus-infected airway epithelial cells].* Zhonghua Jie He He Hu Xi Za Zhi, 2008. **31**(3): p. 213-7.
78. Huang, S.H., X.J. Cao, and W. Wei, *Melatonin decreases TLR3-mediated inflammatory factor expression via inhibition of NF-kappa B activation in respiratory syncytial virus-infected RAW264.7 macrophages.* J Pineal Res, 2008. **45**(1): p. 93-100.
79. Haeberle, H.A., et al., *Respiratory Syncytial Virus–Induced Activation of Nuclear Factor–κB in the Lung Involves Alveolar Macrophages and Toll-Like Receptor 4–Dependent Pathways.* Journal of Infectious Diseases, 2002. **186**(9): p. 1199-1206.
80. Pribul, P.K., et al., *Alveolar Macrophages Are a Major Determinant of Early Responses to Viral Lung Infection but Do Not Influence Subsequent Disease Development.* J. Virol., 2008. **82**(9): p. 4441-4448.
81. Haynes, L.M., et al., *Involvement of Toll-Like Receptor 4 in Innate Immunity to Respiratory Syncytial Virus.* Journal of Virology, 2001. **75**(22): p. 10730-10737.
82. Adam, C., et al., *DC-NK cell cross talk as a novel CD4+ T-cell–independent pathway for antitumor CTL induction.* Blood, 2005. **106**(1): p. 338-344.
83. Arnold, R. and W. Konig, *ICAM-1 expression and low-molecular-weight G-protein activation of human bronchial epithelial cells (A549) infected with RSV.* J Leukoc Biol, 1996. **60**(6): p. 766-71.
84. Tosi, M.F., et al., *Induction of ICAM-1 expression on human airway epithelial cells by inflammatory cytokines: effects on neutrophil-epithelial cell adhesion.* Am J Respir Cell Mol Biol, 1992. **7**(2): p. 214-21.

85. Carpenter, L.R., J.N. Moy, and K.A. Roebuck, *Respiratory syncytial virus and TNF alpha induction of chemokine gene expression involves differential activation of Rel A and NF-kappa B1.* BMC Infect Dis, 2002. **2**: p. 5.
86. McNamara, P.S., et al., *Bronchoalveolar lavage cellularity in infants with severe respiratory syncytial virus bronchiolitis.* Arch Dis Child, 2003. **88**(10): p. 922-6.
87. Domachowske, J.B., et al., *MIP-1α Is Produced but It Does Not Control Pulmonary Inflammation in Response to Respiratory Syncytial Virus Infection in Mice.* Cell Immunol, 2000. **206**(1): p. 1-6.
88. Arnold, R., et al., *Effect of respiratory syncytial virus-antibody complexes on cytokine (IL-8, IL-6, TNF-alpha) release and respiratory burst in human granulocytes.* Immunology, 1994. **82**(2): p. 184-91.
89. Halfhide, C.P., et al., *Neutrophil TLR4 expression is reduced in the airways of infants with severe bronchiolitis.* Thorax, 2009. **64**(9): p. 798-805.
90. Wang, S.Z., et al., *The apoptosis of neutrophils is accelerated in respiratory syncytial virus (RSV)-induced bronchiolitis.* Clin Exp Immunol, 1998. **114**(1): p. 49-54.
91. Garofalo, R., et al., *Eosinophil degranulation in the respiratory tract during naturally acquired respiratory syncytial virus infection.* The Journal of Pediatrics, 1992. **120**(1): p. 28-32.
92. Kim, C.K., et al., *Bronchoalveolar lavage cytokine profiles in acute asthma and acute bronchiolitis.* J Allergy Clin Immunol, 2003. **112**(1): p. 64-71.
93. Kim, H.H., M.H. Lee, and J.S. Lee, *Eosinophil cationic protein and chemokines in nasopharyngeal secretions of infants with respiratory syncytial virus (RSV) bronchiolitis and non-RSV bronchiolitis.* J Korean Med Sci, 2007. **22**(1): p. 37-42.
94. Oh, J.W., et al., *ECP level in nasopharyngeal secretions and serum from children with respiratory virus infections and asthmatic children.* Allergy Asthma Proc, 2000. **21**(2): p. 97-100.
95. Kristjansson, S., et al., *Respiratory syncytial virus and other respiratory viruses during the first 3 months of life promote a local Th2-like response.* Journal of Allergy and Clinical Immunology, 2005. **116**(4): p. 805-811.
96. Ehlenfield, D.R., K. Cameron, and R.C. Welliver, *Eosinophilia at the Time of Respiratory Syncytial Virus Bronchiolitis Predicts Childhood Reactive Airway Disease.* Pediatrics, 2000. **105**(1): p. 79-83.
97. Wills-Karp, M., *Immunological Mechanisms of Allergic Disease*, in *Fundamental Immunology*, W.E. Paul, Editor 2008, Lippincott Williams &Wilkins: Philadelphia, PA. p. 1375-1425.
98. Olszewska-Pazdrak, B., et al., *Respiratory Syncytial Virus-Infected Pulmonary Epithelial Cells Induce Eosinophil Degranulation by a CD18-Mediated Mechanism.* The Journal of Immunology, 1998. **160**(10): p. 4889-4895.
99. Alessandro, M., *The dialogue between human natural killer cells and dendritic cells.* Current Opinion in Immunology, 2005. **17**(3): p. 306-311.
100. Ferlazzo, G. and C. Münz, *NK Cell Compartments and Their Activation by Dendritic Cells.* The Journal of Immunology, 2004. **172**(3): p. 1333-1339.
101. Gerosa, F., et al., *Reciprocal Activating Interaction between Natural Killer Cells and Dendritic Cells.* The Journal of Experimental Medicine, 2002. **195**(3): p. 327-333.
102. Moretta, A., *Natural killer cells and dendritic cells: rendezvous in abused tissues.* Nat Rev Immunol, 2002. **2**(12): p. 957-965.
103. Welliver, T.P., et al., *Severe human lower respiratory tract illness caused by respiratory syncytial virus and influenza virus is characterized by the absence of pulmonary cytotoxic lymphocyte responses.* J Infect Dis, 2007. **195**(8): p. 1126-36.
104. Ehl, S., et al., *The role of Toll-like receptor 4 versus interleukin-12 in immunity to respiratory syncytial virus.* European Journal of Immunology, 2004. **34**(4): p. 1146-1153.
105. Biron, C.A., et al., *NATURAL KILLER CELLS IN ANTIVIRAL DEFENSE: Function and Regulation by Innate Cytokines.* Annual Review of Immunology, 1999. **17**(1): p. 189-220.

106. Christine A, B., *Activation and function of natural killer cell responses during viral infections.* Current Opinion in Immunology, 1997. **9**(1): p. 24-34.
107. Campbell, J.J., et al., *Unique Subpopulations of CD56+ NK and NK-T Peripheral Blood Lymphocytes Identified by Chemokine Receptor Expression Repertoire.* The Journal of Immunology, 2001. **166**(11): p. 6477-6482.
108. Johnson, T.R., et al., *NK T cells contribute to expansion of CD8(+) T cells and amplification of antiviral immune responses to respiratory syncytial virus.* J Virol, 2002. **76**(9): p. 4294 - 4303.
109. Johnson, T.R., et al., *Primary Human mDC1, mDC2, and pDC Dendritic Cells Are Differentially Infected and Activated by Respiratory Syncytial Virus.* PLoS One, 2011. **6**(1): p. e16458.
110. Jones, A., et al., *Differentiation and immune function of human dendritic cells following infection by respiratory syncytial virus.* Clin Exp Immunol, 2006. **143**(3): p. 513-22.
111. Guerrero-Plata, A., et al., *Subversion of pulmonary dendritic cell function by paramyxovirus infections.* J Immunol, 2009. **182**(5): p. 3072-83.
112. Lukens, M.V., et al., *Respiratory syncytial virus-induced activation and migration of respiratory dendritic cells and subsequent antigen presentation in the lung-draining lymph node.* J Virol, 2009. **83**(14): p. 7235-43.
113. Smit, J.J., et al., *The Balance between Plasmacytoid DC versus Conventional DC Determines Pulmonary Immunity to Virus Infections.* PLoS One, 2008. **3**(3): p. e1720.
114. Heufler, C., et al., *Interleukin-12 is produced by dendritic cells and mediates T helper 1 development as well as interferon-γ production by T helper 1 cells.* European Journal of Immunology, 1996. **26**(3): p. 659-668.
115. Liu, B., S.L. Tonkonogy, and R.B. Sartor, *Antigen-presenting cell production of IL-10 inhibits T-helper 1 and 17 cell responses and suppresses colitis in mice.* Gastroenterology, 2011. **141**(2): p. 653-62, 662 e1-4.
116. Kim, H.W., et al., *Respiratory syncytial virus disease in infants despite prior administration of antigenic inactivated vaccine.* Am J Epidemiol, 1969. **89**(4): p. 422-34.
117. Peebles, R.S., Jr., K. Hashimoto, and B.S. Graham, *The complex relationship between respiratory syncytial virus and allergy in lung disease.* Viral Immunol, 2003. **16**(1): p. 25-34.
118. Openshaw, P.J., Y. Yamaguchi, and J.S. Tregoning, *Childhood infections, the developing immune system, and the origins of asthma.* J Allergy Clin Immunol, 2004. **114**(6): p. 1275-7.
119. Becker, Y., *Respiratory syncytial virus (RSV) evades the human adaptive immune system by skewing the Th1/Th2 cytokine balance toward increased levels of Th2 cytokines and IgE, markers of allergy--a review.* Virus Genes, 2006. **33**(2): p. 235-52.
120. Bendelja, K., et al., *Predominant type-2 response in infants with respiratory syncytial virus (RSV) infection demonstrated by cytokine flow cytometry.* Clin Exp Immunol, 2000. **121**(2): p. 332-8.
121. Bont, L., et al., *Peripheral blood cytokine responses and disease severity in respiratory syncytial virus bronchiolitis.* Eur Respir J, 1999. **14**(1): p. 144-9.
122. Chen, Z.M., et al., *Association of cytokine responses with disease severity in infants with respiratory syncytial virus infection.* Acta Paediatr, 2002. **91**(9): p. 914-22.
123. Openshaw, P.J., *RSV bronchiolitis, gammadelta T cells and asthma: are they linked?* Clin Exp Immunol, 2003. **131**(2): p. 197-8.
124. De Weerd, W., W.N. Twilhaar, and J.L. Kimpen, *T cell subset analysis in peripheral blood of children with RSV bronchiolitis.* Scand J Infect Dis, 1998. **30**(1): p. 77-80.
125. Ruckwardt, T.J., et al., *Regulatory T Cells Promote Early Influx of CD8+ T Cells in the Lungs of Respiratory Syncytial Virus-Infected Mice and Diminish Immunodominance Disparities.* J. Virol., 2009. **83**(7): p. 3019-3028.
126. Fulton, R.B., D.K. Meyerholz, and S.M. Varga, *Foxp3+ CD4 Regulatory T Cells Limit Pulmonary Immunopathology by Modulating the CD8 T Cell Response during Respiratory Syncytial Virus Infection.* The Journal of Immunology, 2010. **185**(4): p. 2382-2392.

127. Weiss, K.A., et al., *Multiple CD4+ T Cell Subsets Produce Immunomodulatory IL-10 During Respiratory Syncytial Virus Infection.* The Journal of Immunology, 2011. **187**(6): p. 3145-3154.
128. Legg, J.P., et al., *Type 1 and type 2 cytokine imbalance in acute respiratory syncytial virus bronchiolitis.* Am J Respir Crit Care Med, 2003. **168**(6): p. 633-9.
129. Flores, P., Guimareas, J., Videira Amaral, J.M., *Th1 and th2 cytokine expression in nasopharyngeal secretions during acute bronchiolitis in children younger than two years old.* Allergolia Immunopathologia, 2011. **39**(1): p. 3-9.
130. Mobbs, K.J., et al., *Cytokines in severe respiratory syncytial virus bronchiolitis.* Pediatric Pulmonology, 2002. **33**(6): p. 449-452.
131. Roman, M., et al., *Respiratory syncytial virus infection in infants is associated with predominant Th-2-like response.* Am J Respir Crit Care Med, 1997. **156**(1): p. 190-5.
132. Bem, R.A., et al., *Activation of the granzyme pathway in children with severe respiratory syncytial virus infection.* Pediatr Res, 2008. **63**(6): p. 650-5.
133. Heidema, J., et al., *CD8+ T Cell Responses in Bronchoalveolar Lavage Fluid and Peripheral Blood Mononuclear Cells of Infants with Severe Primary Respiratory Syncytial Virus Infections.* The Journal of Immunology, 2007. **179**(12): p. 8410-8417.
134. Anderson, L.J., et al., *Cytokine Response To Respiratory Syncytial Virus Stimulation Of Human.* Journal of Infectious Diseases, 1994. **170**(5): p. 1201-1208.
135. Lee, F.E.-H., et al., *The balance between influenza- and RSV-specific CD4 T cells secreting IL-10 or IFN[gamma] in young and healthy-elderly subjects.* Mechanisms of Ageing and Development, 2005. **126**(11): p. 1223-1229.
136. de Bree, G.J., et al., *Selective accumulation of differentiated CD8+ T cells specific for respiratory viruses in the human lung.* The Journal of Experimental Medicine, 2005. **202**(10): p. 1433-1442.
137. de Bree, G.J., et al., *Respiratory Syncytial Virus—Specific CD8+ Memory T Cell Responses in Elderly Persons.* Journal of Infectious Diseases, 2005. **191**(10): p. 1710-1718.
138. Bont, L., et al., *Natural reinfection with respiratory syncytial virus does not boost virus-specific T-cell immunity.* Pediatr Res, 2002. **52**(3): p. 363-7.
139. Chang, J. and T.J. Braciale, *Respiratory syncytial virus infection suppresses lung CD8+ T-cell effector activity and peripheral CD8+ T-cell memory in the respiratory tract.* Nat Med, 2002. **8**(1): p. 54-60.
140. Chang, J., et al., *Improved effector activity and memory CD8 T cell development by IL-2 expression during experimental respiratory syncytial virus infection.* J Immunol, 2004. **172**(1): p. 503-8.
141. Chang, J., A. Srikiatkhachorn, and T.J. Braciale, *Visualization and characterization of respiratory syncytial virus F-specific CD8(+) T cells during experimental virus infection.* J Immunol, 2001. **167**(8): p. 4254-60.
142. Ostler, T. and S. Ehl, *Pulmonary T cells induced by respiratory syncytial virus are functional and can make an important contribution to long-lived protective immunity.* European Journal of Immunology, 2002. **32**(9): p. 2562-2569.
143. Ostler, T., et al., *Long-term persistence and reactivation of T cell memory in the lung of mice infected with respiratory syncytial virus.* European Journal of Immunology, 2001. **31**(9): p. 2574-2582.
144. Srikiatkhachorn, A., W. Chang, and T.J. Braciale, *Induction of Th-1 and Th-2 responses by respiratory syncytial virus attachment glycoprotein is epitope and major histocompatibility complex independent.* J Virol, 1999. **73**(8): p. 6590-7.
145. Srikiatkhachorn, A. and T.J. Braciale, *Virus-specific CD8+ T lymphocytes downregulate T helper cell type 2 cytokine secretion and pulmonary eosinophilia during experimental murine respiratory syncytial virus infection.* J Exp Med, 1997. **186**(3): p. 421-32.
146. Hussell, T., et al., *Host Genetic Determinants of Vaccine-Induced Eosinophilia During Respiratory Syncytial Virus Infection.* J Immunol, 1998. **161**(11): p. 6215-6222.

147. Janeway, C.A., Travers, Paul, Walport, Mark, Schlomchik, Mark J., *Immunobiology: The Immune System in Health and Disease*. 5th ed2001, New York: Garland Science.
148. Hemming, V.G., et al., *Intravenous immunoglobulin treatment of respiratory syncytial virus infections in infants and young children.* Antimicrob Agents Chemother, 1987. **31**(12): p. 1882-1886.
149. Wu, H., et al., *Immunoprophylaxis of RSV infection: advancing from RSV-IGIV to palivizumab and motavizumab.* Curr Top Microbiol Immunol, 2008. **317**: p. 103-23.
150. Kasel, J.A., et al., *Relation of serum antibody to glycoproteins of respiratory syncytial virus with immunity to infection in children.* Viral Immunol, 1987. **1**(3): p. 199-205.
151. Murphy, B.R., et al., *Serum and nasal-wash immunoglobulin G and A antibody response of infants and children to respiratory syncytial virus F and G glycoproteins following primary infection.* Journal of Clinical Microbiology, 1986. **23**(6): p. 1009-1014.
152. Kawasaki, Y., et al., *Role of serum neutralizing antibody in reinfection of respiratory syncytial virus.* Pediatr Int, 2004. **46**(2): p. 126-9.
153. Ogilvie, M.M., et al., *Maternal antibody and respiratory syncytial virus infection in infancy.* Journal of Medical Virology, 1981. **7**(4): p. 263-271.
154. Lamprecht, C.L., H.E. Krause, and M.A. Mufson, *Role of Maternal Antibody in Pneumonia and Bronchiolitis Due to Respiratory Syncytial Vims.* Journal of Infectious Diseases, 1976. **134**(3): p. 211-217.
155. Welliver, R.C., et al., *The antibody response to primary and secondary infection with respiratory syncytial virus: Kinetics of class-specific responses.* The Journal of Pediatrics, 1980. **96**(5): p. 808-813.
156. Welliver, R.C., et al., *The development of respiratory syncytial virus-specific IgE and the release of histamine in nasopharyngeal secretions after infection.* N Engl J Med, 1981. **305**(15): p. 841-846.
157. Sung, R.Y., et al., *A comparison of cytokine responses in respiratory syncytial virus and influenza A infections in infants.* Eur J Pediatr, 2001. **160**(2): p. 117-22.
158. Welliver, R.C., et al., *Respiratory syncytial virus-specific IgE responses following infection: evidence for a predominantly mucosal response.* Pediatr Res, 1985. **19**(5): p. 420-4.
159. Domachowske, J.B., et al., *Pulmonary Eosinophilia and Production of MIP-1[alpha] Are Prominent Responses to Infection with Pneumonia Virus of Mice.* Cellular Immunology, 2000. **200**(2): p. 98-104.
160. Domachowske, J.B., et al., *The chemokine macrophage-inflammatory protein-1 alpha and its receptor CCR1 control pulmonary inflammation and antiviral host defense in paramyxovirus infection.* J Immunol, 2000. **165**(5): p. 2677-82.
161. Bonville, C., et al., *Interferon-gamma coordinates CCL3-mediated neutrophil recruitment in vivo.* BMC Immunology, 2009. **10**(1): p. 14.
162. Garvey, T.L., et al., *Inflammatory responses to pneumovirus infection in IFN-alpha beta R gene-deleted mice.* J Immunol, 2005. **175**(7): p. 4735-44.
163. Domachowske, J.B., et al., *Pulmonary eosinophilia in mice devoid of interleukin-5.* J Leukoc Biol, 2002. **71**(6): p. 966-72.
164. Dyer, K.D., et al., *Efficient replication of pneumonia virus of mice (PVM) in a mouse macrophage cell line.* Virol J, 2007. **4**: p. 48.
165. Frey, S., et al., *Role of T cells in virus control and disease after infection with pneumonia virus of mice.* J Virol, 2008. **82**(23): p. 11619-27.
166. Tregoning, J.S., et al., *The Role of T Cells in the Enhancement of Respiratory Syncytial Virus Infection Severity during Adult Reinfection of Neonatally Sensitized Mice.* J. Virol., 2008. **82**(8): p. 4115-4124.
167. Claassen, E.A.W., et al., *Activation and Inactivation of Antiviral CD8 T Cell Responses during Murine Pneumovirus Infection.* J Immunol, 2005. **175**(10): p. 6597-6604.

168. Claassen, E.A., et al., *Identification of a CD4 T cell epitope in the pneumonia virus of mice glycoprotein and characterization of its role in protective immunity.* Virology, 2007. **368**(1): p. 17-25.
169. Heinzel, F.P., et al., *Reciprocal expression of interferon gamma or interleukin 4 during the resolution or progression of murine leishmaniasis. Evidence for expansion of distinct helper T cell subsets.* The Journal of Experimental Medicine, 1989. **169**(1): p. 59-72.
170. Scharton-Kersten, T., et al., *IL-12 is required for natural killer cell activation and subsequent T helper 1 cell development in experimental leishmaniasis.* The Journal of Immunology, 1995. **154**(10): p. 5320-5330.
171. Launois, P., et al., *Early production of IL-4 in susceptible mice infected with Leishmania major rapidly induces IL-12 unresponsiveness.* The Journal of Immunology, 1997. **158**(7): p. 3317-3324.
172. Kuroda, E., T. Kito, and U. Yamashita, *Reduced Expression of STAT4 and IFN-Î³ in Macrophages from BALB/c Mice.* The Journal of Immunology, 2002. **168**(11): p. 5477-5482.
173. Liu, T., et al., *Differences in Expression of Toll-Like Receptors and Their Reactivities in Dendritic Cells in BALB/c and C57BL/6 Mice.* Infect. Immun., 2002. **70**(12): p. 6638-6645.
174. Ulett, G.C., N. Ketheesan, and R.G. Hirst, *Cytokine Gene Expression in Innately Susceptible BALB/c Mice and Relatively Resistant C57BL/6 Mice during Infection with Virulent Burkholderia pseudomallei.* Infection and Immunity, 2000. **68**(4): p. 2034-2042.
175. Morton, D.B. and P.H. Griffiths, *Guidelines on the recognition of pain, distress and discomfort in experimental animals and an hypothesis for assessment.* Vet Rec, 1985. **116**(16): p. 431-6.
176. Mapletoft, J.W., et al., *Intranasal Immunization of Mice with a Bovine Respiratory Syncytial Virus Vaccine Induces Superior Immunity and Protection Compared to Those by Subcutaneous Delivery or Combinations of Intranasal and Subcutaneous Prime-Boost Strategies.* Clin. Vaccine Immunol. **17**(1): p. 23-35.
177. Park, J.K., et al., *Induction of MIP-1[alpha] in Kupffer cell by portal venous transfusion.* Transplant Immunology. **13**(1): p. 33-38.
178. Vogel, C.F.A., et al., *Modulation of the chemokines KC and MCP-1 by 2,3,7,8-tetrachlorodibenzo-p-dioxin (TCDD) in mice.* Archives of Biochemistry and Biophysics, 2007. **461**(2): p. 169-175.
179. Overbergh, L., et al., *The use of real-time reverse transcriptase PCR for the quantification of cytokine gene expression.* J Biomol Tech, 2003. **14**(1): p. 33-43.
180. Pascual, M., S. Fernandez-Lizarbe, and C. Guerri, *Role of TLR4 in ethanol effects on innate and adaptive immune responses in peritoneal macrophages.* Immunol Cell Biol, 2011. **89**(6): p. 716-727.
181. Krempl, C.D. and P.L. Collins, *Reevaluation of the virulence of prototypic strain 15 of pneumonia virus of mice.* J Virol, 2004. **78**(23): p. 13362-5.
182. Domachowske, J.B., et al., *Differential expression of proinflammatory cytokine genes in vivo in response to pathogenic and nonpathogenic pneumovirus infections.* J Infect Dis, 2002. **186**(1): p. 8-14.
183. Bonville, C.A., et al., *Diminished inflammatory responses to natural pneumovirus infection among older mice.* Virology, 2007. **368**(1): p. 182-90.
184. Barr, F.E., et al., *Surfactant protein-A enhances uptake of respiratory syncytial virus by monocytes and U937 macrophages.* Am J Respir Cell Mol Biol, 2000. **23**(5): p. 586-92.
185. Hickling, T.P., et al., *A recombinant trimeric surfactant protein D carbohydrate recognition domain inhibits respiratory syncytial virus infection in vitro and in vivo.* European Journal of Immunology, 1999. **29**(11): p. 3478-3484.
186. Ghildyal, R., et al., *Surfactant Protein A Binds to the Fusion Glycoprotein of Respiratory Syncytial Virus and Neutralizes Virion Infectivity.* Journal of Infectious Diseases, 1999. **180**(6): p. 2009-2013.

187. Henning, L.N., et al., *Pulmonary Surfactant Protein A Regulates TLR Expression and Activity in Human Macrophages.* The Journal of Immunology, 2008. **180**(12): p. 7847-7858.
188. Alcorn, J.L., et al., *Effects of RSV infection on pulmonary surfactant protein SP-A in cultured human type II cells: contrasting consequences on SP-A mRNA and protein.* American Journal of Physiology - Lung Cellular and Molecular Physiology, 2005. **289**(6): p. L1113-L1122.
189. KERR, MARGARET H. and JAMES Y. PATON, *Surfactant Protein Levels in Severe Respiratory Syncytial Virus Infection.* Am. J. Respir. Crit. Care Med., 1999. **159**(4): p. 1115-1118.
190. LeVine, A.M., et al., *Surfactant protein-A enhances respiratory syncytial virus clearance in vivo.* The Journal of Clinical Investigation, 1999. **103**(7): p. 1015-1021.
191. VAN SCHAIK, S.M., et al., *Surfactant Dysfunction Develops in BALB/c Mice Infected with Respiratory Syncytial Virus.* Pediatr Res, 1997. **42**(2): p. 169-173.
192. Atochina, E.N., et al., *Attenuated allergic airway hyperresponsiveness in C57BL/6 mice is associated with enhanced surfactant protein (SP)-D production following allergic sensitization.* Respir Res, 2003. **4**: p. 15.
193. Suzuki, K., et al., *Impaired Toll-like Receptor 9 Expression in Alveolar Macrophages with No Sensitivity to CpG DNA.* Am. J. Respir. Crit. Care Med., 2005. **171**(7): p. 707-713.
194. Punturieri, A., et al., *Specific Engagement of TLR4 or TLR3 Does Not Lead to IFN-β-Mediated Innate Signal Amplification and STAT1 Phosphorylation in Resident Murine Alveolar Macrophages.* The Journal of Immunology, 2004. **173**(2): p. 1033-1042.
195. Kondo, Y., et al., *Regulation of Mite Allergen-pulsed Murine Dendritic Cells by Respiratory Syncytial Virus.* American Journal of Respiratory and Critical Care Medicine, 2004. **169**(4): p. 494-498.
196. Jose, P., et al., *INHIBITION OF INTERLEUKIN-10 SIGNALLING IN LUNG DENDRITIC CELLS BY TOLL-LIKE RECEPTOR 4 LIGANDS.* Exp Lung Res, 2009. **35**(1): p. 1-28.
197. Rodriguez-Martinez, S., et al., *TLRs and NODs mRNA expression pattern in healthy mouse eye.* Br J Ophthalmol, 2005. **89**(7): p. 904-10.
198. Rudd, B.D., et al., *Deletion of TLR3 alters the pulmonary immune environment and mucus production during respiratory syncytial virus infection.* J Immunol, 2006. **176**(3): p. 1937-42.
199. Noah, T.L. and S. Becker, *Chemokines in nasal secretions of normal adults experimentally infected with respiratory syncytial virus.* Clin Immunol, 2000. **97**(1): p. 43-9.
200. Sheeran, P., et al., *Elevated cytokine concentrations in the nasopharyngeal and tracheal secretions of children with respiratory syncytial virus disease.* Pediatr Infect Dis J, 1999. **18**(2): p. 115-22.
201. Bonville, C.A., et al., *Functional Antagonism of Chemokine Receptor CCR1 Reduces Mortality in Acute Pneumovirus Infection In Vivo.* Journal of Virology, 2004. **78**(15): p. 7984-7989.
202. Bonville, C.A., et al., *Altered pathogenesis of severe pneumovirus infection in response to combined antiviral and specific immunomodulatory agents.* J Virol, 2003. **77**(2): p. 1237-44.
203. Domachowske, J.B., et al., *MIP-1alpha is produced but it does not control pulmonary inflammation in response to respiratory syncytial virus infection in mice.* Cell Immunol, 2000. **206**(1): p. 1 - 6.
204. Bont, L., et al., *Local interferon-gamma levels during respiratory syncytial virus lower respiratory tract infection are associated with disease severity.* J Infect Dis, 2001. **184**(3): p. 355-8.
205. Pinto, R.A., et al., *T helper 1/T helper 2 cytokine imbalance in respiratory syncytial virus infection is associated with increased endogenous plasma cortisol.* Pediatrics, 2006. **117**(5): p. e878-86.
206. Davidson, S., et al., *Plasmacytoid dendritic cells promote host defense against acute pneumovirus infection via the TLR7-MyD88-dependent signalling pathway.* J Immunol, 2011. **186**(10): p. 5938-48.

207. Martin, R.M., J.L. Brady, and A.M. Lew, *The need for IgG2c specific antiserum when isotyping antibodies from C57BL/6 and NOD mice.* Journal of Immunological Methods, 1998. **212**(2): p. 187-192.
208. Heer, A.K., et al., *TLR signalling fine-tunes anti-influenza B cell responses without regulating effector T cell responses.* J Immunol, 2007. **178**(4): p. 2182-91.